SEDE AMMINISTRATIVA: UNIVERSITÀ DEGLI STUDI DI PADOVA

DIPARTIMENTO DI MEDICINA MOLECOLARE

SCUOLA DI DOTTORATO DI RICERCA IN BIOMEDICINA

CICLO XXV

A COMBINED COMPUTATIONAL

AND EXPERIMENTAL APPROACH

TO HUMAN OSTEOCALCIN

AND

GPCR FAMILY C GROUP 6 MEMBER A

DIRETTORE DELLA SCUOLA: CH.MO PROF. GIORGIO PALÙ

SUPERVISORE: CH.MO PROF. CARLO FORESTA

DOTTORANDO: DOTT. GIACOMO STRAPAZZON

INDEX

RIASSUNTO

INTRODUZIONE. L'uso di modelli murini transgenici ha permesso la recente identificazione di una regolazione reciproca tra osso, metabolismo energetico e ormoni sessuali. L'osteocalcina, una proteina della matrice ossea che subisce delle modifiche post-traduzionali vitamina-K dipendenti ed è classicamente implicata nella regolazione delle dimensioni e la forma dei cristalli di idrossiapatite, sembra essere nella sua forma circolante un ormone e non un semplice marcatore di rimaneggiamento osseo. La somministrazione di osteocalcina nella sua forma sottocarbossilata regola l'espressione genica e proteica negli adipociti, nelle cellule β pancreatiche e del Leydig attraverso un recettore associato a una proteina G, il recettore GPRC6A, con una selettività genere-specifica. Sono stati condotti numerosi studi che hanno associato i livelli di osteocalcina circolante sia con parametri di controllo gluco-metabolico che con fattori di rischio cardiovascolare. La gran parte degli studi clinici, tuttavia, non ha considerato né l'influenza dei livelli di vitamina K né ha rilevato l'osteocalcina nelle varie forme di differente carbossilazione. È interessante sottolineare, infine, come il recettore GPRC6A sia responsabile della mediazione degli effetti non-genomici degli androgeni e, analogamente, il recettore putativo dell'SHBG sembra essere un recettore associato a una proteina G.

OBIETTIVO dello STUDIO. Obiettivo dello studio è stato studiare in un approccio in due fasi, supportati dalle osservazioni cliniche, le possibili interazioni tra l'osteocalcina, SHBG e il recettore GPRC6A a livello computazionale e, successivamente, verificarle in un modello sperimentale cellulare in vitro.

MATERIALI e METODI. I parametri clinici e di laboratorio sono stati studiati in una coorte di 91 pazienti, che includevano pazienti obesi e soggetti sani di controllo con un disegno trasversale. Un'analisi della struttura proteica tridimensionale e una di docking sono state elaborate con rispettivamente quattro (i.e. TM-align, FATCAT,

TriangleMatch, TopMatch) e tre (i.e. GRAMM-X, ZDOCK, PatchDock) algoritmi bioinformatici. La piattaforma iClickMD-min script é stata utilizzata per l'analisi computazionale della struttura conformazionale dell'osteocalcina, ottenuta tramite il software MOE, in diverse forme di carbossilazione e in presenza o assenza di ioni calcio. Tali analisi sono state integrate con simulazioni di dinamica molecolare, i cui risultati sono stati successivamente confrontati con quelli ottenuti dalle analisi spettroscopiche. I risultati sono stati validati con studi di espressione genica e proteica e saggi di spiazzamento con tecniche di immunofluorescenza e citofluorimetria su colture di cellule HEK-293T.

RISULTATI. Il nostro studio dimostra per la prima volta l'esistenza di una competizione per un sito di legame specifico tra l'osteocalcina e SHBG su cellule umane che esprimono il recettore GPRC6A. Un'analisi predittiva computazionale supporta i risultati, identificando nella sequenza amminoacidica compresa tra i residui residui Gly145 e Leu161 di SHBG l'interfaccia più probabile. I nostri esperimenti descrivono, inoltre, per la prima volta la struttura dell'osteocalcina umana nelle sue varie forme di carbossilazione. L'influenza del legame degli ioni calcio sulla struttura dell'osteocalcina sembra, tuttavia, essere più forte della presenza di un differente stato di carbossilazione. I nostri dati clinici mostrano, infine, uno squilibrio tra le differenti forme di osteocalcina nella coorte di soggetti obesi affetti da ipogonadismo.

CONCLUSIONI. L'approccio utilizzato nel presente studio offre un modello di indagine mirata sull'uomo con il potenziale di poter identificare nuove vie di regolazione e svelare prospettive terapeutiche. Il supporto bioinformatico all'interpretazione degli esperimenti in vitro offre i fondamenti per la sintesi del peptide precedentemente descritto, le cui implicazioni biologiche potranno essere preliminarmente validate sullo stesso modello, al fine di indagare le basi della regolazione integrata tra tessuto osseo, metabolismo energetico e ormoni sessuali.

ABSTRACT

INTRODUCTION. The use of mouse genetics recently highlighted coordination by endocrine regulation between bone, energy metabolism, and endogenous sex hormones. Osteocalcin, a bone matrix protein that regulates hydroxyapatite size and shape through its vitamin‑K-dependent γ‑carboxylated form, unraveled endocrinological functions in its circulating forms, that are not only simple markers of bone formation. Undercarboxylated osteocalcin administration regulates gene and protein expression in adipocytes, in pancreatic β cells, and in Leydig cells by a G protein-coupled receptor, GPRC6A receptor, with a potential gender selectivity. Total serum osteocalcin concentrations in humans are inversely associated with measures of glucose metabolism and cardiovascular risk factors; however, human data are inconclusive with regard to the role of uncarboxylated osteocalcin because most studies do not account for the influence of vitamin K or differentiate between the different γ‑carboxylated forms of osteocalcin. Intriguingly GPRC6A receptor mediates also the non-genomic effects of androgens and, although the information about SHBG-receptor structure is not conclusive, evidence seems to suggest that a G protein-coupled receptor is involved.

AIM of the STUDY. Starting from clinical observations, we investigated the protein-protein interaction computational predictors of osteocalcin and SHBG with GPRC6A receptor, and we validated experimentally in vitro in a two-step approach.

MATHERIAL and METHODS. Clinical and biochemical characteristics were studied in a cohort of 91 obese patients and healthy controls in a cross-sectional study. 3-D protein structure alignment analysis and protein docking analysis were resolved with a four (i.e. TM-align, FATCAT, TriangleMatch, TopMatch) and three (i.e. GRAMM-X, ZDOCK, PatchDock) different algorithms approach, respectively. ClickMD-min script was used as a molecular dynamic platform for computational analysis of the

conformational structure of osteocalcin in presence or absence of Ca^{2+}, developed with MOE software. Steered molecular dynamics simulations related to the carboxylation state were performed, and the data compared with the spectroscopic techniques results. Gene and protein expression analysis and cell-surface receptor binding assays (i.e. immunofluorescence and flow cytometry analysis) on HEK-293T cells experimentally validated the former results in vitro.

RESULTS. Our study shows for the first time the existence of the competition for a specific binding site between osteocalcin and SHBG on human cells expressing GPRC6A receptor. The results are supported by a computational prediction analysis, describing amino acid residues of SHBG from Gly145 to Leu161 as a highly predicted interface. Our experiments describe the structure of human osteocalcin in its carboxylated and undercarboxylated forms for the first time. The influence of the binding of Ca^{2+} on osteocalcin structure seems to be stronger than the presence of γ-carboxylated glutamic acid residues. Our clinical data show an imbalance between the γ‑carboxylated forms of osteocalcin in a cohort of hypogonadic obese an overweight patients, with decreased levels of SHBG and altered levels of the other sex hormones.

CONCLUSIONS. The current two-step approach offers a target approach of investigation directly in humans, that has the potential to identify novel pathophysiological pathways as well as novel therapeutic possibilities. The computational basis of the possible binding of SHBG and osteocalcin has been experimentally validated and can directly lead to the synthesis of a peptide, whose physiological and therapeutic implications represent a feasible perspective for future research in an area of paramount importance, such as the cross-talk between bone, energy metabolism, and endogenous sex hormones.

INTRODUCTION

Osteocalcin synthesis and catabolism

Osteocalcin, also called bone Gla protein or BGP, was the first member of the calcium binding and vitamin K-dependent protein family not associated with blood coagulation to be described, sequenced, and characterized (Price et al., 1976[a]; Price et al., 1976[b]). Osteocalcin (OC) is secreted mainly by osteoblasts, only in the late stage of their differentiation, after the arrest of proliferation and under the control of the Runx2/Cbfa1 transcription factor (Carvallo et al., 2008). Lower levels of osteocalcin has been reported in endothelial progenitor cells (Gössl et al., 2008), myeloid calcifying cells (Fadini et al., 2011), in vascular smooth muscle cells (VSMCs) (Spronk et al., 2001), and in the brain, intestine and kidney (Fleet et Hock, 1994). Moreover, our group reported evidence for osteocalcin production, storage, and secretion, upon activation with an endogenous mechanism, in peripheral blood platelets and in bone marrow megakaryocytes (Thiede et al., 1994; Foresta et al., 2012), and in adipose tissue and during all stages of adipogenesis (Foresta et al., 2010). *Osteocalcin* mRNA has also been detected in several non-osseous tissues, but the RNA splicing was found to be incomplete (Jung et al., 2001).

Osteocalcin is encoded in human by the *Bone γ-Carbossiglutamate* gene, a single-copy gene located on chromosome gene 1q25.31 (Puchacz et al., 1989; Raymond et al., 1999). The transcription of this gene requires modifications in the chromatin structure and nucleosome organization, that render the regulatory sequences at promoter level accessible to the cognate transcription factors (Shen et al., 2003). The key regulators of *Osteocalcin* transcription have been recognized by Runx2, the essential regulator of basal bone-specific transcription, and vitamin D3, the principle enhancer of *Osteocalcin* expression (by 3 to 5-fold times) (Price et Baukol, 1981; McDonnell et al., 1989; Ozono et al., 1990), after the initiation of basal transcription. The transcription starts at the proximal region of the promoter, which contains

Runx2 and TCF/LEF sites, and continues at the distal regions which contains Runx2 and AP-1 binding sites and regulatory sequences responsive to vitamin D3. Other regulatory factors include parathyroid hormone (PTH) (Yu et Chandrasekhar, 1997), estrogens (E) (Qu et al., 1998), glucocorticoids, (Shalhoub et al., 1998), growth factors (Hughes-Fulford et Li, 2011) and cyclic adenosine monophosphate (cAMP) (Boudreaux et Towler, 1996). Besides its role in the regulation of the transcription gene, vitamin D3 regulates *Osteocalcin* gene expression at post-translational level, by stabilizing the *Osteocalcin* mRNA, as demonstrated in osteoblast-like cells (Mosavin et Mellon, 1996).

After the synthesis of pre-promolecule with 98 amino acids and 11 KDa molecular weight, several post-translational modifications are required to obtain the active form of 49 residues and around 5.8 KDa molecular weight. A 23-signal peptide is cleaved and three carboxyl groups in propeptide are added to three glutamic acid residues (Glu) in the presence of vitamin K, the cofactor of carboxylase. (Lian et Friedman, 1978; Price et al., 1983) The vitamin K group consists of structurally similar, fat-soluble, 2-methyl-1,4-naphtoquinones, which transform Glu residues into γ-carboxyglutamic acid residues (Gla), through carboxylation process (Figure 1).
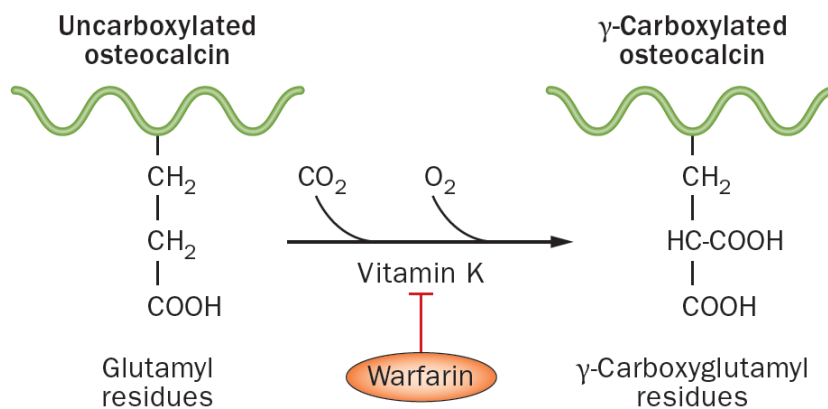

Figure 1. Vitamin K is required for the formation of γ‑carboxyglutamic acid residues (Gla). γ‑carboxyglutamic acid residue is a unique amino acid that is created by vitamin-K-dependent post-translational modification of specific glutamic acid residues in all Gla-containing proteins, including osteocalcin. This process is inhibited by warfarin. (modified from Booth et al., 2012)

The vitamin K dependent carboxylation of osteocalcin has been shown to occur in bone tissue in organ culture (Lian et Friedman, 1978) and in isolated bone cells in tissue culture (Nishimoto and Price, 1980). The carboxylase has a high affinity binding site for the sequence contained in the mature form (Stanley et al., 1999; Frazao et al., 2005). Moreover, the carboxylase enzyme has high affinity for the domain formed by Gla residues (Benton et al., 1995). In most species, all three Glu residues are fully carboxylated. However, in humans, osteocalcin in bone is incompletely carboxylated.

At the end of post-translational modifications, the mature form is released in bone matrix, where the major part binds calcium ions (Ca^{2+}) (Hoang et al., 2003). The unbound fraction is released into the bloodstream (Price et Nishimoto, 1980); circulating osteocalcin consists of intact osteocalcin (one-third), N-terminal osteocalcin fragments 1-43 (one-third) and unidentified fragments (one-third), due to the action of proteolytic enzymes. Recently, Ferron et al. demonstrated a pH-dependent mechanism of activation for osteocalcin in mouse and human osteoblasts (Ferron et al., 2010). Since an acid pH is the only known chemical condition allowing protein decarboxylation (Poser and Price, 1979; Engelke et al., 1991), bone resorption, which occurs at pH 4.5, provides an ideal setting to decarboxylate and activate osteocalcin, using the huge amount of osteocalcin stored in the bone extracellular matrix (ECM). The levels of carboxylated osteocalcin and undercarboxylated osteocalcin in cultured differentiated osteoclasts on bovine cortical bone slides devitalized (to exclude any endogenous osteoblastic) resulted in a 2-fold increase in the undercarboxylated/carboxylated osteocalcin ratio (Ferron et al., 2010). However, this mechanism account only for a part of the undercarboxylated osteocalcin, another *in vitro* study, in fact, showed that warfarin increases undercarboxylated osteocalcin from 29% to 54% (Henneicke et al., 2009). Human osteocalcin concentrations in bone and in the circulation are only 20% of those found in other species.

Osteocalcin structure

Osteocalcin proteins have of 46-50 amino acid residues depending on the species (Frazao et al., 2005). Compared with the human sequence, the overall protein sequence is highly conserved in most species (80-95%), but to a lesser extent in the frog and chicken (70%), mouse (60%) and bony fish (40%) (Hoang et al., 2003). However, considerable sequence variation exists at other regions (Figure 2).
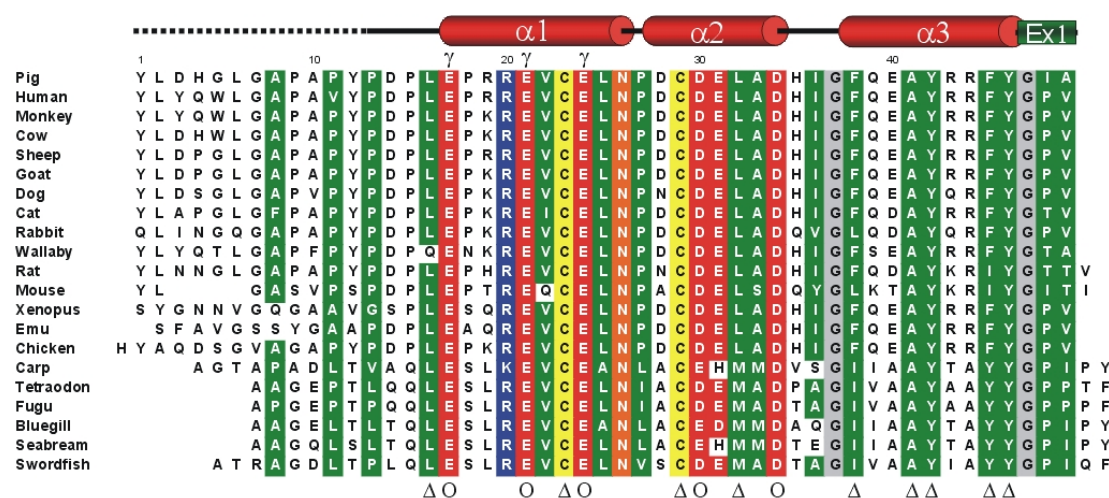
Figure 2. Sequence alignment of osteocalcin. Protein sequence with the secondary structure elements are indicated and the conserved residues highlighted (green, red, blue, yellow, orange and grey indicate conserved, acidic, basic, cysteine, asparagine and glycine residues, respectively). Positions are identified as conserved if more than 85% of the residues are identical, or similar if hydrophobic in nature. γ indicates a Gla residue, open triangles and circles indicate hydrophobic core and Ca^{2+}-coordinating surface, respectively. (modified from Hoang et al., 2003)

Conserved elements in all osteocalcin sequences examined include a single disulfide-bonded loop (i.e. Cys23-Cys29), and the homology of the EXXXEXCEXXXXC motif (i.e. GluXXXGluXCysGluXXXXCys). EXXXEXCEXXXXC motif, in particular, including the three Glu residues located at positions 17, 21, and 24 (according the numbering of in human and porcine osteocalcin) undergoing to the γ- carboxylation process, is highly conserved (Hoang et al., 2003; Frazao et al., 2005), arguing for its functional importance. Carboxylation is an ordered process with Glu21 and Glu24 residues being carboxylated first, followed by Glu17 in humans (Benton et al., 1995).

However, Glu17 is γ-carboxylated only in about 9% of human osteocalcin (Poser et al., 1980). The partial carboxylation of human osteocalcin was proposed to be due, at least in part, to defective post-translational carboxylation prior to secretion, not to decarboxylation of the mature protein after secretion (Frazao et al., 2005). γ-carboxylation of Glu residues is thought to increase affinity of osteocalcin for Ca^{2+} and is essential for the interaction of osteocalcin with bone in vivo and for the specific interaction with bone hydroxyapatite (HA) in vitro, thus contributing to bone formation (Poser and Price, 1979; Pastoureau et al., 1993). Circular dichroism (CD) (Hauschka and Carr, 1982; Atkinson et al., 1995) and nuclear magnetic resonance (NMR) (Atkinson et al., 1995; Dowd et al., 2001; Dowd et al., 2003) analysis indicate that fully γ-carboxylated chicken and bovine osteocalcin in solution are largely unstructured in the absence of calcium and that only after addition of physiological Ca^{2+} concentrations (1-2 mM), they undergo a transition to a folded state displaying highly flexible N- and C-terminal regions and characterized by a protein core formed by three α-helices stabilized by the previously described single disulfide bridge and orienting the Gla residues on the same face of osteocalcin molecule. Similar conclusions were also drawn from the crystallographic structures of porcine (Hoang et al., 2003) and fish (Frazao et al., 2005) osteocalcin. Specifically, porcine osteoalcin (i.e. from residues Pro13 to Ala49) formed a tight globular structure comprising a previously unknown fold (no matches in the DALI database, Hohm and Sander, 1993) with a topology consisting, from its N-terminal, of three α-helices and a short extended strand. α-helices H1 and H2 are connected by a type III turn structure from Asn26 to Cys29 and formed a V-shaped arrangement that was stabilized by an interhelix disulphide bridge involving Cys23 and Cys29 (Figure 3) (Hoang et al., 2003). α-helix H3 was connected to α-helix H2 by a short turn and was aligned to bisect the V-shape arrangement of α-helices H1 and H2. The three α-helices together composed a tightly packed core involving conserved hydrophobic residues Leu16, Leu32, Phe38, Ala41, Tyr42, Phe45 and Tyr46. The overall tertiary structure

was further stabilized by a hydrogen bond (HB) interaction between two invariant residues, Asn26 in the α-helices H1 and H2 linker and Tyr 46 in α-helices H3 (Hoang et al., 2003).

Projection of conserved residues onto the molecular surface of the porcine osteocalcin structure showed an extensive negatively charged surface centering on α-helices H1 (solvent-exposed surface area 586 $Å^2$). Notably, all three Gla residues implicated in HA binding were located on the same surface of α-helices H1 and, together with the conserved residue Asp30 from α-helices H2, coordinated five Ca^{2+} in an elaborate network of ionic bonds (Figure 3) (Hoang et al., 2003).
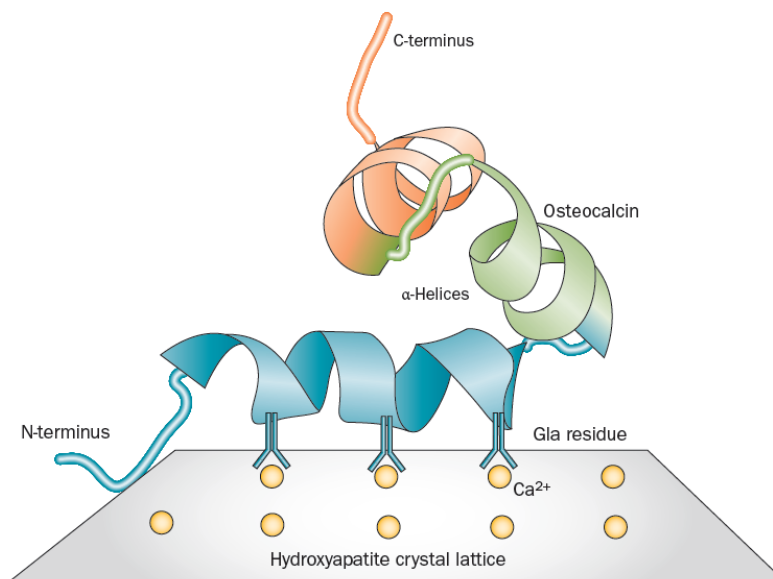
Figure 3. Direct structural analysis of osteocalcin by NMR imaging and X‑ray crystallography predicted a tight globular structure comprised of three α‑helices, a C‑terminal hydrophobic core and an unstructured N‑terminus. All three Gla residues were found in the first helical region (α‑helix H1). The γ‑carboxyglutamic acid residues are complementary to the calcium ions on the c‑axis of the hydroxyapatite crystal lattice, and are positioned to control crystal size and shape within the constraints of the collagen fibril. (modified from Hoang et al., 2003)

The N-terminal part of OC exhibits a considerable sequence variation (Hauschka et al, 1989; Viegas et al., 2002), but unfortunately was not considered in the Hoang model (Hoang et al., 2003). The C-terminal part of osteocalcin seems to possess

chemotactic activity (Mundy and Poser, 1983). However, Frazao states that the residues at N- and C-terminal regions, out of the tight globular arrangement of the three α-helices, have essentially no secondary structure characteristics in the porcine and fish models (Frazao et al., 2005). Finally, sedimentation equilibrium data suggested that osteocalcin exists as a monomer *in vivo* (Hoang et al., 2003).

Osteocalcin function

The several interesting properties of osteocalcin were highlighted since long ago: (i) extremely abundance in the bone ECM (Hauschka et al., 1989); (ii) low-level of circulating osteocalcin in blood plasma (Price and Nishimoto, 1980); (iii) derivation from higher molecular weight precursor proteins (Hauschka, 1979; Nishimoto and Price, 1980) (iv) specific Gla-dependent binding of Ca^{2+} ions (Hauschka et Gallop, 1977; Poser and Price, 1979; Gallop et al., 1980); and (v) Ca^{2+}-induced transition to the α-helical conformation (Hauschkan et Carr, 1982).

The first piece of evidence that osteocalcin is a determinant of bone formation was obtained in mice lacking of *Osteocalcin* (*Osteocalcin*^{-/-} mice), that developed a late-onset phenotype marked by modestly increased bone mass and bones of improved functional quality (Ducy et al., 1996), suggesting that osteocalcin directly inhibits osteoblastic bone formation without impairing bone resorption or mineralization. Bone mineral content was unaffected, but subsequent analysis of the crystal properties of hydroxyapatite showed altered mineral composition in the cortical bone of *Osteocalcin*^{-/-} mice (Boskey et al., 1998), being immature at small-angle X-ray scattering. Conversely, subsequent studies suggested that osteocalcin improved both the initial adherence of osteoblast-like cells to biocement, without affecting the proliferation of cells (Knepper-Nicolai et al., 2002), and to hydroxyapatite/collagen composites (Rammelt et al., 2005). Further studies showed that osteocalcin was implicated in bone resorption, promoting differentiation of osteoclast progenitors and enhancing chemotaxis and activity in studies in vivo (Lian

et al., 1984; Chenu et al., 1994, Ingram et al., 1994) and in vitro (Malone et al., 1982; Liggett et al., 1994; Mundy et Poser, 1983). Finally, despite osteocalcin abundance in a mineralized bone ECM and protein's high affinity for mineral ions due to Gla residues suggested that this protein was involved in bone ECM, loss- and gain-of-function mutations in *Osteocalcin* have unambiguously established, that this was not the only action (Figure 4) (Ducy et al., 1996; Murshed et al., 2004). *Osteocalcin*^{-/-} mice, given the abundance of osteocalcin and its restriction to bone and specificity to hydroxyapatite, had no overt phenotypic abnormalities (Ducy et al., 1996), despite that changes in optimal crystal size and orientation of HA, affecting both bone quantity and quality, were revealed at small-angle X‑ray scattering (Boskey et al., 1998; Poundarik et al., 2011)

All three Glu residues in the osteocalcin molecule are fully carboxylated in most species. However, osteocalcin in bone and serum is incompletely carboxylated and Ca^{2+}-free osteocalcin can be detected in circulating plasma in humans, as previously specified, and its levels are generally associated both with higher osteoblast activity (Garnero et al., 1994) and with bone turnover (Ivaska et al., 2004). Moreover, since Ducy`s *Osteocalcin*^{-/-} mice model, circulating osteocalcin showed important endocrine functions. The first hypothesis that skeleton may act as an endocrine organ regulating energy metabolism, arose observing the abnormal amount of visceral fat in *Osteocalcin*^{-/-} mice. This hypothesis was verified by showing that, unlike wild-type osteoblasts, *Osteocalcin*^{-/-} osteoblasts cannot induce insulin secretion by pancreatic β cells (Lee et al., 2007). Accordingly, *Osteocalcin*^{-/-} mice were hyperglycemic, hypoinsulinemic, and insulin resistant in liver, muscle, and white adipose tissue. Islets' size and number, β-cell mass, pancreas insulin content, and insulin immunoreactivity were all markedly decreased in *Osteocalcin*^{-/-} mice. Fat mass was increased and associated with a higher adipocytes number and serum triglyceride levels in *Osteocalcin*^{-/-} mice (Lee et al., 2007). These features were associated with decreased levels of serum adiponectin, an adipokine known to

enhance insulin sensitivity. In particular, the decrease in osteocalcin-induced insulin sensitivity occurs, at least in part, through adiponectin, though the decrease in insulin secretion is a direct consequence of osteocalcin deficiency (Lee et al., 2007). Surprisingly, the metabolic phenotype of *Osteocalcin*^{-/-} mice were the mirror image of the one observed in mice lacking of *Embrionic stem cell phosphatase* (*Esp*^{-/-} mice), suggesting that in the latter there is a gain of osteocalcin activity (Figure 4). *Esp* (also known as the protein tyrosine phosphatase receptor type *Ptprv* gene) is expressed in the mouse osteoblast and the mouse Sertoli cells and the embryonic stem cell and encodes the protein tyrosine phosphatase termed OST-PTP (Mauro et al., 1994). *Esp*^{-/-} mice were hypoglycemic and hyperinsulinemic (Lee et al., 2007; Ferron et al., 2008). Insulin secretion and sensitivity were increased in *Esp*^{-/-} mice, whereas mice overexpressing *Esp* in osteoblasts were glucose intolerant because of a decrease in insulin secretion and sensitivity, in pancreatic β cells and in liver, muscle, and white adipose tissue, respectively (Lee et al., 2007). In a co-culture assay, in which wild type (WT) cells were separated by a filter, osteoblasts enhanced *Insulin* expression of 40%, next to insulin secretion by islets or β cells, and *Adiponectin* expression, and subsequently adiponectin secretion, by adipocytes. The enhancement of the expression was to a higher extent with *Esp*^{-/-} osteoblasts than wild-type osteoblast (Lee et al., 2007). Moreover, the glucose intolerance phenotype of *Osteocalcin*^{-/-} mice was corrected by removing one allele of *Esp* from these mice (Lee et al., 2007). Overall the previous data indicate that *Esp*^{-/-} mice are a gain-of-function model for osteocalcin the newly discover actions of osteocalcin on metabolism.

Lee et al. showed that the level of γ-carboxylation, the main post-translational modification of osteocalcin, was different in wild-type and *Esp*^{-/-} mice (Lee et al. 2007). Following a 15 min incubation period, 90% of osteocalcin present in the serum of wild-type mice was bound to HA, whereas only 74% was present using serum from *Esp*^{-/-} mice. Moreover, wild-type osteoblasts treated with warfarin, an inhibitor of γ-carboxylation (Berkner, 2005), resulted in a marked decrease in the

percentage of osteocalcin bound to HA, and warfarin-treated osteoblasts induced *Adiponectin* expression to a significantly higher extent than vehicle-treated osteoblasts. Only undercarboxylated osteocalcin in cell-based in vitro assays showed that could induce expression of *Adiponectin* in adipocytes, and of *Insulin* and *CyclinD1*, a molecular marker of cell proliferation, in islets (Lee et al., 2007). No effects were demonstrated in the former model by co-incubation with osteocalcin with fully carboxylated Gla residues. Ferron et al. data confirmed the previously, in fact when rat insulinoma INS-1 cells treated with carboxylated osteocalcin (i.e. at pH 7.5) or undercarboxylated osteocalcin (i.e. at pH 4.5), only the latter form could increase insulin secretion to the same extent of recombinant undercarboxylated osteocalcin (i.e. bacterially produced), used as a positive control (Figure 4) (Ferron et al., 2008).

$Esp^{-/-}$ mice fed with a high fat diet gained significantly less weight than wild-type mice and did not develop glucose intolerance or insulin resistance as wild-type mice did (Lee et al., 2007), showing in vivo that $Esp^{-/-}$ mice are intrinsically protected. The protein encoded by *Esp*, in fact, is not secreted and therefore cannot be a hormone. On the other side, $Osteocalcin^{-/-}$ mice receiving exogenous osteocalcin had a decreased blood glucose levels at the 30, 60, and 120 min time points of this glucose tolerance test assay and an increased insulin secretion compared to those not receiving recombinant undercarboxylated osteocalcin (Lee et al., 2007). Moreover, wild-type mice receiving exogenous osteocalcin (3 ng/h) did not develop an obesity phenotype or a glucose intolerance phenotype when fed a high-fat diet (Ferron et al, 2008). Pico to nanomolar amounts of exclusively recombinant undercarboxylated osteocalcin were able to regulate glucose metabolism, to affect insulin sensitivity, and to regulate fat mass in wild-type mice (Ferron et al, 2008). In wild-type mice fed a high-fat diet, daily injections of osteocalcin partially restored insulin sensitivity and glucose tolerance, displaying additional mitochondria in their skeletal muscle, having

increased energy expenditure, being protected from diet-induced obesity and hepatic steatosis (Ferron et al., 2012).
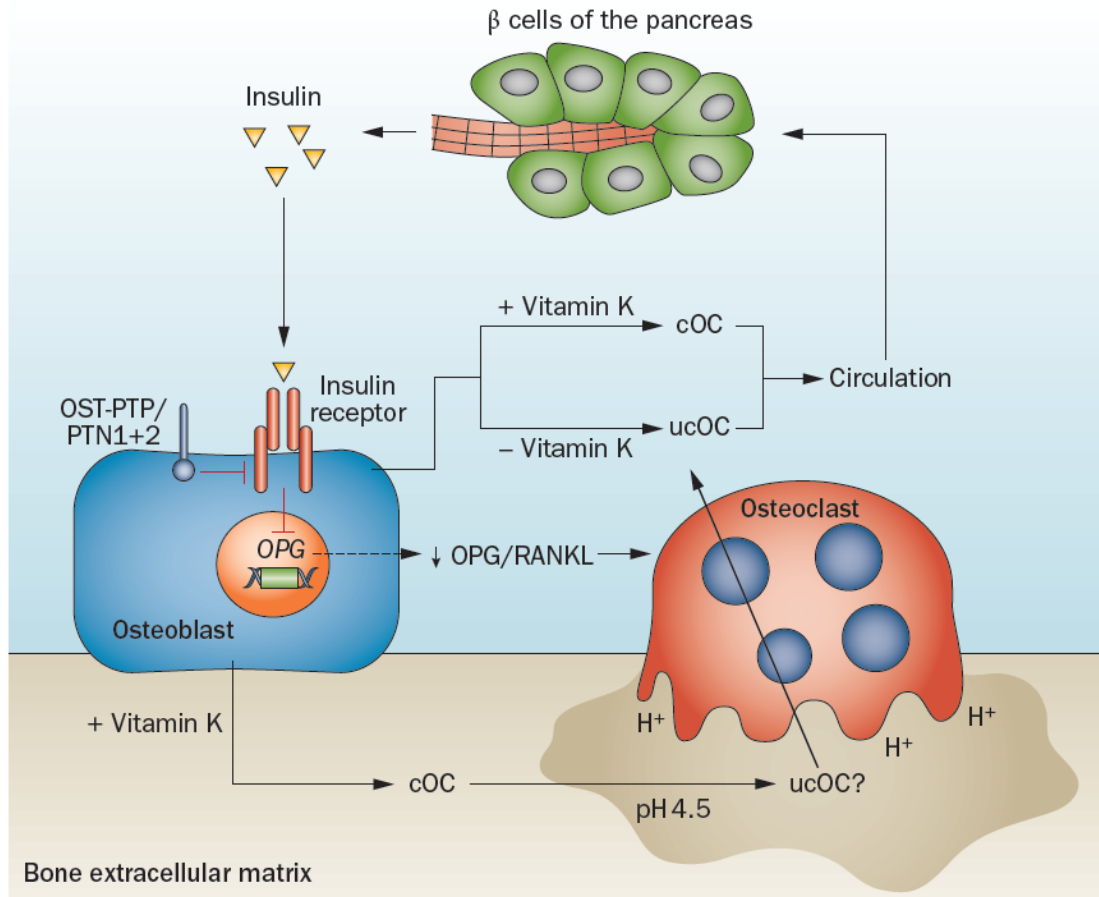
Figure 4. Model of the role of osteocalcin in glucose metabolism in mice. The presence of undercarboxylated osteocalcin in human circulation could be the consequence of two separate processes: incomplete carboxylation of osteocalcin, linked or not to suboptimal vitamin K intake, or decarboxylation during osteoclast resorption. Insulin signaling in osteoblasts limits the production of osteoprotegerin, an inhibitor of osteoclast maturation. This mechanism facilitates osteoclast bone resorption, producing an acid environment that decarboxylates (and hence activates) intact osteocalcin. OST-PTP/PTN 1+2 dephosphorylates the insulin receptor in osteoblasts leading to inhibition of insulin signaling. abbreviations: cOC, carboxylated osteocalcin; OPG, osteoprotegerin; ucOC, undercarboxylated osteocalcin. (modified from Booth et al., 2012)

These experiments are consistent with the notion that osteocalcin is a molecule secreted and represent a hormone, whose action and regulation seems to be linked to osteocalcin secretion in mice.

Osteocalcin G protein-coupled receptor

The final element necessary to complete a putative endocrine loop mediated by osteocalcin was the identification of a tissue-specific receptor. G protein-coupled receptors make up one of the largest protein families in humans and are cell-surface receptors that can be activated by a broad range of ligands (Bockaert et Pin, 1999). A large proportion of physiological stimuli and of current drugs (27%–45%) exerts their effect via G protein-coupled receptors, but the majority of the receptors in this protein superfamily are as yet untapped for potential therapies (Overington et al., 2006).

The first evidence that the signaling pathway of osteocalcin could be mediated by a protein-coupled receptor, was the discovery that an orphan G protein-coupled Ca^{2+} receptor, widely expressed in bone and osteoblasts, was responsive to osteocalcin (Pi et al., 2005). Osteocalcin in the presence of extracellular Ca^{2+} significantly enhanced serum response element (SRE)-luciferase activity in a cell line stably expressing GPRC6A receptor, depending on the prevailing level of extracellular Ca^{2+} (Pi et al., 2000; Pi et al., 2005). Oury et al. achieved the same goal with an interesting indirect approach (Oury et al. 2011). After characterization of the signaling pathway used by osteocalcin (i.e. induction of cAMP production, but not tyrosine phosphorylation, ERK activation, or intracellular calcium accumulation in Leydig cells), a G protein-coupled receptor emerged to be the most appropriate candidate. Moreover, taking the advantage of the dichotomy of fertility regulation of osteocalcin between male and female mice, only 22 out of 103 orphan GPCRs tested were predominantly expressed in testes compared to ovary. 4 out of these 22 were enriched in Leydig cells, including $Gprc6a^{-/-}$, whose deletion resulted in a metabolic and fertility phenotype similar to that of $Osteocalcin^{-/-}$ mice, characterized by glucose intolerance, impaired insulin secretion, and under-masculinization in vivo (Pi et al., 2008). Moreover, osteocalcin directly bound to wild-type cells expressing $Gprc6a$ but not to $Gprc6a^{-/-}$ cells (Oury et al., 2011). Interestingly, GPRC6A receptor

is highly expressed in mouse pancreatic tissue and in the mouse TC-6 pancreatic β-cell line, and recombinant osteocalcin stimulates insulin secretion in the pancreas (Pi et al., 2011)

GPRC6A receptor belongs to a small family of dimeric G protein-coupled receptor, Family C/Glutamate family, which includes eight metabotropic glutamate receptors (mGluR1-8), one calcium sensing receptor (CaR), two γ-aminobutyric acid receptor (GABA$_B$R1-2) as well as several taste (e.g. T1R1, T1R2, and T1R3) and orphan receptors (RAIG1, GPRC5B-5D, and GABABL) (Wellendorph et Braüner-Osborne, 2004; Braüner-Osborne et al., 2007). GPRC6A receptor was conserved through evolution.

Gprc6A gene is located on chromosome band 6q22.31. The longest and most abundant variant was named isoform 1 and displayed an open-reading frame of 2778 nt (926 aa). The existence of two additional *Gprc6a* isoforms (2 and 3); the two isoforms carry in-frame deletions in the ATD (Wellendorph et al., 2004). *Gprc6a* has a broad expression profile in humans, mice, and rats (Kuang et al., 2005; Pi et al., 2005; Wellendorph and Braüner-Osborne, 2004; Wellendorph et al., 2007). *Gprc6a* is expressed nearly all tissues tested (except the small and large intestines and parathyroid gland), with highest levels in kidney, skeletal muscle, testis, brain, and leucocytes (Wellendorph et al., 2004; Kuang et al., 2005; Pi et al., 2005). All three isoforms are expressed in mammalian cells, but are poorly expressed on the cell surface. Except for the kidney, where isoforms 1 and 2 appear equally expressed, isoforms 2 and 3 are generally less abundant than isoform 1.

The Family C receptors have a characteristic large, extracellular, ligand-binding venus fly trap domain (VFTM), a Cys-rich region, a seven-transmembrane (7-TM) bundle and an intracellular C-terminal (Braüner- Osborne et al., 2007). The calcium-sensing receptor is its closest homologue with a 34% amino acid residues sequence identity, despite the bears the highest resemblance is with an odorant goldfish 5.24 receptor (Wellendorph et al., 2004) (Figure 5).
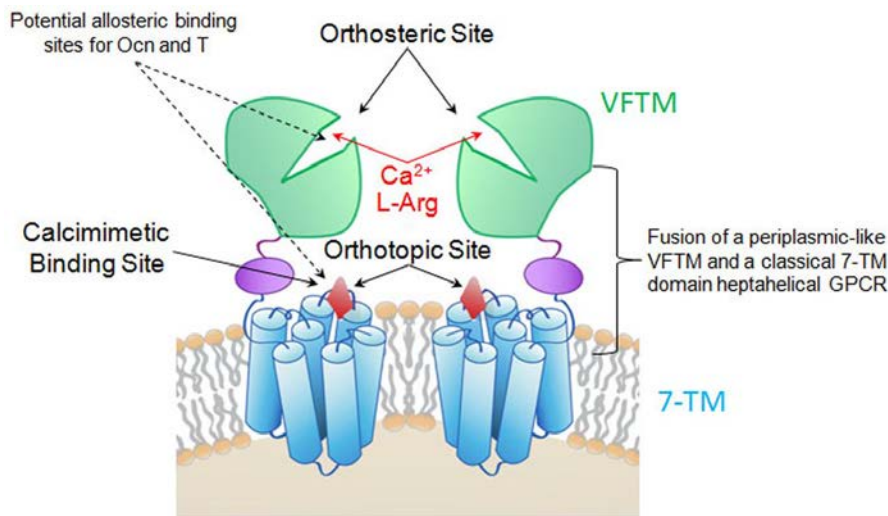
Figure 5. Hypothetical model of ligand activation and allosteric modulation of GPRC6A. GPRC6A consists of a VFTM for sensing nutrients and the 7-TM domain and like other members of this family may function as a dimer. The orthotopic agonists, such as L-Arg and Ca^{2+}, which are likely to be the natural ligands, binding sites are located adjacent to each other in the VFTM, whereas binding sites for allosteric modulators, such as calcimimetics (i.e. osteocalcin), are located in the 7-TM region, possibly representing a retained (cryptic) ligand binding site in the classical GPCR region. Pi et al. hypothesize that osteocalcin (Ocn) and testosterone (T) are also allosteric activators of GPRC6A with mechanism of activation similar to calcimimetics because they require the presence of a threshold concentration of Ca^{2+} for signaling to occur. (modified from Pi et Quarles., 2012[a])

GPRC6A receptor has structure/functional characteristics that permit it to sense dissimilar ligands. VFTM and 7-TM domains of GPRC6A receptor creates, in fact, the structural basis for both independent biological and pharmacological actions of orthosteric ligands and allosteric modulators with different affinities and efficacies; VFTM and 7-TM domains supports also for the possible cooperative interactions between the orthosteric and allosteric ligand binding sites (Figure 5). Accordingly, ample evidence exists for the involvement of GPRC6A receptor in the regulation of biological processes in humans.

GPRC6A receptor is physiologically activated by L-α-amino acids, with a preference for the naturally occurring basic amino acids Arg, Lys and ornithine (Kuang et al., 2005; Wellendorph et al., 2005). Interestingly, depending on which signaling pathway is studied, the receptor is also positively modulated (Christiansen et al., 2007; Kuang et al., 2005), or directly activated (Pi et al., 2005) by divalent cations.

The broad ligand recognition, and the previously described wide tissue expression, have obscured the elucidation of the physiological function of the GPRC6A receptor. The generation of *Gprc6a*^{-/-} mice elucidated potential physiological roles, including severe metabolic and endocrinological disturbances (Oury et al., 2011; Pi et al., 2008; Wellendorph et al., 2009). Interestingly, large discrepancies have been observed between different *Gprc6a*^{-/-} mice of two separate laboratories (Pi et al., 2008; Wellendorph et al., 2009). Pi et al. reported the previously described *Osteocalcin*^{-/-}-like phenotype, feminization of male mice, and decreased bone mineral density and impaired mineralization (Pi et al., 2008). Whereas, Wellendorph et al. found mice were viable and fertile, developed normally and exhibited no significant differences in body weight or skeletal manifestations compared with their wild-type littermates. (Wellendorph et al., 2009).

Given the known physiological importance of the CaR receptor as a metabolic regulator (Tfelt-Hansen et Brown, 2005), the phenotype of *Gprc6a*^{-/-} mice (Pi et al., 2008), the ability of GPRC6A to mediate osteocalcinin-induced insulin release in vivo (Pi et al., 2011), and the novel role of osteocalcin (Lee et al., 2007), it is tempting to speculate that GPRC6A receptor could also be implicated in regulation of energy metabolism. However, given the wide expression of this receptor, the question remains how osteocalcin functions as a cell-specific ligand of GPRC6A receptor. Perhaps a co-receptor is required for tissue specificity, as seen for FGF‑23 (another bone-derived factor) and its co-receptor, Klotho (Urakawa et al., 2006).

Osteocalcin in metabolic and cardiovascular diseases

Clinical studies show that osteocalcin is involved in glucose homeostasis and cardiovascular diseases in humans are small in number and limited in size, but there are some evidence supporting a correlation with indicators of metabolic phenotype and cardiovascular risk factors.

The levels of circulating osteocalcin have mainly be reported to be inversely associated with measures of glycemia in cross-sectional studies of nondiabetic adults and children, consistent with the hypothesis that osteocalcin influences β‑cell function and insulin sensitivity (Lee et al., 2007) (Table 1). Interestingly, in prospective analyses, exposure to higher osteocalcin levels during follow-up was associated with a significantly lower rise in fasting glucose at 3 years (Pittas et al, 2009).

Description of association with osteocalcin	N of Subjects	Reference
Inverse with HOMA-IR, fasting glucose and insulin	2493 adults; M + F	Saleem et al., 2010
Inverse with HOMA-IR, fasting glucose	1597 adults; M	Iki et al., 2012
Inverse with HOMA-IR	580 adults; M + F	Gravenstein et al., 2011
Inverse with HOMA-IR, fasting glucose and insulin	380 adults; M + F	Pittas et al., 2009
Inverse with HOMA-IR and fasting glucose	348 adults; M + F	Shea et al., 2009
Inverse with fasting glucose	64 adults; M + F	Iglesias et al., 2011

Table 1. Cross-sectional association between osteocalcin and glucose metabolism in nondiabetic adults. F, females; HOMA-IR, Homeostasis Model of Assessment - Insulin Resistance; M, males; osteocalcin, total osteocalcin. Only significantly statistically (P < .05) associations are reported.

Fernandez-Real et al. reported a positive association between insulin sensitivity and osteocalcin in a cross-sectional study of 149 lean adult men (Fernandez-Real et al., 2009), and other did not find any association, like in our cohort of 83 male adults patients between osteocalcin and fasting glucose and insulin (Foresta et al., 2010) Most of the cross-sectional studies with cohort of nondiabetic children showed no association with Homeostasis Model of Assessment - Insulin Resistance (HOMA-IR) and fasting insulin (Misra et al., 2007; Pollock et al. 2011; Boucher-Berry et al., 2012).

Since the 80s human studies reported that osteocalcin were lower in patients with established diabetes and microangiopathic complications (Pietschnann et al., 1988). Recently, Im et al. studied glucose metabolism and osteocalcin in 339

postmenopausal Japanese women (Im et al., 2010). Circulating osteocalcin was significantly lower among patients with type 2 diabetes when compared to patients without diabetes and showed an inverse relationship with fasting glucose, glycosylated haemoglobin (HbA1c), and HOMA-IR (Im et al., 2010). A multivariate analysis adjusting for age and body weight revealed circulating osteocalcin as an independent predictor for glucose and HbA1c levels. Concurrently, an interim analysis of the large-scale prospective Fenofibrate Intervention and Event Lowering in Diabetes (FIELD) trial (Keech et al., 2005; Sullivan et al., 2011), which included 661 patients with diabetes mellitus revealed lower fasting glucose, insulin, and HOMA-IR levels with increasing levels of circulating osteocalcin (Sullivan et al., 2011). HbA1c (7.10 vs. 6.4%) declined substantially from the lowest to the highest tertile of osteocalcin in the same population (Sullivan et al., 2011).

Circulating osteocalcin seem to be inversely associated with measures of adiposity, such as percentage body fat and body max index (BMI) (Table 2), despite in our cohort of 83 male obese and overweight we did not find any association (Foresta et al., 2010).

Description of association with osteocalcin	N of Subjects	Reference
Inverse with and BMI	2493 adults; M + F	Saalem et al., 2010
Inverse with % body fat (only in F)	443 adults; M	Shea et al., 2010
Inverse with % body fat	307 adults; M + F	Pitroda et al., 2009
Inverse with % body fat and BMI	380 adults; M + F	Pittas et al., 2009
Inverse with % body fat and BMI	106 child; M + F	Boucher-Berry et al., 2012
Inverse with visceral fat	86 adults; M	Kim et al., 2010

Table 2. Cross-sectional association between osteocalcin and measures of adiposity in nondiabetic adults and children. F, females; BMI, body max index; M, males; osteocalcin, total osteocalcin. Only significantly statistically (P < .05) associations are reported.

Fernandez-Real et al. showed that change in visceral fat was the best predictor of change in osteocalcin after controlling for age, BMI, and change in insulin sensitivity (P = .002) (Fernandey-Real et al., 2009). A subsequent study from the same group

used an hypocaloric diet to achieve weight loss of −22.3 ± 2.3% and a decline in BMI of 30.9 ± 5.2% (Fernandez-Real et al., 2010). These changes were accompanied by a doubling of circulating osteocalcin from 2.8 ± .75 at baseline to 5.9 ± .9 ng/mL and a substantial improvement in HOMA-IR at closeout.

Bae et al. showed that in patients with a multifactorial pathology like metabolic syndrome, osteocalcin was independently associated to its presence (Bae et al., 2012), according to Saleem et al. observations (Saleem et al., 2010).

The discrepancies of results from the different studies can be ascribed to multiple factors as it is the regulation of osteocalcin synthesis and catabolism and the one of energy metabolism. Osteocalcin has been reported to vary by age, sex, smoking status, and physical activity (Nimptsch et al., 2007). Unfortunately, most studies di not include independent measures of bone formation and resorption, and vitamin K status, which limits our ability to address the question of whether osteocalcin acts as a mediator or marker. Moreover, cohorts with different pathologies have often been included.

An important point is also the paucity of studies that have measured undercarboxylated osteocalcin critically considering possible relationships with the etiology of the pathologies of the population, and possible confounding factors. Ueland et al. observed a strongly increase in total and undercarboxylated osteocalcin levels in acromegalic patients when compared to healthy controls, but only total osteocalcin was a significant independent predictor of the HOMA-IR index (Ueland et al., 2010). Ferron et al. showed that patients with osteopetrosis had an increased ratio of undercarboxylated osteocalcin to carboyalated osteocalcin, accompanied by markedly low insulin levels (Ferron et al., 2010). Kanazawa et al. showed an increment of total osteocalcin by 90%, while undercarboxylated osteocalcin exhibited a non-significant rise of only 17% in 50 poorly controlled diabetics study during a month of intensified glycemic control (Kanazawa et al., 2009[a]). The same group has subsequently extensively described in diabetic patients

the previous data, overall showing total and undercarboxylated osteocalcin were inversely associated with fasting glucose and visceral fat, and positively with serum adiponectin level, parameters of insulin secretion, and its sensitivity in humans (Kanazawa et al., 2009[b]; Kanazawa et al., 2011[a]; Kanazawa et al., 2011[b]). Moreover, Kanazawa et al. showed an association between osteocalcin and atherosclerosis in diabetic patients (Kanazawa et al, 2009[b]), in agreement with the observation of Pietschnann et al. (Pietschnann et al., 1988). Our group showed that undercarboxylated osteocalcin to total osteocalcin ratio was negatively correlated to body mass index (ρ = .233; P $\leq$ .05) in a cohort of 83 patients; undercarboxylated osteocalcin was negatively correlated with waist circumference (ρ = .362; P $\leq$ .05) and fasting glucose (ρ = .430; P $\leq$ .05) in the overweight and obese group, suggesting the importance of the excess of the adipose tissue and the associated possible hypogonadsim (Foresta et al., 2010).

The poor association between undercarboxylated osteocalcin and glucose metabolism in humans contrasts with findings in mouse models. If osteocalcin, but not its undercarboxylated form, it is inversely correlated with glucose metabolism and adiposity in humans, and becomes important to discern if osteocalcin is mediating this effect or if it is an independent indication of an impaired osteoblast, as suggested by studies in an insulin-resistant rat model of diabetes mellitus (Hamann et al., 2011). However, the low number of studies that directly measured both the total and the undercarboxylated forms of osteocalcin, precludes forming conclusions regarding the importance of osteocalcin carboxylation in glucose metabolism. Similarly, very few studies used assays that measure the percentage of undercarboxylated osteocalcin, which would address any concern related to the strong correlation between total and undercarboxylated osteocalcin concentrations. Finally, it is likely that the association with osteocalcin in its different γ-carboxylated forms can differ between cohorts due to the different etiologies, but this observation also highlight the importance of other modulating co-factors.

Endogenous sex steroid hormones in metabolic and cardiovascular diseases

Testosterone (T) and other endogenous sex hormones are important signaling molecule in regulating energy metabolism. Testosterone is known to have a role in glucose homeostasis as well as obesity and lipid metabolism (Pi et al., 2010; Pi et Quarles, 2012[a]). This suggests that testosterone deficiency (i.e. hypogonadism) may contribute to the etiology of obesity, metabolic syndrome and its sequels, namely type 2 diabetes mellitus and other cardiovascular diseases. Low testosterone concentrations were associated with a higher incidence of type 2 diabetes mellitus in men, with the converse seen in women. A systematic review and meta-analysis including 36 cross-sectional and 7 prospective studies reported a significantly lower testosterone concentration in men with type 2 diabetes mellitus (-2.7 nmol/L, 95% CI -3.4 to -1.9 nmol/L). Men with a higher testosterone concentration (>15.6 nmol/L) had a 42% lower risk of type 2 diabetes mellitus (relative risk .58, 95%CI .39-.87) (Ding et al., 2006).

Epidemiological evidence associate additional biological significance to the principal transport protein for sex steroid hormones, the sex hormone binding globulin (SHBG). Low SHBG concentration were associated with increased risk of development of type 2 diabetes mellitus. Two genetic studies demonstrated an association between three SNPs, SHBG concentration and the incidence of type 2 diabetes mellitus, suggesting that the relationship between SHBG and the risk of developing diabetes may well be causal (Ding et al., 2006; Ding et al., 2009; Perry et al., 2010; Le et al., 2012).

Multiple factors and unraveled hormones may confound the association between endogenous sex hormones, energy metabolism and bone, including age, gender, obesity, body composition, osteocalcin, and risk factors of metabolic and cardiovascular diseases.
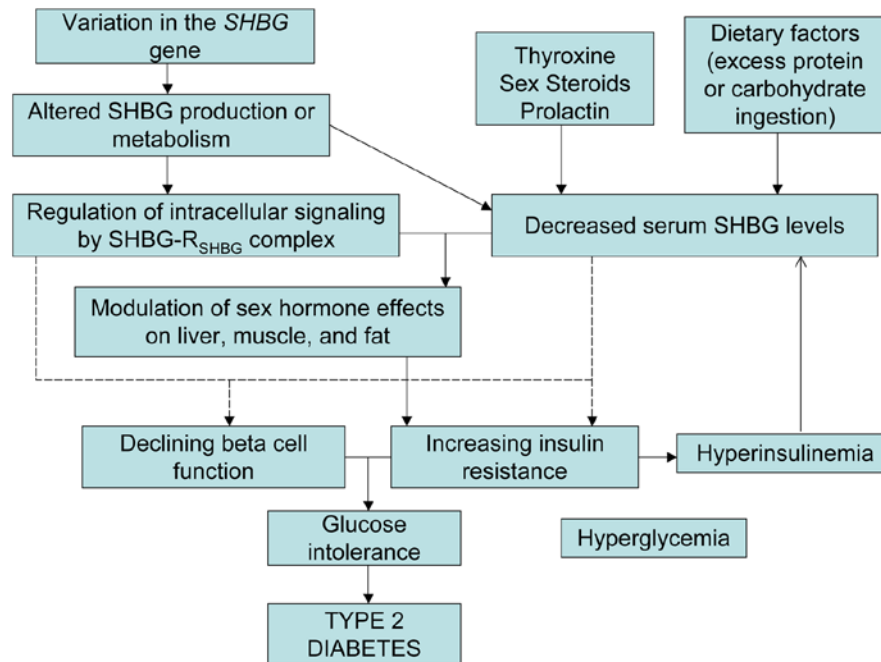
Figure 5. Potential mechanisms for the relationship between sex hormone binding globulin (SHBG) and type 2 diabetes mellitus. Alterations in SHBG may contribute to derangements in glucose homeostasis through modulation of sex hormone bioavailability. Recent findings also support a specific SHBG receptor, implying a more direct role of the protein in certain intracellular signaling pathways. Aside from influencing sex-steroid bioavailability, decreases in SHBG, either directly or via SHBG receptor activation, may have hypothetical effects (represented by dotted lines) that increase insulin resistance and reduce β cell function leading to glucose intolerance and ultimately overt diabetes. RSHBG, SHBG receptor. (modified from Le et al., 2012)

Osteocalcin and endogenous sex steroid hormones: a common receptor?

Osteocalcin and endogenous sex hormones appear to potentially share a common receptor, GPRC6A receptor.

GPRC6A appears to mediate the non-genomic effects of testosterone as evidence by the loss of the rapid signaling responses to testosterone administration in *Gprc6a*^{-/-} mice (Pi et al., 2010). Testosterone also has rapid effects on insulin secretion in β - cells (Grillo et al., 2005), which also appear to be mediated through activation of GPRC6A receptor (Pi et al., 2010). Thus, testosterone may have both effects on

insulin sensitivity as well as a direct effect on insulin secretion that are at least partially mediated via GPRC6A receptor (Pitteloud et al. 2005).

SHBG has an own receptor, but it has not been cloned yet. Hryb et al. showed that SHBG bound to human prostatic cell membranes with high specificity and affinity (Hryb et al., 1985). The specific binding of SHBG to cell membranes has been demonstrated in a limited number of tissues, including endometrium, breast cancer cells, normal breast, prostate, proximal convoluted tubule cells of the kidney, liver and epididymis (Rosner et al., 2010), thus making the interaction reasonably specific to tissues that are responsive to the steroids which bind to SHBG. SHBG receptor is thought to be a G protein-coupled receptor. Activation of the G protein-coupled second messenger system leads to release of cAMP and then to activation of protein kinase A (PKA) (Nakhla et al., 1999).

Osteocalcin from mouse to human

Overall, some translational data support the notion that osteocalcin activity is determined in humans in a similar way that in mice, highlighting the importance of the γ -carboxylation status of Glu residues for structure and function. Moreover, no molecule identified as a hormone in the mouse has lost this function in humans. However, the strength and reciprocity of the interactions and their physiological relevance in humans remain to be explored, clarifying the inconsistencies that has emerged from the current literature and the known physiology of the two different species.

We reported previously how human *Osteocalcin* is encoded by a single-copy gene. Mice have a cluster of three *Osteocalcin* genes in a 23 kb span oriented in the same transcriptional direction. Two of the genes (*Bglap* and *Bglap2*, also known as *OG1* and *OG2*) are expressed only in bone, while the third, the osteocalcin-related gene (*Bglap-rs1*, also known as *ORG*), is expressed at low levels in brain, lung and kidney, but not in bone (Desbois et al., 1994). Examination of the promoters of the human

and rat genes reveal that they are very similar with respect to the organization of regulatory elements and their response to hormones and growth factors, whereas the mouse gene exhibits differences, particularly in response to vitamin D3, the formers being dose-dependently up-regulated, whereas the latter being down-regulated (Kerner et al., 1989; Lian et al., 1989).

Esp is a pseudogene in humans (Cousin et al., 2004). Ferron et al., starting from the identification of the insulin receptor as a substrate of the phosphatase OST-PTP, hypotesized that tyrosine-protein phosphatase nonreceptor type 1 (PTN1, also known as PTP-1B, ubiquitously expressed) partially exerts in human the regulatory action of OST-PTP, being able to dephosphorylate insulin receptor. OST-PTP in mouse seem to regulate insulin signaling in osteoblasts, enhancing osteocalcin activity by promoting the ability of osteoblasts to enhance bone resorption and, indeed, potentially also in human the osteocalcin decarboxylation due to the previously described acid pH in the resorption lacuna (Silver et al., 1988; Ferron et al., 2010). Patients with a missense mutation in ClCN7, a gene required for acid secretion in the resorption lacuna (Schaller et al., 2005), and in others with a decrease of acidification ability of osteoclasts, circulating undercarboxylated osteocalcin was significantly decreased in all patients (Ferron et al., 2010). Zee et al. demonstrated that another tyrosine-protein phosphatase nonreceptor type 2 (PTN2, also known as TC‑PTP) also regulates insulin receptor phosphorylation in human osteoblasts and is, in fact, more highly expressed in bone than either OST-PTP or PTP-1B (Zee et al., 2012).

Neither mice osteocalcin cristallographyc structure nor human osteocalcin one have been resolved yet. Mouse and human and osteocalcin show extensive amino acid sequence homology in the region containing the three Glu residues (i.e. EXXXEXCEXXXXC motif), with a different length in total amino acids residues. Frazao et al. described possible differences between Gla residues in the 3-D structure of osteocalcin from different species (Frazao et al., 2005) (Figure 6).
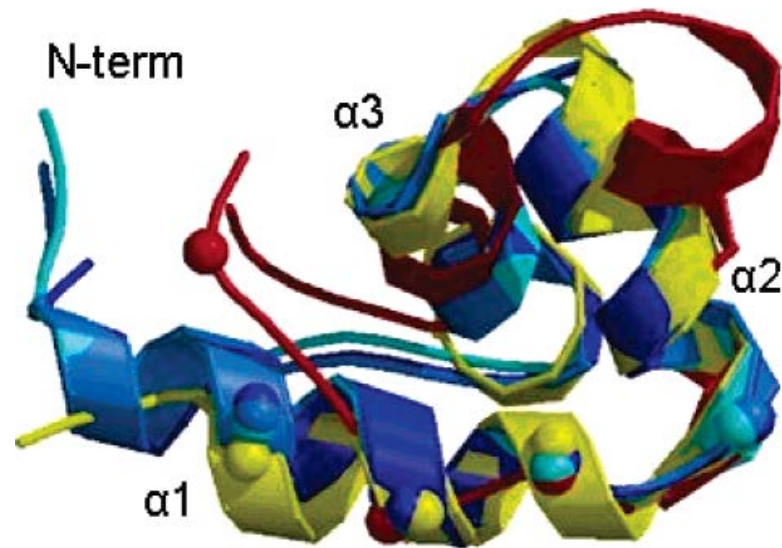
Figure 6. Cartoon representation of the superposition of different types of osteocalcin. *A. regius molecules* A (cyan), B (medium blue), and C (dark blue), with Gla residues positions represented as spheres, superpose clearly with the porcine structure (yellow), while the bovine structure (red) shows much less secondary structure and a poor match of Gla residues. (modified from Frazao et al., 2005)

Finally, adult mice do not express SHBG, whereas SHBG concentration have been associated in humans with increased incidence of type 2 diabetes (Ding et al., 2006), despite the exact nature has still to be elucidate. It is interesting to underline again that SHBG have a putative G protein-coupled receptor (Rosner et al., 2010), but the details of the molecular mechanism are not elucidated yet.

AIM of the STUDY

The use of mouse genetics recently highlighted coordination by endocrine regulation between bone, energy metabolism, and endogenous sex hormones. Osteocalcin, a bone matrix protein that regulates hydroxyapatite size and shape through its vitamin‑K-dependent γ‑carboxylated form, unraveled endocrinological functions in its circulating forms, that are not only simple markers of bone formation. In particular, recombinant undercarboxylated osteocalcin administration regulates gene expression not only in adipocytes, but also in pancreatic β cells and in Leydig cells in animal models, with a potential gender selectivity. Despite that circulating concentrations of osteocalcin in humans are inversely associated with measures of glucose metabolism, human data are inconclusive regarding the role of different γ-carboxylated forms of osteocalcin in energy metabolism and endogenous sex hormones. Most human studies do not differentiate between total and undercarboxylated forms of osteocalcin and do not take into account endogenous sex hormones, whose circulating concentration and tissue transport are regulate in a species-specific way in humans and mice. Intriguingly, the recently identified receptor of osteocalcin (i.e. GPRC6A receptor) is a G protein-coupled receptor that mediates also the non-genomic effects of androgens and, although the information about SHBG-receptor structure is not conclusive, evidence seems to suggest that a G protein-coupled receptor is involved.

Computational prediction   Experimental validation
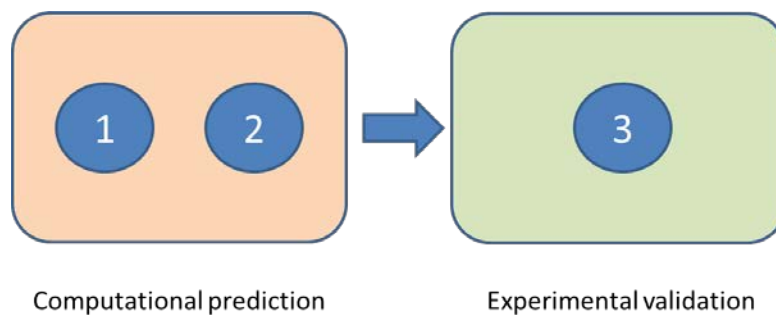
Figure 7. Two-step approach to human osteocalcin physiology and unraveled endocrinological functions.

Starting from clinical observations, we investigated the protein-protein interaction computational predictors of osteocalcin and SHBG with GPRC6A receptor, and we validated experimentally in vitro in a two-step approach (Figure 7).

In particular, due to the lack of data about osteocalcin γ-carboxylated forms, we focused on the determinants of osteocalcin structure between its carboxylated and uncarboxylated forms, and the effects of Ca^{2+} binding.

MATERIALS and METHODS

Study subjects

The study groups consisted of 63 male patients with obesity (BMI ≥ 25 kg/m^2), referred to the Obesity Clinic of the University of Padova, and 28 age male healthy controls (BMI ≥ 18.5–24.9 kg/m^2) consecutively recruited. Nobody had hepatic or renal failure. All subjects were free from drugs known to influence bone and calcium metabolism (e.g. steroids, vitamin D and K, calcitonin, bisphosphonates, and thiazolidinediones). All patients underwent physical examination, including anthropometric and blood pressure measurement, and a venous blood sample was collected after overnight fasting and stored at -80 °C after plasma separation. Our institutional review board approved this study and each participant provided informed consent. The investigation was conformed to the principles of the Declaration of Helsinki.

Biochemical markers measurements

Biochemical markers were measured by standard methods. Total testosterone and estradiol were measured by a commercial electrochemiluminescence immunoassay (Elecsys 2010, Roche Diagnostics, Mannheim, Germany). SHBG was measured by chemiluminescence assay (Immulite 2000, Siemens, Milano, Italy). The interassay coefficient of variation (CV) was below 10%.

The value of free T was estimated by calculation from total T and SHBG concentrations, which is comparable to free T concentration obtained by equilibrium dialysis, except in pregnancy (Vermeulen et al., 1999). Apart from albumin, the only other protein that binds T is SHBG. As the binding of other steroid hormones normally present in plasma can be omitted from the calculation (Vermeulen, 1973), it follows: free T = ([T] - (N x [FT]))/(K_t{SHBG x [T] + N[FT]}) (Eq IV), where K_t is the

association constant of SHBG for T, and N = K_aC_a + 1. This yields a second degree equation that can be solved either for free T or SHBG (Vermeulen et al., 1999).

Carboxylated and undercarboylated osteocalcin were measured in blood serum by enzyme-linked immunosorbent assay (ELISA) according to the manufacturer's instruction (Takara, Basel, Switzerland). The detection limits of the kit for carboxylated osteocalcin were 0.5-16 ng/ml. Inter-assay CV for this kit were 1% and 2.4% for 12.10 and 0.62 ng/ml cOC, respectively, and the intra-assay CV were 3.3% and 4.8% for 12 and 0.60 ng/ml, respectively. The detection limits of the kit for undercarboxylated osteocalcin were 0.25–8 ng/ml. Inter-assay CV for this kit was 5.67% and 9.87% for 6.47 and 0.69 ng/ml for ucOCN, and the intra-assay CV were 4.6% and 6.7% for 6.87 and 0.79 ng/ml, respectively. Total osteocalcin was estimated as the sum of the carboxylated osteocalcin and undercarboxylated forms of osteocalcin. ucOC/OC ratio was used as one of the parameters.

Others biochemical markers, including fasting blood glucose, insulin, C-peptide, and leptin, were measured by standard biochemical methods. All measurements were performed in duplicate.

Protein sequence alignment analysis

It has been postulated that the native tertiary structure of a given protein is determined solely by the protein's amino acid sequence in a given environment (Anfinsen, 1973), and that proteins with similar sequences adopt similar structures (Chothia et Lesk, 1986). Conserved structural domains can originate from sequences with less than 12% sequence identity (Holm et Sander, 1996; Hubbard et al., 1997; Rost, 1999). Thereafter, comparative methodology started form an approach involving a primary structure alignment through NW-align algorithm.

NW-align (http://zhanglab.ccmb.med.umich.edu/NW-align/) is a simple and robust alignment program based on the standard Needleman-Wunsch dynamic programming algorithm for the prediction of homologue surface motives and

clusters of amino acids, owning to protein predicted interactions (Needleman et Wunsch, 1970). An alignment of two sequences is represented by three lines. The first line shows the first sequence, and the third line shows the second sequence. The second line has a row of symbols. The symbol is a vertical linking simbol where ever characters in the two sequences match, and a space where ever they do not. Dots may be inserted in either sequence to represent gaps.

The algorithm was applied between SHBG and osteocalcin, whose primary sequences were obtained from UniPROTKB/Swiss-Prot (O'Donovan et al., 2002; Bairoch et al., 2004). In particular, sequence of osteocalcin precursor (UniProtKB/Swiss-Prot entry P02818.2) were:

MRALTLLALLALAALCIAGQAGAKPSGAESSKGAAFVSKQEGSEVVKRPRRYLYQWLGAPVPYPDPLEP
RREVCELNPDCDELADHIGFQEAYRRFYGPV

and sequence of SHBG precursor (UniProtKB/Swiss-Prot entry P04278.2) was:

MESRGPLATSRLLLLLLLLLLRHTRQGWALRPVLPTQSAHDPPAVHLSNGPGQEPIAVMTFDLTKITKTSS
SFEVRTWDPEGVIFYGDTNPKDDWFMLGLRDGRPEIQLHNHWAQLTVGAGPRLDDGRWHQVEVKMEG
DSVLLEVDGEEVLRLRQVSGPLTSKRHPIMRIALGGLLFPASNLRLPLVPALDGCLRRDSWLDKQAEISAS
APTSLRSCDVESNPGIFLPPGTQAEFNLRDIPQPHAEPWAFSLDLGLKQAAGSGHLLALGTPENPSWLSLH
LQDQKVVLSSGSGPGLDLPLVLGLPLQLKLSMSRVVLSQGSKMKALALPPLGLAPLLNLWAKPQGRLFL
GALPGEDSSTSFCLNGLWAQGQRLDVDQALNRSHEIWTHSCPQSPGNGTDASH

3-D protein structure alignment analysis

An approach with four different algorithms for three dimensional (3-D) alignments was used to recognize possible alignments between the query and the target structures, based on different criteria (Figure 8).
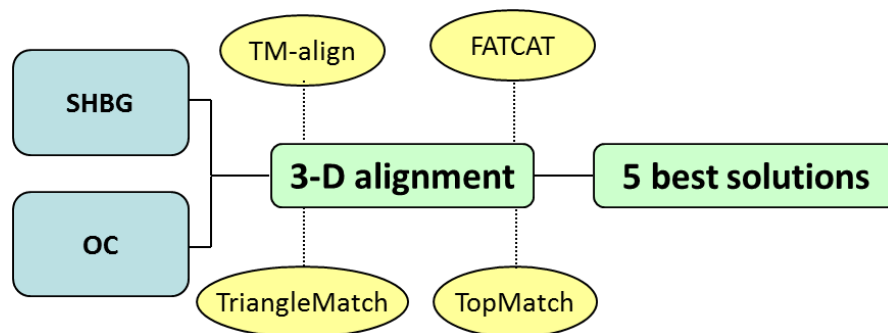
Figure 8. 3-D protein structure alignment analysis workflow between SHBG and osteocalcin (OC).

TM-align (http://bioinformatics.buffalo.edu/TM-align) is a structural alignment algorithm to identify the best structural alignment between protein pairs that combines the TM-score rotation matrix and Dynamic Programming (DP) (Zhang et Skolnick, 2005). The TM-score, in particular, (Zhang et Skolnick, 2004) weights the residue pairs at smaller distances relatively stronger than those at larger distances, exploiting a variation of Levitt–Gerstein (LG) weight factor (Levitt et Gerstein, 1998), implementing the root-mean-square deviation (RMSD). An optimal alignment between two proteins, as well as the TM-score value, will be reported for each comparison. TM-align can be used to match the predicted models for solved non-homologous proteins in the Protein Data Bank (PDB). For both folded and mis-folded models, TM-align can almost always find close structural analogs, with an average RMSD of 3 Å and 87% alignment coverage, whose data are given in the final output. The value of TM-score lies in between 0 to 1. In general, a comparison of TM-score < 0.2 indicates that there is no similarity between two structures; a TM-score > 0.5 means the structures share the same fold.

Flexible structure AlignmenT by Chaining Aligned Fragment Pairs (FATCAT, http://fatcat.burnham.org/) is a an algorithm that allows structural alignment of proteins, simultaneously addressing the two major goals of flexible structure alignment: (i) optimizing the alignment and (ii) minimizing the number of rigid-body movements (twists) around pivot points (hinges) introduced in the reference protein (Ye et Godzik, 2003). Therefore, it avoids the problem of existing flexible structure alignment programs that separate these two goals, such as introducing too many hinges into the alignment or missing the optimal alignment because of significant errors in the initial rigid-body alignment of structure obtained by X-ray crystallography. In particular, the structure alignment is formulated as the AFPs chaining process allowing at most t twists, and the flexible structure alignment is transformed into a rigid structure alignment when t is forced to be 0. Moreover, a dynamic programming is used to find the optimal chaining. A final chaining score is

given, including information regarding RMSD (dk), length (L), mis-matched regions (p) and/or gaps (q), and the required number of twists T(k).

TriangleMatch (http://bioinfo3d.cs.tau.ac.il/TriangleMatchBeta/index.html) is an algorithm designed to find non-topographical, sequence independent similarities between protein structural motifs, suitable for quick scanning of structural data bases (Nussinov et Wolson, 1991). The method is truly 3-D, sequence-order independent, and thus insensitive to gaps, insertions, or deletions. This algorithm is based on the geometric hashing paradigm, which allows the program to find structural matches that are independent of the amino-acid reside sequence. The algorithm used finds, in particular, pairs of sub-structures from the two proteins that after under-going a rigid transformation will give the largest match possible. The algorithm uses protein structures, atomic labels, and the respective 3-D coordinates; protein's backbones are structurally compared using their Cα atoms coordinates. A set of high scoring conformations, whose P value is based on results of an all-against-all matching of superfamilies representatives, is output and the user may view these conformations in a PDB file viewer. The number of best matches can be set and are shown by score, and secondarily by RMSD.

TopMatch (http://services.came.sbg.ac.at) is not only a computational algorithm for protein structure alignment, but also for the visualization of structural similarities, and for highlighting relationships found in protein classifications (Sippl et Wiederstein, 2008). Given a pair of protein structures, TopMatch calculates a ranked list of alignments based on the computing of a sequence score using a structure derived substitution matrix (Prlic et al., 2000). The alignments are characterized by a small set of parameters, including again the length of an alignment and the absolute similarity $S(q,t)$. Additional useful parameters are the root-mean-square error of superposition (RMES), percentage of sequence identity (Identity), the relative similarity $s(q,t) = 100 \times 2S(q,t)/(L_q+L_t)$, and the relative query and target cover

defined as cq=100 x S(q,t)/L_q and ct=100x S(q,t)/L_t, respectively (here L_q and L_t are the respective sequence lengths).

Protein docking analysis

A computational prediction of the 3-D structures of molecular interactions was retrieved to produce structural predictions with atomic-level accuracy. The use of protein docking to distinguish binding versus non-binding proteins is based on docking scores (Wass et al., 2011). Protein docking analysis and detailed comparative analyses of the performance of different docking algorythms (Wang et al. 2003) demonstrate the dependence of docking accuracy on the conformational search methods, the quality of the protein-ligand potentials describing binding enthalpy, and the scoring methods for estimation of protein-ligand binding entropy.

Both osteocalcin and SHBG with the putative plasma membrane receptors in target tissues of osteocalcin (i.e. GPRC6A receptor), underwent to a molecular docking approach.

Sequence of GPRC6A receptor from Swiss-Prot database (UniProtKB/Swiss-Prot entry Q5T6X5.1) was:

MAFLIILITCFVIILATSQPCQTPDDFVAATSPGHIIIGGLFAIHEKMLSSEDSPRRPQIQECVGFEISVFLQTL
AMIHSIEMINNSTLLPGVKLGYEIYDTCTEVTVAMAATLRFLSKFNCSRETVEFKCDYSSYMPRVKAVIGS
GYSEITMAVSRMLNLQLMPQVGYESTAEILSDKIRFPSFLRTVPSDFHQIKAMAHLIQKSGWNWIGIITTD
DDYGRLALNTFIIQAEANNVCIAFKEVLPAFLSDNTIEVRINRTLKKIILEAQVNVIVVFLRQFHVFDLFNK
AIEMNINKMWIASDNWSTATKITTIPNVKKIGKVVGFAFRRGNISSFHSFLQNLHLLPSDSHKLLHEYAMH
LSACAYVKDTDLSQCIFNHSQRTLAYKANKAIERNFVMRNDFLWDYAEPGLIHSIQLAVFALGYAIRDLC
QARDCQNPNAFQPWELLGVLKNVTFTDGWNSFHFDAHGDLNTGYDVVLWKEINGHMTVTKMAEYDL
QNDVFIIPDQETKNEFRNLKQIQSKCSKECSPGQMKKTTRSQHICCYECQNCPENHYTNQTDMPHCLLCN
NKTHWAPVRSTMCFEKEVEYLNWNDSLAILLLILSLLGIIFVLVVGIIFTRNLNTPVVKSSGGLRVCYVILL
CHFLNFASTSFFIGEPQDFTCKTRQTMFGVSFTLCISCILTKSLKILLAFSFDPKLQKFLKCLYRPILIIFTCTG
IQVVICTLWLIFAAPTVEVNVSLPRVIILECEEGSILAFGTMLGYIAILAFICFIFAFKGKYENYNEAKFITFG
MLIYFIAWITFIPIYATTFGKYVPAVEIIVILISNYGILYCTFIPKCYVIICKQEINTKSAFLKMIYSYSSHSVSSI
ALSPASLDSMSGNVTMTNPSSSGKSATWQKSKDLQAQAFAHICRENATSVSKTLPRKRMSSI

Previous studies developed homology model of the trans-membrane bundle of GPRC6A receptor from the group-to-group alignment against the crystallized sequences of both β1 and rhodopsin as templates (Pi et al., 2010) using MOE

(Chemical Computing Group, Montreal, Canada) software. We chose an homology model for the isoform 1 of GPRC6A receptor form MODBASE database, developed on the crystallographic structure of a metabotropic glutamate receptor (mGluR-II3) (Pieper et al., 2004; Muto et al., 2007), due to Family identity reasons.

An approach with three different algorithms for 3D alignments for Protein docking analysis was used to recognize a possible relationships between the query and the target (Figure 9), according to the work-flow explained in the "3-D protein structure alignment analysis" section.
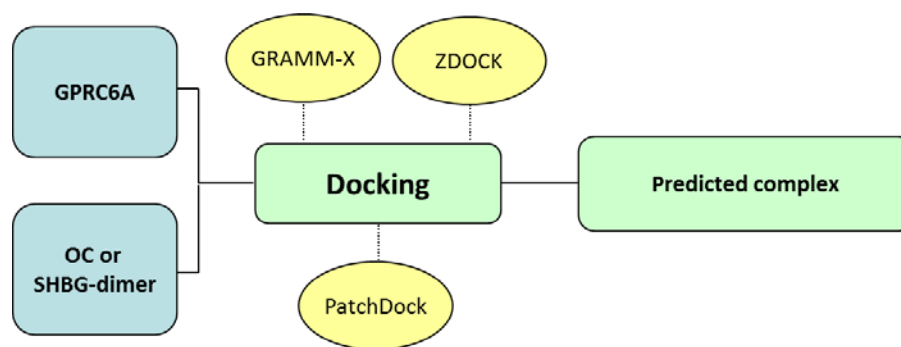
Figure 9. Protein docking analysis workflow between GPRC6A and SHBG/osteocalcin (OC).

GRAMM-X protein docking algorithm (http://vakser.bioinformatics.ku.edu/resources/gramm/grammx) is an extention of the original Global RAnge Molecular Matching (GRAMM) Fast Fourier Transformation (FFT) methodology (Tovchigrechk et Vakser, 2006). GRAMM-X requires only the atomic coordinates of the two molecules To predict the structure of a complex (no information about the binding sites is needed). The program performs an exhaustive 6-D search through the relative translations and rotations of the molecules. The quality of the prediction depends on the accuracy of the structures. The GRAMM methodology use an empirical approach to smoothing the intermolecular energy function by changing the range of the atom-atom potentials, locating the area of the global minimum of intermolecular energy for structures of different accuracy with a correlation technique based on the so called FFT

(Katchalski-Katzir et al., 1992). GRAMM-X has been implemented by employing smoothed potentials, refinement stage, and knowledge based scoring.

ZDOCK (http://zdock.umassmed.edu/) is a protein docking algorithm using FFT to perform a 3-D search of the spatial degrees of freedom between two proteins (Pierce et al., 2011). ZDOCK searches all possible binding modes in the translational and rotational space between the two proteins, and evaluates each by an energy scoring function, including shape complementarity, electrostatics, and a pairwise atomic statistical potential. In particular, utilizing a pairwise atomic potential, ZDOCK has notably gained in docking accuracy. Finally, the incorporation of the 3-D convolution library into ZDOCK, and the additionally modified ZDOCK to dynamically (e.g. optimal centering of the input proteins, rotation of the receptor, switching of the ligand and receptor) has oriented the input proteins for more efficient convolution. Interestingly, search speed is greatly increased by converting each protein's structure to a digital signal.

PatchDock (http://bioinfo3d.cs.tau.ac.il/PatchDock/patchdock.html) is a geometry-based molecular docking algorithm. It is aimed at finding docking transformations that yield good molecular shape complementarity (Schneidman-Duhovny et al. 2005). Such transformations, when applied, induce both wide interface areas and small amounts of steric clashes. A wide interface is ensured to include several matched local features of the docked molecules that have complementary characteristics. The PatchDock algorithm divides the Connolly dot surface representation of the molecules into concave, convex and flat patches (Stage I, Molecular Shape Representation) (Connolly, 1983). Thereafter, the complementary patches are matched in order to generate candidate transformations employing a hybrid of the Geometric Hashing and Pose-Clustering matching techniques (Stage II, Surface Patch Matching). Each candidate transformation is further evaluated by a scoring function that considers both geometric fit and atomic desolvation energy

(Stage III, Filtering and Scoring) (Zhang et al., 1997). Finally, an RMSD clustering is applied to the candidate solutions to discard redundant solutions.

The docking output analysis, presenting the series of top solutions of the predicted interactions between proteins, underwent to a comparative analysis between the frequencies of the predicted interfaces between SHBG and GPRC6A receptor, their spatial position in SHBG crystallographic structure and the similarity to osteocalcin, supported by PDBePISA (European Bioinformatics Institute[©]). PDBePISA (http://www.ebi.ac.uk/msd-srv/prot_int/) is an interactive tool for the exploration of macromolecular (protein, DNA/RNA and ligand) interfaces, prediction of probable quaternary structures (assemblies), database searches of structurally similar interfaces and assemblies, as well as searches on various assembly and PDB entry parameters.

Molecular modeling studies

Homology molecular modeling is a computational approach to predict the approximate tertiary structure (3-D) of a protein based on the known 3-D structure of a closely related protein.

The protein model is performed in four steps (Schwede et al. 2003), including:

1.   Structural template selection (at least one known protein structure protein);

2.   Alignment of template and target sequences;

3.   Model building (protein backbone assignment, placing and energy minimization of side-chain conformations);

4.   Model evaluation of protein geometry with respect to sterical hindrance, potential energy (dihedral angles, angles, bond-length and electrostatic interactions).

The structure of the human osteocalcin was carried out using a conventional homology modeling approach implemented in MOE (Chemical Computing Group, Montreal, Canada; version 2010.11) software (http://www.chemcomp.com) and

using porcine osteocalcin as a structural template, having 88% sequence identity with human osteocalcin (Protein Data Bank entry 1Q8H) (Hoang et al., 2003). Hydrogen atoms and electric charges were added using the "Protonate-3D" tool implemented in MOE. To minimize contacts among hydrogens, the structures were subjected to Amber94 force field minimization (Okur et al., 2003; Ponder et Case, 2003) until the *rms* of conjugate gradient was <0.1 kcal/mol/Å, keeping heavy atoms fixed at their crystallographic positions. Model quality was evaluated using the MOE Protein Geometry stereochemical quality evaluation tools.

Molecular dynamics studies

tLeap (Case et al., 2005) and Amber FF99SB (Hornak et al., 2006**)** were employed for the parametrization of the protein models osteocalcin in different γ-carboxylated forms. Gla residues were parameterized "from scratch" using molecular information from the available crystal structures, while Ca^{2+}-ions were parameterized as previously detailed (Bradbrook et al., 1998). The protein models were equilibrated in TIP3P water boxes and finally added counterions (e.g., Na^{+}) to assure the neutrality of the molecular systems. ClickMD-min script (Cristiani et al., 2011) was used as a molecular dynamic platform for minimizing Gla and Glu osteocalcin structures in Ca^{+2}-bound form. ClickMD-min uses NAMD 2.7b3 as MD engine and produced 100,000 steps of conjugated-gradient minimization using a 32 cores Intel Core2Quad Q9600 2.66Ghz. ClickMD-eq script was used for equilibrating the protein models and their solvatation systems (0.5 ns, Cα positional restrains), while ClickMD-prod was employed to simulate large-scale MD for 100 ns in osteocalcin systems in the presence of Ca^{2+} (100 ns NVT, P=1atm, T=300K). Analysis of trajectories was performed with VMD 1.8.7 (Humphrey et al., 1996**)**, RMSD Trajectory Tools 2.01 (http://physiology.med.cornell.edu/faculty/hweinstein/vmdplugins/rmsdtt/), RAINBOWRMSD and NRGPLOT (Cristiani et al., 2011).

Steered molecular dynamics studies

Steered molecular dynamics (SMD) was performed with YASARA (Krieger et al. 2002: Krieger et al., 2006) applying a constant pulling acceleration of 35,000 pm/ps^2 on the Ca^{2+} ions. The pulling direction of the acceleration is represented by the distance between the centre of mass of the protein and the respective ion. SMD simulations of 50 ps has been repeated three times after the assignment of different initial atom velocities to each molecular system, highlighting converging results.

Spectroscopic techniques

Human Gla osteocalcin and murine Glu osteocalcin were purchased form Bachem (Bachem AG, Bubendorf, Switzerland) and their purity and chemical identity was checked by reverse phase high-performance liquid chromatography (RP-HPLC) and mass spectrometry. An aliquot (20 µg) of osteocalcin was loaded onto a Vydac C18 column (4.6 × 250 mm, 5 µM) (Hesperia, CA, USA) eluted with an acetonitrile 0.078% TFA gradient from 20 to 60% in 30 min at the flow rate of 0.8 ml/min. Mass spectrometry analysis was carried out on a Mariner (PerSeptive Biosystems, Stafford, TX, USA) ESI-TOF spectrometer, yielding mass values in agreement with theoretical mass within 50 ppm accuracy. Binding of Ca^{2+} to Gla osteocalcin or Glu osteocalcin was studied by fluorescence and circular dichroism (CD) spectroscopy. Aliquots (2-50 µl) of a $CaCl_2$ stock solution (150 mM) were added under gentle magnetic stirring to a solution of OC (1.5 ml; 1 µM) in a 1-cm pathlength quartz cuvette for fluorescence measurements. All measurements were carried out in 20 mM Tris-HCl, pH 7.4, at 25 ± 0.2 °C on a Jasco (Tokyo, Japan) FP-6500 spectrofluorimeter equipped with a Peltier temperature control system ETC-273T. Samples were excited at 280 nm and the emission intensity was recorded at 344 nm, using an excitation emission slit of 5/10 nm. Each spectrum was the average of two accumulations after baseline subtraction.

Aliquots (2-50 µl) of a CaCl$_2$ stock solution (150 mM) were added under gentle magnetic stirring to a solution of OC (1.5 ml; 20 µg/ml) in a 1-cm pathlength cuvette for CD measurements. Ellipticity data (θ) at 220 nm are expressed as millidegrees without further normalization. All measurements were carried out in 20 mM Tris-HCl at pH 7.4 and 25 ± 0.2 °C on a J-810 spectropolarimeter equipped with a Peltier temperature control system PTC-423S. Each spectrum was the average of four accumulations, after base line subtraction. Data points were fitted using the equation:

$$\theta = \theta_0 + [\theta_{max} \cdot ([Ca^{+2}]/K_d)) / (1 + [Ca^{+2}]/K_d)$$

(eq. 1)

where θ$_0$ and θ$_{max}$ are the ellipticity values of OC in the absence and at saturating calcium concentration, respectively, and K$_d$ is the dissociation constant of the complex Ca^{2+}-osteocalcin.

Cell line HEK-293T

The human kidney cell line 293 was generated by transfection of adenovirus DNA into normal human embryonic kidney (HEK) cells (Graham et al., 1977), whereas the human kidney cell lines STt-4i (293T) were generated by transfection of HEK cells with plasmids encoding SV40 viral oncogene (Robinson et al., 1991). In the initial seed stock at the American Type Culture Collection, ATCC (Manassas, VA, USA), HEK293 was described as an hypotriploid human epithelial cell line. The modal chromosome number was 64, occurring in 30% of cells. The rate of cells with higher ploidies was 4.2%. The der(1)t(1;15) (q42;q13), der(19)t(3;19) (q12;q13), der(12)t(8;12) (q22;p13), and four other marker chromosomes were common to most cells. There were four copies of N17 and N22. Noticeably in addition to three copies of X chromosomes, there were paired Xq$^+$, and a single Xp$^+$ in most cells. However, cytogenetic instability has been reported in the literature for some cell lines.

HEK-293T were cultured in 75 cm^2 cell culture flasks with ATCC-formulated Dulbecco's Modified Eagle's Medium, adding fetal bovine serum to a final concentration of 10% and 10,000 µg/ml penicillin/streptomycin at pH 7.7 under an air/5% CO_2 mixture, as previously described (Aulestia et al., 2011).

RNA extraction, cDNA synthesis and RT-PCR

Total RNA was purified and extracted from cell pellets using the Qiagen RNeasy Mini Kit (Quiagen, Germantown, MD, USA). First strand cDNA synthesis from total RNA was catalyzed by SuperScript® III RT using random hexamers, including a deoxyribonuclease treatment according to the manufacturer protocol. All isolated RNA was quantified by spectrophotometry by determining the ratio of optical density at 260/280 nm, using a Nano-Drop® spectrophotometer (Wilmington, DE, USA).

Total cDNA was amplified by PCR using specific primers for each gene to verify cDNA presence and quality. As a negative control, cDNA was omitted.

The primers used to amplify various gene from HEK-293T cells were internally designed. The primers were *hGprc6a*_1 forward 5'-AAGACTCTCCCAGACGACCA-3' and reverse 5'-CTCAATGCTGTGTATCATGGC-3' (92 bp, exon spanning), *hGprc6a*_3 forward 5'- AAGACTCTCCCAGACGACCA-3' and reverse 5'-CATACCCCAGTTTGACTCCAG-3' (138 bp, exon spanning), and h*Gprc6a*_ART forward 5'-CAGGAGTGTGTTGGCTTTGA-3' and reverse 5'- AAAGCAATGGCTCACCTGAT-3' (428 bp, exon spanning). To control for intact RNA recovery and the uniform efficiency of each RT reaction *β-actin* was amplified by PCR using after primers, including forward 5'-CACTCTTCCAGCCTTCCTTCC-3' and reverse 5'-CGGACTCGTCATACTCCTGCT-3'.

The melting temperature was 60°C for all primer pairs. RT-PCR products were electrophoretically analyzed on 2% agarose gel and confirmed by direct sequencing.

Quantitative Real-Time PCR analysis

The products of the first strand cDNA synthesis were directly amplified by PCR using specific primers for GPRC6A gene to verify cDNA presence and quality. As a negative control, cDNA was omitted. GPRC6A expression was quantified by real-time PCR, using the Bio-Rad iQ™5 system according to manufacturer instructions with Power SYBR® Green PCR Master Mix. Amplification reactions were performed in a 20 µl final volume containing 10 µl Power SYBR Green PCR Master Mix, 1 µl primers (10 µM) and 4 µl (20 ng) cDNA from HEK-293 cells. Amplification was done for 40 cycles. After an initial hot start for 10 min each cycle consisted of 15 sec denaturation, 30 sec annealing at 60°C and 30 sec extension at 60°C.

To normalize the amount of expressed mRNA the internal housekeeping gene glyceraldehyde-3-phosphate dehydrogenase (primer forward 5'-AAGGTGAAGGTCGGAGTCAA-3' and reverse 5' AATGAAGGGGTCATTGATGG-3') was used and each cDNA product was tested in triplicate. To calculate data we used the comparative Ct method for relative quantification (ΔΔCt), which describes the change in expression of the target gene in the tested sample relative to a calibrator sample from a cDNA library and provides accurate comparison between the initial level of template in each sample (Livak et Schmittgen, 2001). Data were analyzed with Bio-Rad iQ™5.

End-point PCR analysis

An end-point PCR reaction was performed. The PCR mixture consisted of 2,5 µL TaqGold Buffer 10X without $MgCl_2$, 1,5 µL $MgCl_2$ (50 mM), 1 µl dNTPs (10 mM), 20 pmol of each primer, 0,2 µL TaqGold enzyme, sterile H_2O in a final volume of 25 µL and 4 µl (20 ng) cDNA from HEK-293T cells. The amplification program was as follows: denaturing at 94°C for 10 min, 40 cycles each at 94°C for 1 min, annealing at 56°C for 1 min and extension at 72°C for 1 min, followed by a final extension at 72°C

for 10 min. The amplification products were analyzed by staining with SYBR safe DNA gel stain, after electrophoresis on 1% agarose gel.

Flow cytometry analysis

About 16 hr before the beginning of an experiment, cells were starved in serum-free medium. Thereafter, cells were detached mechanically with a scraper (UltraCruz™ Cell Scrapers, sc-213229, Santa-Cruz Biotechnology), providing uniform contact with all growth surfaces to ensure efficiency and to minimize mechanical strain. All sample were rinsed once with PBS + BSA 5%, suspended in serum-free medium, and splitted into different tubes. Each sample was incubated for 1 h at room temperature according to the different experimental conditions (see "Cell-surface receptor binding assays" section). Thereafter, all samples were fixed in 4% paraformaldehyde (Sigma-Aldrich, St. Louis, MO, USA) in PBS for 15 min and rinsed in PBS + BSA 5%. All samples were then incubated for staining-procedure with a goat anti-OC polyclonal antibody (1:100; sc-18319, Santa-Cruz Biotechnology) or a goat anti-SHBG polyclonal antibody (1:100; sc-32467, Santa-Cruz Biotechnology) for 15 min at room temperature. Primary immunoreaction was properly detected by the use an anti-goat biotinylated secondary antibody (1:200; Dako Italia) for 15 min at room temperature and, successively, after rinsed in PBS + BSA 5%, with a streptavidina/FITC-conjugated tertiary reagent (1:200; DBA Italia) for other 15 min at room temperature. Multiple biotinylated secondary antibodies molecules can be conjugated to a protein of interest, which allows binding of multiple streptavidin-coniugated reagents, increasing the sensitivity of detection of the protein of interest. Samples were finally analyzed with the FACScan flowcytometer (BD Biosciences, San Jose, CA, USA) and 10,000-15,000 events gated in the region of the specific cell type were acquired (Figure 10). The value of fluorescence intensity subtending the highest 1% of the untreated control curve was considered as the threshold for quantification of specific agonist binding (Oury et al., 2011).
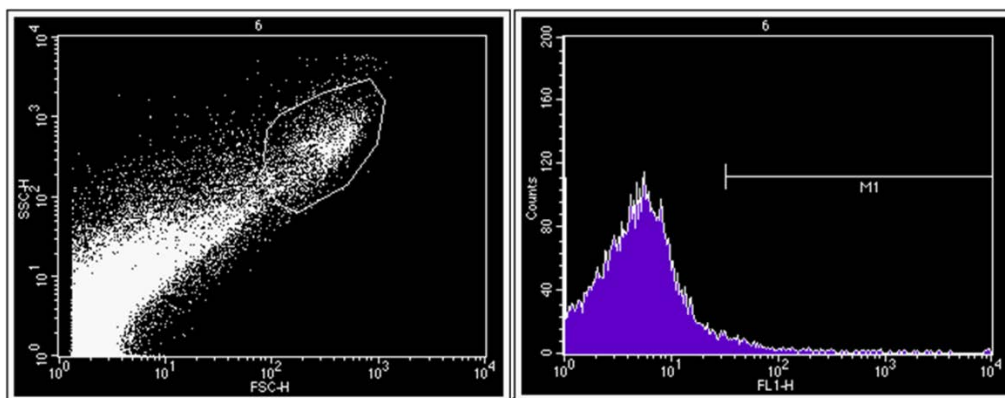
Figure 10. Flow cytometry analysis on HEK-293T cells. Morphological gate (left panel) and establishment of value of fluorescence intensity subtending the highest 1% of the untreated control curve (right panel), as threshold for quantification analysis of specific agonist binding.

Immunofluorescence assays

Cells were cultured in a 8-well flat-bottomed microculture dish as previously described in the "Cell line HEK-293T" section. About 16 hr before the beginning of an experiment, cells were rinsed once with PBS + BSA 5% and starved in the same condition described in the "Flow cytometry analysis" section. Thereafter, all sample were rinsed with PBS + BSA 5% and incubated for two hours at room temperature according to the different experimental conditions. The samples were fixed in 4% paraformaldehyde (Sigma-Aldrich) in PBS for 15 min at room temperature and rinses in PBS + BSA 5%. All samples were then treated for staining-procedure by co-incubation with the respective primary antibody (1:100) (see "Cell-surface receptor binding assays" section). Primary immunoreaction were detected as previously described.

Finally, samples were counterstained with 40,6-diamidino-2- phenylindole (DAPI, 1:10,000; Boehringer), mounted on microscope slides with antifade buffer, and analyzed by laser confocal microscopy VICO fluorescence microscope (Nikon, Firenze, Italy).

Cell-surface receptor binding assays

A single concentration of ligand (usually an agonist) was used in every assay tube. The ligand (e.g. undercarboylated osteocalcin) was used at a low concentration, usually at or below its dissociation constant (K_d) value. The level of specific binding of the ligand (e.g. undercarboylated osteocalcin) was then determined in the presence of other competing compounds (e.g. SHBG), in order to determine the specificity with which they competed for the binding of the previous ligand. In order to verify the working hypothesis, the samples underwent to the following experimental conditions (Table 3):

Sample (1h at room temperature)
Medium without serum
SHBG 73,7ng/mL
ucOC 10ng/mL
ucOC 10ng/mL + SHBG 50-fold [cOC]
cOC 10ng/mL
cOC 10ng/mL + SHBG 50-fold [cOC]

Table 3. Cell-surface receptor binding assays. Different experimental conditions. The concentration of SHBG is equimolar to osteocalcin. cOC, carboylated osteocalcin; ucOC, undercarboylated osteocalcin; SHBG, sex-hormone binding globulin.

A group of samples were pre-treated for 30 min at room temperature with a rabbit anti-hGPRC6A polyclonal antibody (H-68, sc-67302; Santa-Cruz Biotechnology) in an oversaturating concentration in order to better assess the specificity of the binding. hGPRC6A antibody raised against an epitope corresponding to amino acids 343-410 mapping within an extracellular domain of GPRC6A receptor of human origin. hGPRC6A antibody was recommended for detection of GPRC6A receptor of human origin by western blot, immunofluorescence, and ELISA assays.

A preparatory phase, in order to titolate the optimal concentration of the different reagents balancing specificity and sensitivity, was performed.

STATISTICAL ANALYSIS

All statistics were performed using SPSS software (version 19.0; SPSS Inc. Chicago, IL, USA) and R software (version 2.11.0; Free Software Foundation, Auckland, CA, USA). Comparisons between biochemical markers and clinical variables were made using Mann-Whitney U and Kruskall-Wallis non parametric tests across groups. Relationships between continuous markers and variables were assessed using nonparametric Spearman's ρ correlation test. A multiple regression model using the ucOC/OC ratio as the dependent variable adjusted for presence of diabetes was performed. Variables are given as mean ± standard error of the mean (SEM), except when otherwise indicated.

A multivariate clustering analysis on 3-D protein structure alignment analysis outputs was performed. Cluster analysis is a major technique for classifying a 'mountain' of information into manageable meaningful piles. It is a data reduction tool that creates subgroups that are more manageable than individual datum. Like factor analysis, it examines the full complement of inter-relationships between variables. Each alignment (of the 3-D protein structure alignment analysis) was a point in the ideal 188 dimensions space (one for each amino acid) of SHBG amino acid residues to which the different osteocalcin models were compared. One case was the output of an algorithm, having categorized each amino acid as a nominal variable in accordance to the similarity to osteocalcin (0 not comparable; 1 comparable).

Comparison of experimental data was done by the unpaired 2-tailed Student t test after acceptance of normal distribution with the Kolmogorov-Smirnov test. Data are shown as the mean ± standard deviation of the mean (SD). All experiments were performed in triplicate, except when otherwise indicated. The significance level was set as P value < .05.

RESULTS

Clinical and biochemical characteristics of the patients

Seventeen patients were overweight (19%, BMI = 25.0-29.9 kg/m^2), 21 class I-II obese (23%, BMI = 30.0-39.9 kg/m^2), and 25 class III obese (27%, BMI ≥ 40.0 kg/m^2) according to the WHO-recommended classification for BMI (WHO, 2000).

Differences between clinical and biochemical characteristics among all groups, overweight and obese patients (BMI ≥ 25.0 kg/m^2) vs. healthy controls are showed in the table (Table 4). Body weight (data not shown), BMI, systolic and diastolic blood pressure (data not shown), leptin, total and free T, SHBG, E, ucOC, and ucOC/OC ratio were different between all groups, whereas there were no differences in body height (data not shown), total OC, and cOC across groups. Within each group, patients with diagnosis of diabetes were as follows: 1/17 (5.9%) in overweight patients, 1/21 (4.8%) in class I-II obese patients and 4/25 (16%) in class III obese patients.

Free T was negatively correlated to BMI (ρ = -.71, P < .05) and positively correlated to ucOC/OC ratio (ρ = .22, P < .05) in the whole cohort, but no correlation was found with cOC (ρ = .11) and ucOC (ρ = .19). The positive correlation between free T and ucOC/OC ratio was not significantly influenced by the presence of diabetes through a multiple regression model (P = 0.12 using Fisher's test comparing the simple model, without inclusion of diabetes as independent variable, β = .20 and SE = .12, to the multiple model, including diabetes, β = .23 and SE = .12). There was no correlation between either total T or SHBG and cOC (ρ = -.066 and -.51, respectively), ucOC (ρ = .18 and .04, respectively) or ucOC/OC ratio (ρ = .19 and .02, respectively). There was no significant correlation between E and ucOC or E and ucOC/OC ratio (ρ = -18 and -15, respectively). Leptin was negatively correlated to total T (β = -.68, P < .001), free T (β = -.60, P < .001) and SHBG (β = -.51, P < .001),

and positively with E (β = .47, P < .001), but we could not find any correlation between leptin and osteocalcin in different γ-carboxylated forms.

	Group 1 normal (n=28)	Group 2 overweight (n=17)	Group 3 cl. I-II obese (n=21)	Group 4 cl. III obese (n=25)	among all groups (P value)	Group 2+3+4 (BMI ≥ 25) (n=63)	Group 1 vs. Group 2+3+4 (P value)
Age (years)	39.0 ± 1.2	42.3 ± 1.5	41.5 ± 2.7	45.2 ± 2.3	.099	43.2 ± 1.4	**.029**
BMI (kg/m²)	23.5 ± .3	26.5 ± .3	34.1 ± .7	49.3 ± 1.8	**< .001**	38.1 ± 1.4	**< .001**
Leptin (pmol/L)	199 ± 35	254 ± 55	656 ± 96	1438 ± 101	**< .001**	848 ± 85	**< .001**
Total T (nmol/L)	19.74 ± .83	16.68 ± 1.34	12.99 ± .98	8.59 ± .67	**< .001**	12.23 ± .69	**< .001**
Free T (nmol/L)	.44 ± .02	.41 ± .03	.32 ± .02	.22 ± .02	**< .001**	.30 ± .02	**< .001**
SHBG (nmol/L)	31.6 ± 1.59	24.37 ± 1.94	23.20 ± 2.57	19.71 ± 1.63	**< .001**	22.13 ± 1.2	**< .001**
E (nmol/L)	65.51 ± 4.93	79.27 ± 8.47	97.77 ± 10.45	113.79 ± 7.36	**< .001**	99.13 ± 5.31	**< .001**
cOC (ng/mL)	8.26 ± .6	8.1 ± .97	8.41 ± .87	9.66 ± 1.16	.885	8.82 ± .60	.897
ucOC (ng/mL)	3.78 ± .43	2.72 ± .59	3.68 ± .72	2.02 ± .22	**.028**	2.75 ± .33	**.016**
OC (ng/mL)	12.04 ± .85	10.82 ± 1.34	12.09 ± 1.25	11.68 ± 1.22	.549	11.58 ± .73	.593
ucOC/OC ratio	.31 ± .02	.24 ± .03	.27 ± .04	.20 ± .02	**.022**	.23 ± .02	**.013**

Table 4. Cross sectional clinical and biochemical data of 63 obese and overweight patients (Group 2, 3, and 4) vs. 28 healty controls. BMI, body mass index; cl, class; cOC, carboxylated osteocalcin; SHBG, sex-hormone binding globulin; T, testosterone; E, 17-β-estradiol; OC, total osteocalcin; ucOC, undercarboxylated osteocalcin. Values are shown as means ± standard error of the mean (SEM). Significantly staoistical results (P < .05) are in bold.

Osteocalcin and SHBG sequence alignment analysis

Sequence alignment between template sequences SHBG (170 aa, first line) and OC (49 aa, third line) showed an alignment length of 48 amino acid residues, with an identical length of 11 and a sequence identity of 22.9% (Figure 11).

```
SHBG  -PPAVHLSNGPGQEPIAVMTFDLTKITKTSSSFEVRTWDPEGVIFYGDTNP
                                     :      :           :
OC    Y------------------------------LYQWLGAPVPYPDPLEP
      12345678901234567890123456789012345678901234567890 1
             21        31        41        51        61


      KDDWFMLGLRDGRPEIQLHNHWAQLTVGAGPRLDDGRWHQVEVKMEGDSVL
                   :  :                        :      :
      -----------RREV--------------------CELNPDCDELA
      2345678901234567890123456789012345678901234567890 12


      LEVDGEEVLRLRQVSGHPIMRIALGGLLFPASNLRLPLVPALDGCLRRDSWL
           :   :      :  :
      DHIGFQEAYR--RFYG-PV--------------------------------
      34567890123456789012345678901234567890123456789012 34


      DKQAEISASAPTSLRSC

      -----------------
      56789012345678901
```

Figure 11. Sequence alignments of SHBG (first line) and osteocalcin (third line) with NW-align. Amino acid residues are classified with the one-letter code.

Crystallographic structure of osteocalcin and SHBG

The electronic database of Medline was searched via Structure with the search terms (osteocalcin [All Fields]) and (OCN [All Fields]) and (OC [All Fields]), or (sex hormone binding protein [All Fields]) and (SHBG [All Fields]). Additional hand searching of articles, reference texts and reference lists was also performed. From a total of 54 and 42 retrieved citations, respectively 0 and 6 results were classified as relevant and were subjected to full review.

Despite no article depicted the crystallographic structure of SHBG alone (Table 5), SHBG in complex with dihydrotestosterone (DHT) was chosen, representing the endogenous ligand that binds with the greater affinity to SHBG (K_D 5.5 10^9 M^{-1}), to

undergo to analysis of 3-D protein alignments analysis with human osteocalcin. The crystallographic structure of SHBG in complex with DHT was retrieved from the Protein Data Bank (PDB code entry 1D2S).

PDB code	Description	Reference
1D2S	SHBG in complex with **dihydrotestosterone**	Grishkovskaya et al. 2000
1LHU	SHBG in complex with **estradiol**	Grishkovskaya et al. 2002[a]
1LHV	SHBG in complex with **norgestrel**	Grishkovskaya et al. 2002[a]
1LHW	SHBG in complex with **2-methoxyestradiol**	Avvakumov et al. 2002
1LHN	SHBG in complex with **5α-androstane-3β,17α-diol**	Grishkovskaya et al. 2002
1LHO	SHBG in complex with **5α-androstane-3β,17β-diol**	Grishkovskaya et al. 2002
1F5F	SHBG in complex with **zinc**	Avvakumov et al. 2000
1KDK	SHBG in crystals soaked with EDTA	Grishkovskaya et al. 2002[b]
1F5F	SHBG (tetragonal crystal form)	Grishkovskaya et al. 2002[b]

Table 5. Crystallographic structure of SHBG in PDB (last update February, the 1st 2012). EDTA, ethylenediaminetetraacetic acid; PDB, Protein Data Bank; SHBG, sex hormone binding globulin.

Human osteocalcin homology modeling

The homology model of human osteocalcin was built starting from the crystallographic structure of porcine osteocalcin (PDB code: 1Q8H) (Hoang et al., 2003). Due to the high conformational flexibility of the N-terminal in the template structure, only the amino acid residues from Pro13 to Val49 could be modelled. The resulting human osteocalcin model displayed three α-helices H1(Asp14-Leu25), H2(Asp28-Ile36), and H3(Gln39-Tyr46), stabilised by numerous HB involving Asp14, Gla17 and Arg20 in α-helix H1, Glu31 and His35 in α-helix H2, and Glu40 and Arg43 in α-helix H3. The orientation of α-helices H1 and H2 was locked by a disulphide bridge between Cys23 and Cys29 in the protein core. A distinctive structural feature of human osteocalcin entailed the asymmetric distribution of positive and negative

amino acids within the model structure (Figure 12). A wide negatively charged surface (in red) was generated by clustering of acidic amino acids in α-helices H1 (Gla17, Gla21 and Gla24) and H2 (Asp28, Asp30, and Asp34), whereas a few positively charged amino acids (Arg19, Arg43 and Arg44) were located on the opposite face of the protein (in blue).
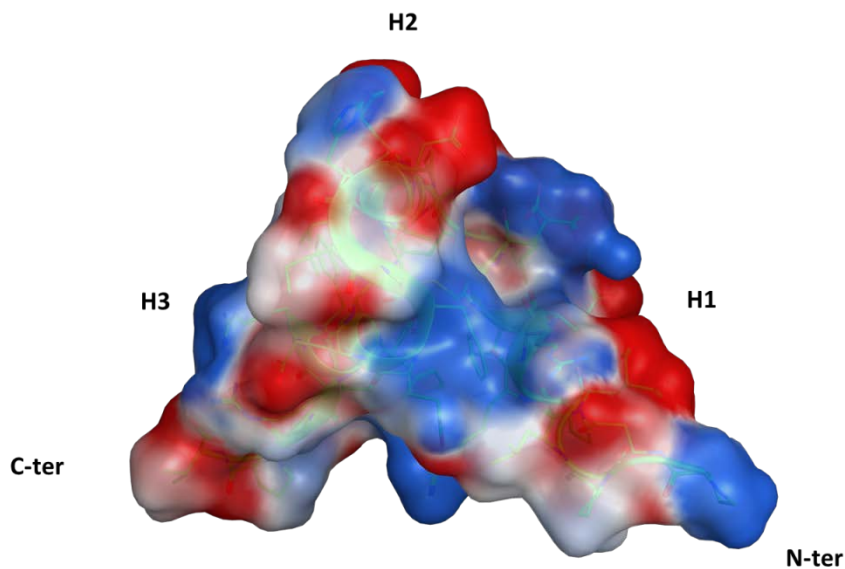
Figure 12. Surface electrostatic distribution on Gla osteocalcin. The charge distribution on the surface of molecule is shown. The concentration of acidic residues near the convergence of α-helices H1 and H2 produces a localized, highly negative surface region (in red) suited for coupling with cations. This suggests that in bone the protein may associate with Ca^{2+} on the bone mineral surface. C-ter, C-terminal; H, α-helix; N-ter, N-terminal; blue colour, positively charged surface region; red colour, negatively charged surface region.

The clustering of negative amino acids in Gla osteocalcin is suited for coupling with cations, represented by the three Ca^{2+} ions (Figure 13).
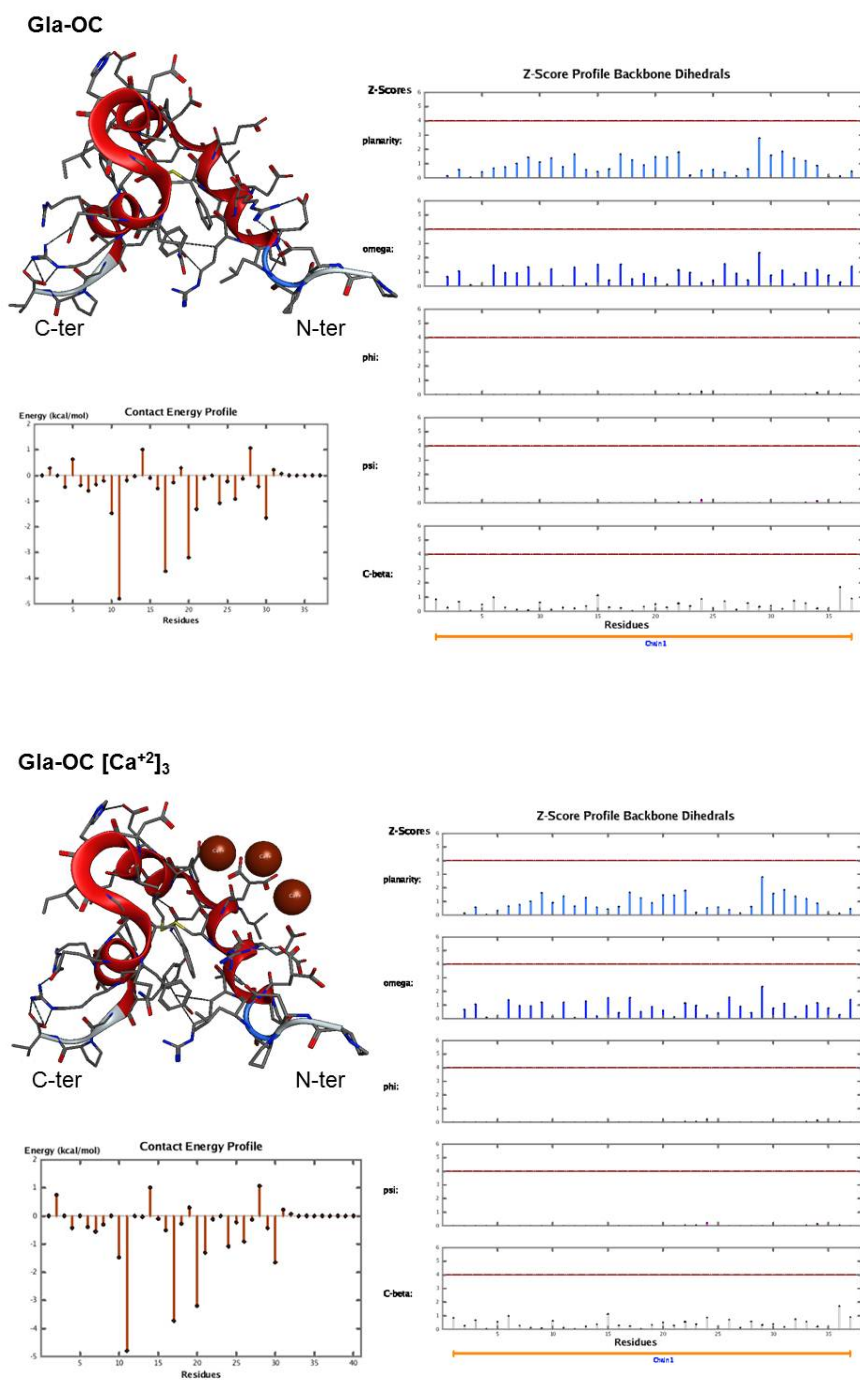
Figure 13. 3-D structure of Gla osteocalcin (upper panel, un-complexed with Ca^{2+}; lower panel, complexed with Ca^{2+}) and the model validation through MOE version 2010.11 suite. Contact energy profile and the Z-Score of the protein backbone dihedrals have been evaluated, being the red line the maximum limit accepted. C-ter, C-terminal; N-ter, N-terminal; OC, osteocalcin.

Molecular dynamics simulations and Ca^{2+} binding of osteocalcin

Classical molecular dynamics (MD) simulations were performed on osteocalcin containing three Gla residues at position 17, 21 and 24 (Gla-OC) and in osteocalcin in which all Gla residues were replaced by Glu residues (Glu-OC).

Gla osteocalcin (Gla17/Gla21/Gla24). Gla osteocalcin model, as described in the was simulated at 100 ns NVT, 1 atm and 300K. The maximal protein RMSD was 3.5 Å, while the minimum fluctuation was 0.9 Å. The average RMSD was 2.1 Å. At the beginning of the simulation the C-terminal of the protein pointed into the bulk solvent, while after 1 ns the C-terminal interacted with Tyr42. At 10 ns of simulation it made a stable polar interaction with Arg19. The latter interaction was broken at 34 ns and after 50 ns the interaction was reformed, remaining stable until the end of the simulation at 100 ns. This final stabilization was due to the participation in the polar environment of Gln39 after 67 ns of MD. After the minimization and equilibration phase, the three Ca^{2+} were coordinated by Gla21, Gla24, Asp30, and Glu31 forming a "carboxy-cage" bridging α-helices H1 to H2 via Ca^{2+} bonds. Notably, Gla17 did not seem to participate in Ca^{+2} binding, consistently with the low frequency of γ-carboxylation (9%) occurring at this position in human osteocalcin (Poser et al., 1980).

Glu osteocalcin (Glu17/Glu21/Glu24). Applying the same simulation protocol, the maximal protein RMSD was 3.3 Å, while the minimum fluctuation was 0.5 Å. The average RMSD was 2.3 Å. The disruption in the polar interaction between the C-terminal carboxylate group and Arg43 after 21 ns and a subsequent (24 ns) HB formation between the backbone of Gly47 and the side chain of Tyr42 was observed. Despite that this last interaction caused the re-orientation of the C-terminal towards Arg19 side chain, no stable interaction was formed at this stage as observed for Gla osteocalcin. After 34 ns of simulation, Gly47-Tyr42 HB was broken and the C-terminal was oriented towards Arg19 after 48 ns; the C-terminal carboxylate formed a stable polar interaction with Arg19, which was stabilized by

Tyr42. The latter conformation was detectable until the end of MD simulation. Gln39 was not involved in the stabilization of the C-terminal, as observed with Gla osteocalcin. In Glu osteocalcin Ca^{2+} were coordinated by Glu21, Glu24, Asp30, Glu31, and Asp34. The initial interaction between the side chains of Glu31 and His35 was broken and replaced by Glu31-Ca^{2+}-Asp34 coordination. Generally, Ca^{2+} ions moved less when compared to the Gla osteocalcin. Moreover, the "carboxy-cage" of Glu osteocalcin model oriented the 3 Ca^{2+} in a different conformation compared to Gla osteocalcin, the major difference resulting in the coordination of Ca^{2+} by Glu24 and Asp30 in Glu osteocalcin. The different calcium-binding network enabled Phe38 in Glu osteocalcin to flip around the Cα-Cβ bond, and thus filling a hydrophobic pocket formed by Ala33 side chain, the Arg20 methylene-groups and the disulphide bridge (Cys23-Cys29), after 25 ns of MD simulation. Re-orientation of Phe38 aromatic side chain resulted in a more compact 3-D structure of Glu osteocalcin compared to the more open structure of Gla osteocalcin.

Ca^{2+} effect in the models of Gla osteocalcin and Glu osteocalcin was monitored analysing the protein RMSD over 100 ns of large-scale NVT molecular dynamics simulation. Both the protein RMSD of Gla osteocalcin and of Glu osteocalcin in presence of Ca^{2+} (in black) was lower compared to the simulations of the same proteins in absence of Ca^{2+} ions (in red) (Figure 14).
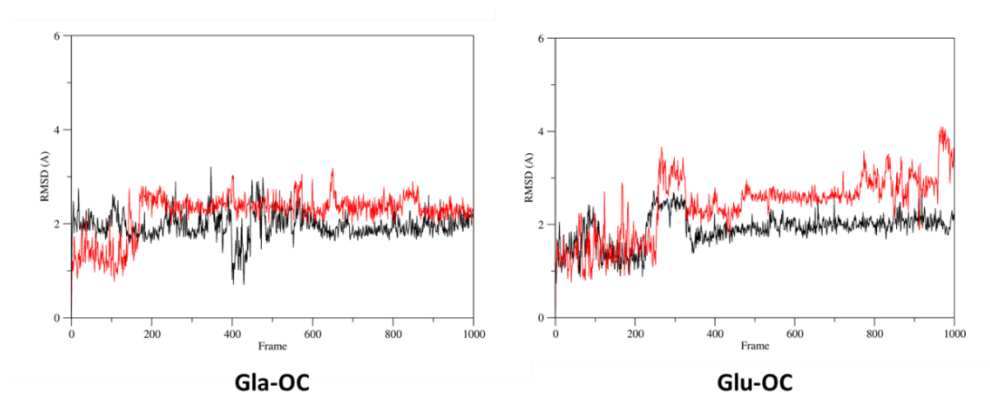
Figure 14. Protein RMSD of Gla osteocalcin (left panel) and Glu osteocalcin (right panel) with overtime of 100 ns NVT 300K MD simulations complexed with Ca^{2+} (black) and un-complexed (red). Gla-OC, carboxylated osteocalcin; Glu-OC, uncarboxylated-OC; RMSD, root-mean-square deviation.

This effect was particularly underlined within Glu osteocalcin molecular dynamics runs and a plausible explanation could be searched in the involvement of the counter ions added to the molecular system during the molecular dynamics parameterization. Gla osteocalcin had 3 COO^- groups more than Glu osteocalcin, whose effect was balanced by 3 Na^+, which were not present in Glu osteocalcin molecular system.

The average values of the protein backbone RMSD and of the residues 17-21-24 RMSD of Gla-OC, and Glu-OC models are reported in the table (Table 6).

	Gla-OC	Glu-OC
Protein backbone RMSD (AVG Å)	2.0	1.9
Residues 17-21-24 RMSD (AVG Å)	0.8	1.2

Table 6. Average values of the protein backbone RMSD and of the residues 17-21-24 RMSD of Gla-OC, and Glu-OC. AVG, average values; Gla OC, carboxylated osteocalcin; Glu-OC, uncarboxylated OC; RMSD, root-mean-square deviation.

Osteocalcin ClickMD analysis

A ClickMD RAINBOW RMSD (Cristiani et al., 2011) analysis (Figure 15) over the two protein systems analysed indicated for both protein structures high conformational changes in the N-terminal and especially in the C-terminal (in green and yellow range). Gla osteocalcin showed larger conformational changes compared to not-carboxylated osteocalcin in absence of Ca^{2+}. This was probably due to the charge repulsion due to the presence of the carboxylation. Whereas, Glu osteocalcin showed larger conformational changes compared to Gla osteocalcin in presence of Ca^{2+}. In particular, Gla osteocalcin exhibited a major stability in the region of the Ca^{2+} interactions. This last observation, together with the above described protein RMSD analysis, suggests a potential key role of Glu residues in the protein conformational stability: the presence of Ca^{2+} ions complexed by carboxylated acid glutamic residues stabilize the protein conformation of Gla-OC compared to Glu-OC.
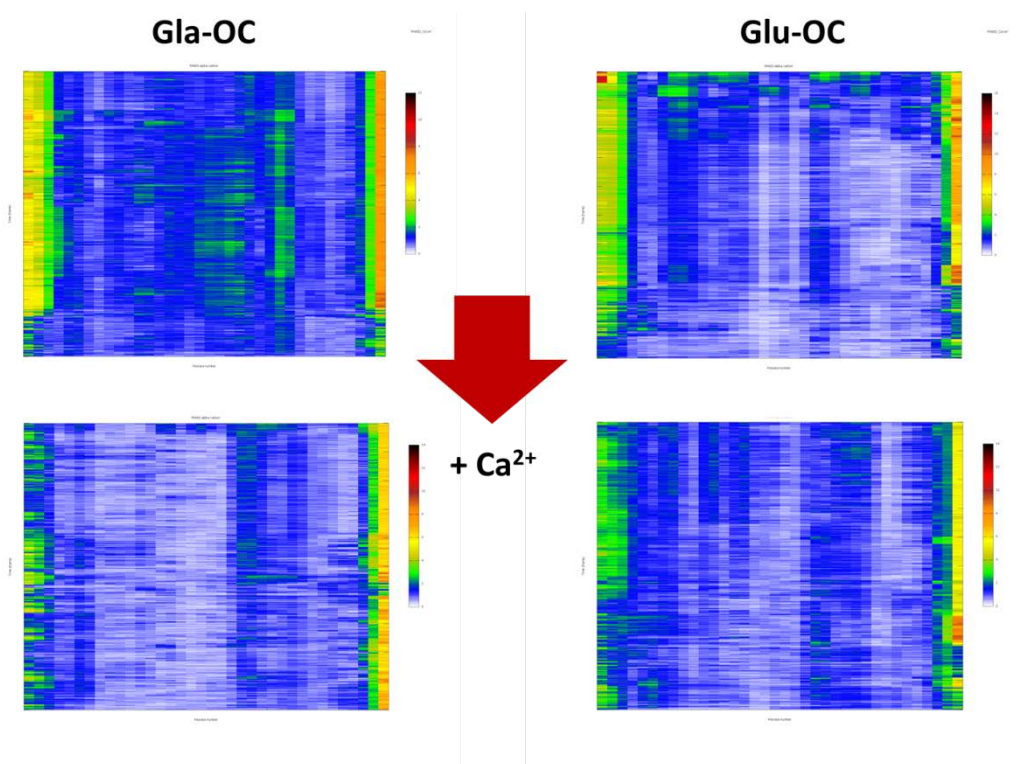
Figure 15. ClickMD RAINBOW RMSD analysis performed overtime of 100 ns NVT 300K MD. Gla osteocalcin (left panels), and Glu osteocalcin (right panels), un-complexed (upper panels) and complexed with Ca^{2+} (lower panels). Amino acid residues (lateral axis); time (vertical axis); white color, RMSD 0 Å; black color, RMSD 14 Å.

A heatmap analysis (performed with VMD 1.8.7 software) described the analysis of trajectories. The heatmap analysis showed unstable (in red/black) and stable (in white) amino acid residues across the time, and confirmed the previous observation between Gla and Glu osteocalcin: Ca^{2+} ions seem to influence more the protein conformation compared to protein carboxylation (Figure 16).

Steered molecular dynamics on osteocalcin carboxy-state and Ca^{2+} binding

Starting from the average osteocalcin structures obtained during MD trajectories, further investigations were carried out through SMD simulations applied on the complexes between Ca^{2+} and all three γ-carboxylated forms of osteocalcin described in the literature, respectively Gla osteocalcin, Glu17 osteocalcin (i.e. osteocalcin γ-carboxylated only on the amino acid residues Glu21 and Glu24), and Glu osteocalcin (Figure 17).
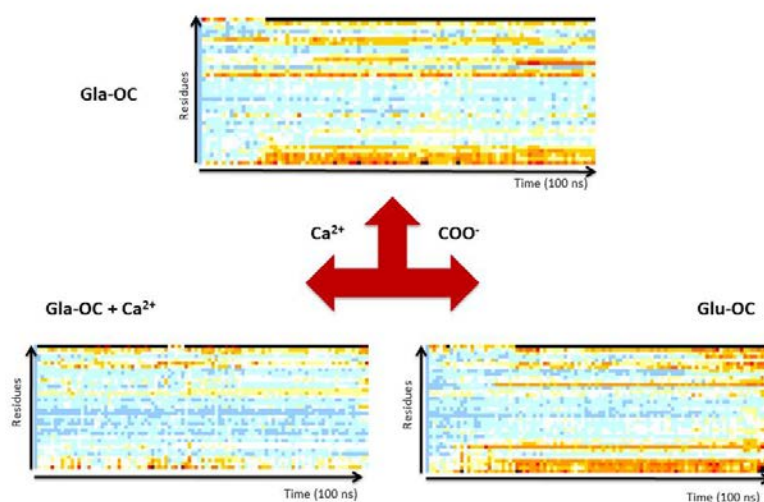
Figure 16. VMD heatmap analysis performed over 100 ns of MD simulation with VMD 1.8.7 software. Gla osteocalcin, un-complexed (upper panel) and complexed with Ca^{2+} (lower-left panel), and Glu osteocalcin un-complexed with Ca^{2+} (lower-right panel). The Ca^{2+} ions influences more the protein conformation compared to the protein γ-carboxylation. COO$^-$, carboxyl group.

SMD experiments showed the strength of the binding between Ca^{2+} and osteocalcin proteins in a rough and fast evaluation way. Briefly, during an SMD simulation an external force was applied to the ligand in the protein complex, in order to facilitate its unbinding from the protein. The analysis of interactions of the dissociating ligand with its binding region, as well as the recording (as a function of time) of the applied forces and the ligand position can yield important structural information about the

structure-function relationships of the ligand-receptor complex, binding pathways, and mechanisms underlying the selectivity of enzymes. In our simulations a constant acceleration (equal to 35,000 pm/ps^2) was applied to Ca^{2+}. Different "distance profiles" were obtained in relation to the degree of γ-carboxylation of the protein, showing a qualitative correlation between the degree of γ-carboxylation of osteocalcin and the strength of the Ca^{2+} binding to the protein. Using the same external acceleration on the Ca^{2+} ions, the unbound process appeared after only 7 ps of SMD simulation in Glu osteocalcin, after 14 ps in Glu17 osteocalcin, after 42 ps of SMD simulation in Gla osteocalcin. These results suggest that the strength of the interactions between Ca^{2+} and osteocalcin depends on the degree of γ-carboxylation of the protein and support the validity of our model.
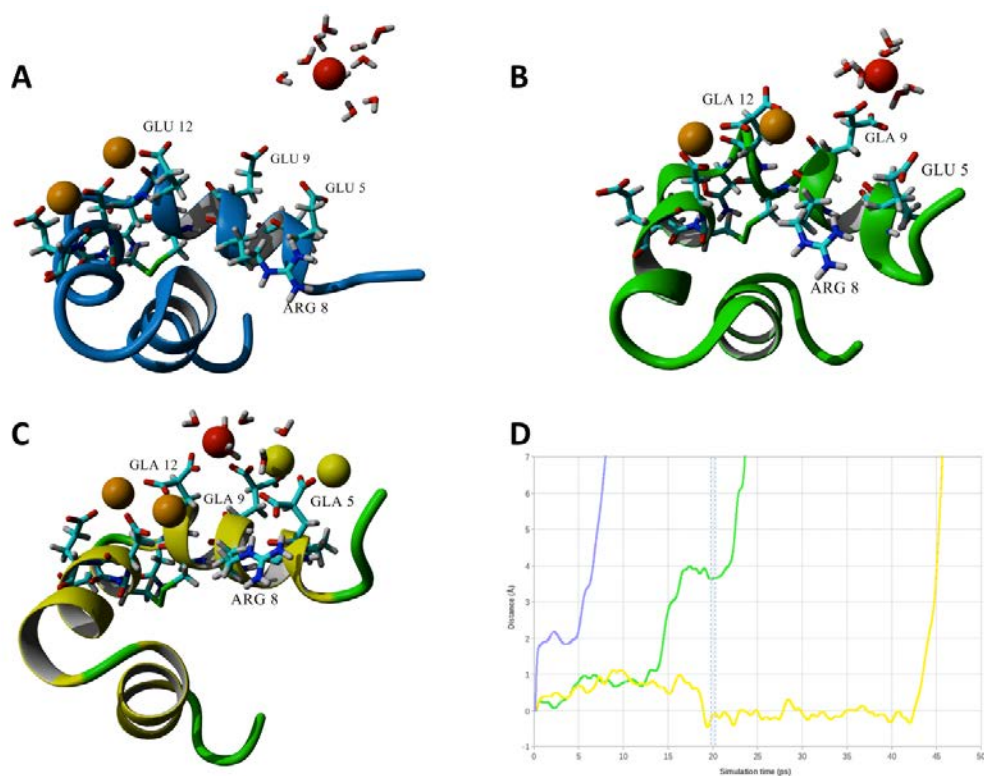
Figure 17. Glu-OC (A, in blue), Glu17-OC (B, in green) and Gla-OC (C, in yellow) after 20 ps of SMD after 20 ps of SMD analysis. The graph (D) represents quantitatively the distance profiles of Ca^{2+} (red) during the SMD. The amino-acid sequence numbering starts at N-terminal of the homology model (i.e. Pro13), thus, e.g., Gla5 correspond to Gla17 of human carboxylated osteocalcin.

Osteocalcin at RP-HPLC and mass analysis

Human Gla osteocalcin and mice Glu osteocalcin purity and chemical identity, were checked by RP-HPLC and mass spectrometry (Figure 18).
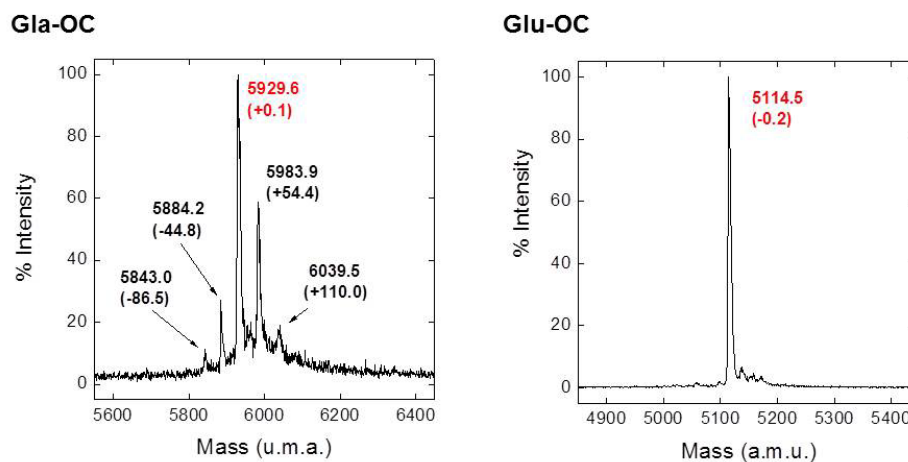
Figure 18. Deconvoluted ESI-TOF mass spectrum of LC-MS purified Gla osteocalcin (left panel) and Glu osteocalcin (right panel). a.m.u./u.m.a, atomic mass units.

The results confirmed the available data from the literature (Table 7).

	aa number	Theoretical MW (a.m.u.)	Gla number	Trp Number	Tyr Number	ε at 280 nm (M^{-1}*cm^{-1})	e$^{0.1\%}$ at 280 nm (mg^{-1}*cm^2)
Human Gla-OCN	49	5929.52	3	1	5	13075	2.205
Mouse Glu-OCN	46	5114.75	0	0	4	6085	1.189

Table 7. Chemical data of human (Human Gla-OCN) and mouse osteocalcin (Mouse Glu-OCN). aa, amino acid residue; a.m.u., atomic mass units; MW, molecular weight; ε, absorbance.

Osteocalcin Ca^{2+} binding at spectroscopic techniques

The effect of γ-carboxylation on Ca^{2+} binding to osteocalcin was investigated by using human osteocalcin, containing Gla residues at positions 17, 21 and 24, and mouse osteocalcin, where γ-carboxylation does not occur and Gla residues are replaced by Glu.

The results of fluorescence spectroscopy in the far-UV region showed that the single Trp5 in human Gla osteocalcin in the absence of Ca^{2+} emitted fluorescence at 350 nm, indicating that Trp5 was fully exposed to the water solventin (Figure19). Upon increasing calcium concentration, the fluorescence of Trp5 was quenched and the λ_{max} value was slightly blue-shifted, suggesting that in the presence of Ca^{2+} the N-terminal of human Gla osteocalcin undergoes to significant conformational changes. Unfortunately, mouse Glu osteocalcin does not contain any residue of Trp; no information from fluorescence measurements could be obtained.
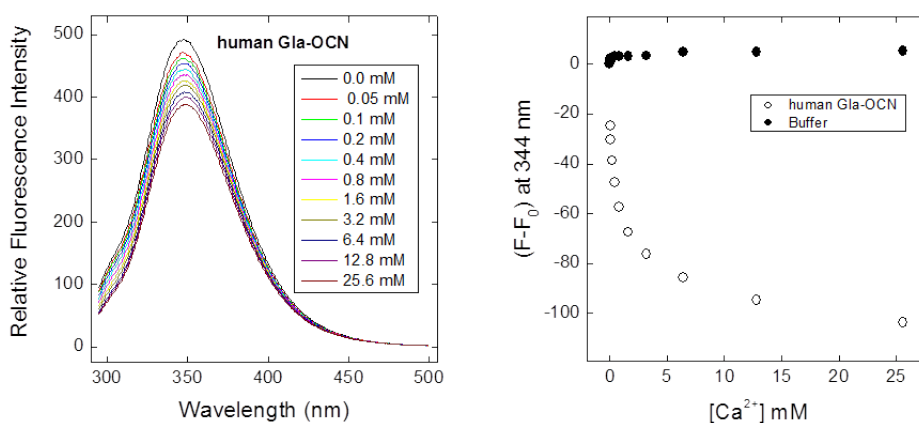
Figure 19. Binding of Ca^{2+} to human Gla osteocalcin monitored by fluorescence spectroscopy in the presence of 0.15 M NaCl. Samples were excited at 280 nm and the emission was recorded at 344 nm. The fluorescence intensity was recorded as a function of Ca^{2+} concentration. Each spectrum was the average of two accumulations after baseline subtraction.

The spectra of human Gla osteocalcin and mouse Glu osteocalcin at CD spectroscopy exhibited a negative band around 204 nm consistent with a random coil (Figure 20). A shift in the negative band to 208 nm, as well as a strong increase in the ellipticity (θ) value at 222 nm, was observed when Ca^{2+} was added. The former results indicate that when Ca^{2+} is added, Ca^{2+} induces a α-helical conformational shift in both proteins with the maximal conformational change occurring at about 3 mM and 28 mM Ca^{2+} for human Gla osteocalcin and mouse Glu osteocalcin, respectively. The change in ellipticity signal at 222 nm as a function of Ca^{2+} concentration was

obtained (Figure 20). The affinity of human and mouse osteocalcin for Ca^{2+} was determined by CD spectroscopy. The best fit yielded a K_d for Ca^{2+}- human Gla osteocalcin of .11 ± .01 mM and a K_d for Ca^{2+}- mouse Glu osteocalcin of 3.64 ± .23 mM. This data showed that Gla residues bind Ca^{2+} with an affinity which is over one order of magnitude greater than that of Glu residues.
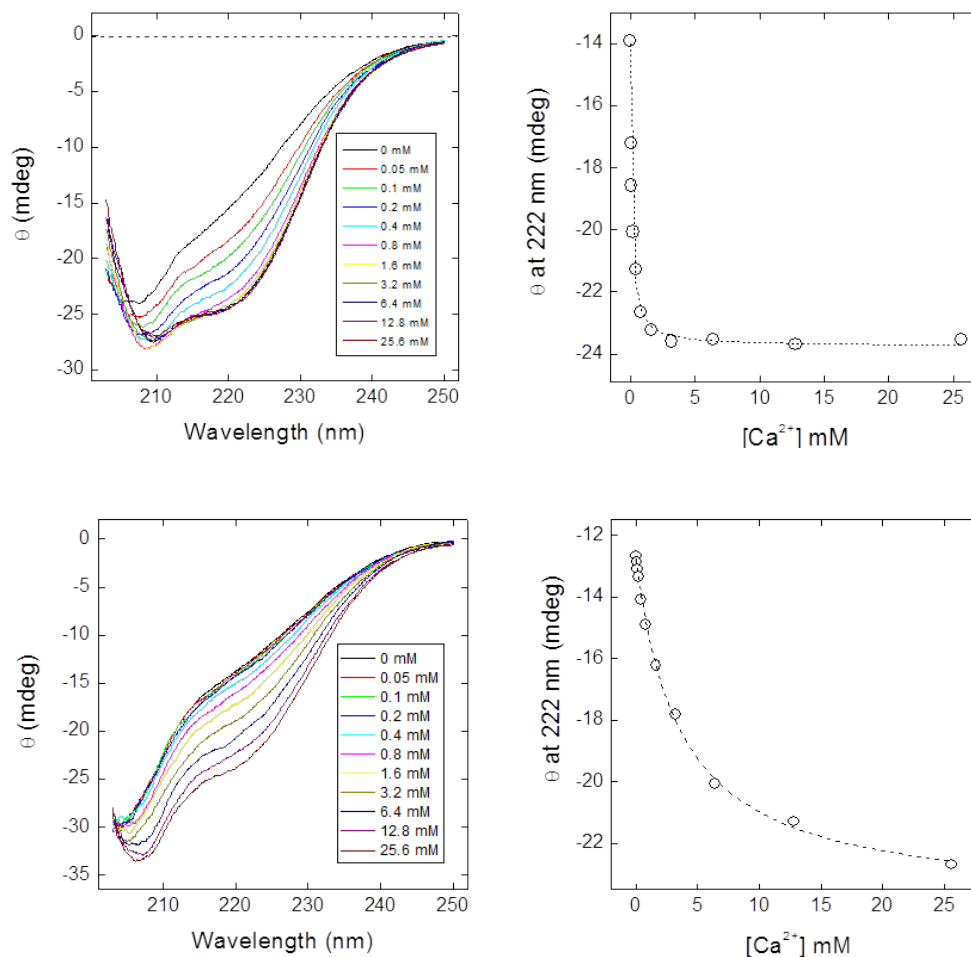
Figure 20. Affinity of Ca^{2+} for human Gla osteocalcin (upper panels) and mouse Glu osteocalcin (lower panels) determined by circular dichroism spectroscopy. The ellipticity signal of osteocalcin was recorded as a function of Ca^{2+} concentration. Each spectrum is the average of four accumulations, after baseline subtraction. Ellipticity data are expressed as millidegrees without further normalization. Θ, ellipticity.

Cluster analysis of 3-D alignments between osteocalcin and SHBG
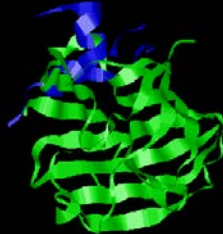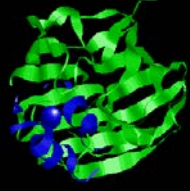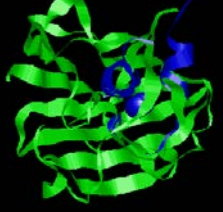
The output solutions was obtained by the comparison of the 3-D protein structure of SHBG (PDB code entry 1D2S) to, respectively, the human internally developed ones of Gla osteocalcin and Glu osteocalcin. TM-align, as well as FATCAT algorithm, gave a single output; whereas the best five matches scored by TopMatch and TriangleMatch were chosen. Overall the output solutions (188 element vectors were defined as 0 not comparable, 1 comparable; see "APPENDIX" section) underwent to a multivariate cluster analysis (as explained in the "Statistical analysis" section) to identify SHBG regions characterized by a good similarity with osteocalcin. The best three clusters of the comparisons are summarized in the table (Table 8).

Proteins	Cluster	Alignments classified (%)	Similarity surface motifs[§]
SHBG/ Glu-OC	1	35	33-38; 170-177
	2	25	143-155
	3	40	15-18; 26-29; 53-56; 159-164
SHBG/ Gla-OC	1	15	171-177
	2	60	16-18; 46-56; 142-146; 159-165
	3	25	75-85

[§] aa sequences shared by the majority of the alignments classified in the same cluster using SHBG aa sequence numbering

Table 8. Cluster analysis of 3-D alignments between osteocalcin and SHBG. The percentage of the solutions classified in each the best three clusters are shown.

Overall, three regions of similarity were identified between SHBG and human Gla or Glu osteocalcin. However, amino acids residues from 75 to 85 of SHBG correspond to the region implied into the dimerization of SHBG. Representative positions of testosterone are presented to support the previous interpretation (Figure 21 e 22).

Region	Example alignment	

1	OC 16 35
	        LEPRRE … HIGFQEAYR
	SHBG **DLTKIT … DSWLDKQAE**
	        33 168	

2	OC 25 41
	        LNPDC … AYRRFYGPV
	SHBG **GGLLF---PASNLRLPL**
	        144	

3	OC 16
	        P-L---EPRREVCELNPDCDELADX
	SHBG **PPA … E--V-RT-WDPE--GVIFY**
	        13 45	

Figure 21. Analysis of 3-D alignments SHBG/undercarboxylated osteocalcin (OC). Examples of alignments which were randomly chosen.
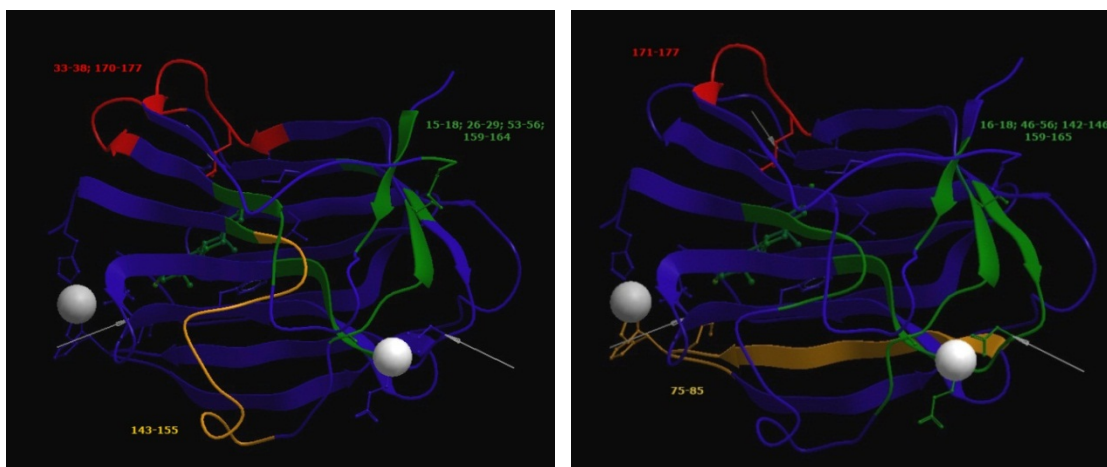
Figure 22. Cluster analysis of SHBG/undercarboxylated osteocalcin (left panel) and SHBG/carboxylated osteocalcin alignments (right panel) on SHBG 3-D structure. Representative positions of testosterone are presented to support the interpretation

Osteocalcin and SHBG (dimer)-GPRC6A receptor docking analysis

The best-scored comparative protein structure model describing the extracellular loops and upper third of the trans-membrane bundle of GPRC6A receptor was used as the docking site, due to the lacking of the crystallographic resolution of GPRC6A receptor. Either SHBG or Glu osteocalcin was docked to GPRC6A receptor to determine the preferred binding site on the receptor. The best five outputs of each of the three docking algorithms underwent to a frequency analysis of the amino acids involved in the predicted surfaces interaction SHBG-GPRC6A receptor (Figure 23). The three highly predicted interfaces were, respectively, 145-161, 59-67 and 19-41, numbered according the SHBG sequence amino acid residues (Figure 24).

Inferring about those showing a 3-D protein structure osteocalcin-like, only the first and the latter showed it. In particular, the first one included amino acids Gly145 Leu145 Leu147 Phe148 Pro149 Ala150 Ser151 Asn152 Leu153 Arg154 Leu155 Pro156 Leu157 Val158 Pro159 Ala160 Leu161, forming a loop between the β-motifs, opposite to the steroid-binding site (Figure 25). The central part of the sequence was predicted with a rate above 50% compared to the other amino acid residues of

SHBG. The nature of the amino acids (e.g. Pro) of the predicted interface could support the synthesis of a potentially structured peptide.

Predictor	Solution	Interface	aa
GRAMM_X	1	136-140	5
		146-159	14
	2	24-26	3
		31-36	6
		60-66	7
		146-156	11
	3	19-24	6
		49-52	4
		72-77	6
		88-97	10
		122-126	5
		149-162	14
	4	20-31	12
		146-160	15
		178-186	9
	5	24-36	13
		60-66	7
		145-159	15

Predictor	Solution	Interface	aa
PatchDock	1	13-36	24
		168-188	21
	2	22-33	12
		60-64	5
		146-160	15
		177-183	7
	3	45-51	7
		93-107	15
	4	49-52	4
		72-75	4
		92-101	10
		158-162	5
	5	13-22	10
		35-45	11
		102-109	8
		165-188	24

Predictor	Solution	Interface	aa
ZDock	1	34-40	7
		60-65	6
		107-110	4
		125-139	14
	2	61-66	6
		148-159	2
	3	33-40	8
		83-85	3
		107-110	4
		125-139	15
	4	34-40	7
		60-64	5
		107-110	4
		125-139	15
	5	61-66	6
		81-87	7
		151-156	6

Figure 23. Best five outputs of SHBG (dimer)-GPRC6A receptor docking analysis with GRAMM-X; PatchDcock and ZDOCK algorithms. The predicted interfaces are numbered according to the sequence of SHBG amino acid residues.
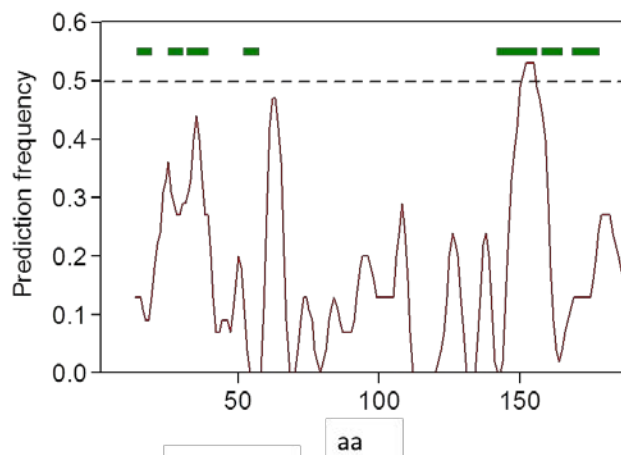
Figure 24. Frequency of the prediction of each amino acid residues of SHBG as shown by the best outputs of the SHBG (dimer)-GPRC6A receptor docking analysis. Green color represents the amino acid residue of SHBG which participated to osteocalcin-like (OC-like) motifs. aa, amino acid residue.
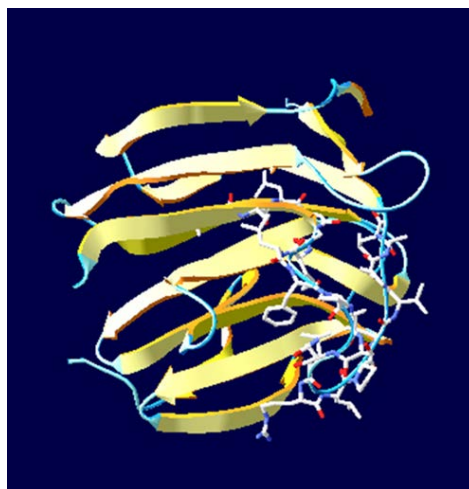
Figure 25. Cartoon of SHBG monomer. The amino acid residues from Gly145 to Leu161 are shown as sticks. The former amino acid residues (the most predicted interface in SHBG (dimer)-GPRC6A receptor docking analysis) form a loop between the β-motifs, opposite to the steroid-binding site.

Gprc6a gene expression in HEK-293T cells

End-point PCR analysis of amplified cDNA extracted from HEK-293T showed that *Gprc6a* is endogenously expressed (Figure 26). A clear band could be observed with each of the three primers; the quality of the experiments was confirmed by the expression of the internal housekeeping gene, glyceraldehyde-3-phosphate dehydrogenase (*GADPH*).
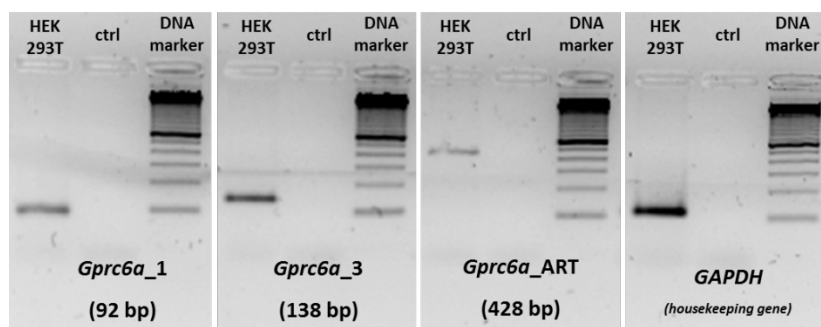
Figure 26. End-point PCR of *Gprc6a* gene expression from HEK-293T cells with three pairs of primers, respectively *Gprc6a*_1, Gprc6a_3, and Gprc6a_1ART. ctrl, negative control; *GADPH*, glyceraldehyde-3-phosphate dehydrogenase.

To confirm these results, RT-PCR experiments were performed. A human kidney library served as a positive control. The expression of *Gprc6a* was further confirmed, despite to a lower level compared to the human kidney library (data not shown).

GPRC6A receptor protein expression on HEK-293T cells

GPRC6Areceptor expression on the surface of HEK-293T cells was confirmed by immunofluorescence assay and VICO technology to minimize the influence of the background signal (Figure 27). The staining of GPRC6A appeared as a specific dotted signal.
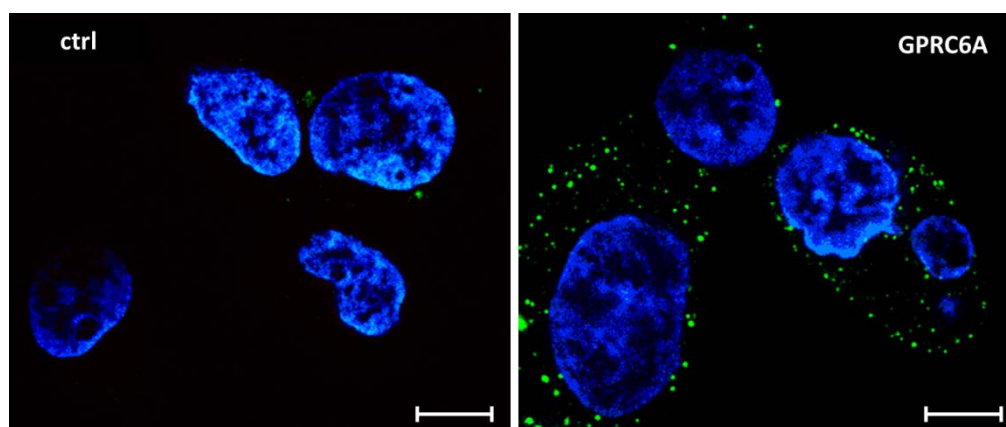
Figure 27. Immunofluorescence (confocal fluorescence microscope) for GPRC6A receptor on HEK-293T cells. Negative control (left panel) and example of a sample treated with Ab anti-GPRC6A (green). Counterstaining of nuclei was performed with 4,6-diamidino-2-phenylindole (DAPI) (blue). Scale bars: 20 μm.

Characterization of osteocalcin and SHBG binding on HEK-293T cells

A binding assay was performed on HEK-293T cells to evaluate the binding of undercarboxylated osteocalcin, carboxylated osteocalcin and SHBG, respectively, and any non-specific binding. Undercarboxylated osteocalcin, carboxylated osteocalcin and SHBG binding were confirmed by immunofluorescence assay and VICO technology, with SHBG and undercarboxylated osteocalcin showing a higher signal (Figure 28 and 29). No meaningful signal was detected when the samples

were pre-incubated with an antibody anti-GPRC6A, and thereafter treated with osteocalcin.
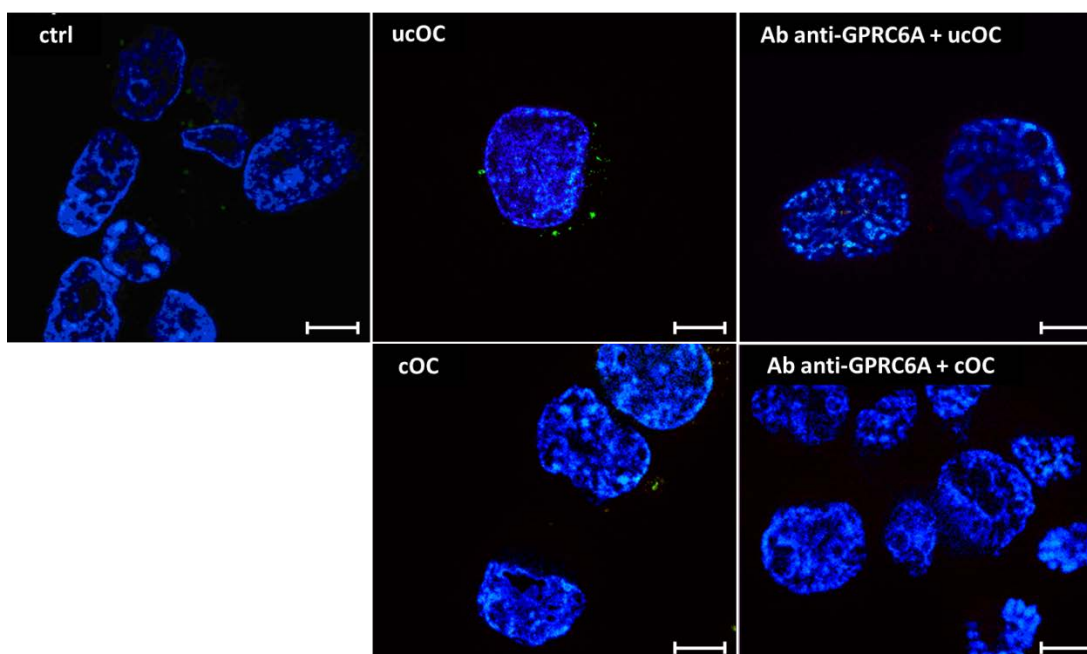
Figure 28. Immunofluorescence (confocal fluorescence microscope) for osteocalcin binding on HEK-293T cells. Negative control (left panel); example of a sample treated with osteocalcin (green) (central panels; ucOC upper panel, cOC lower panel); example of a sample pre-incubated with Ab anti-GPRC6A (right panels). Counterstaining of nuclei was performed with 4,6-diamidino-2-phenylindole (DAPI) (blue). Scale bars: 20 μm.

Interestingly, the signal was meaningfully decreased also when the former pre-incubated samples (i.e. antibody anti-GPRC6A) were treated with SHBG (Figure 29).
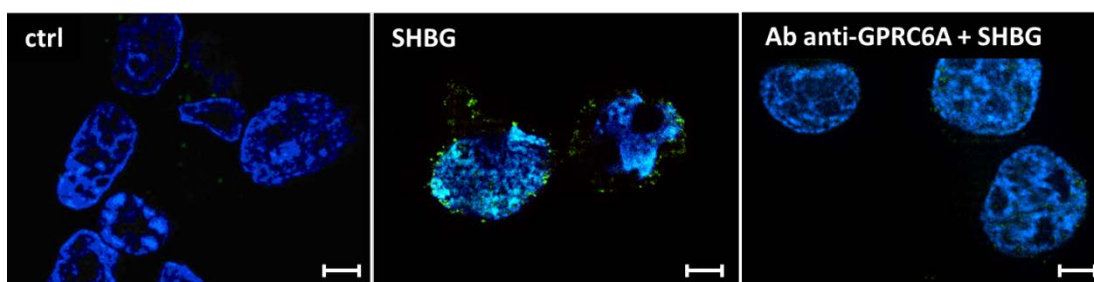
Figure 29. Immunofluorescence (confocal fluorescence microscope) for SHBG binding on HEK-293T cells. Negative control (left panel); example of a sample treated with SHBG (green) (central panel); example of a sample pre-incubated with Ab anti-GPRC6A (right panel). Counterstaining of nuclei was performed with 4,6-diamidino-2-phenylindole (DAPI) (blue). Scale bars: 20 μm.

Osteocalcin *vs.* SHBG binding assay on HEK-293T cells

A binding assay was performed on HEK-293T cells to evaluate any competition for the same binding site between, respectively, undercarboxylated osteocalcin, carboxylated osteocalcin and SHBG. The co-incubation both of ucOC and cOC with an excess of SHBG (50-fold equimolar) showed a meaningful qualitative decrement of the signal detected by the primary antibody anti-osteocalcin by immunofluorescence assay and VICO technology (Figure 30).

In a parallel experiment performed by flowcytometry assay was quantified a relative decrement by the mean staining signal of respectively 85% (for ucOC) and 37% (for cOC) when samples were co-incubated with an excess of SHBG (100-fold equimolar).
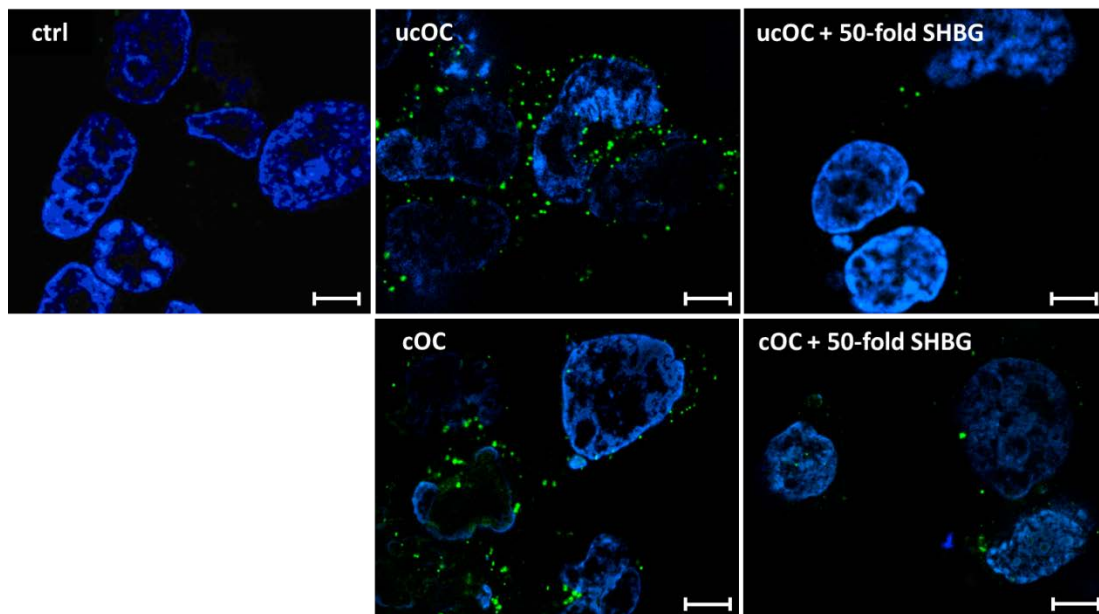
Figure 30. Immunofluorescence (confocal fluorescence microscope) for osteocalcin vs. SHBG binding on HEK-293T cells. Negative control (left panel); example of a sample treated with osteocalcin (green) (central panels; ucOC upper panel, cOC lower panel); example of a sample co-incubated with osteocalcin and an excess (50-fold) of SHBG (right panels). Counterstaining of nuclei was performed with 4,6-diamidino-2-phenylindole (DAPI) (blue). Scale bars: 20 µm.

DISCUSSION

Our study shows for the first time the existence of the competition for a specific binding site between osteocalcin and SHBG on human cells expressing GPRC6A receptor, which was supported by a computational prediction analysis. Concurrently, our clinical data show an imbalance between the γ‑carboxylated forms of osteocalcin in a cohort of hypogonadic obese and overweight patients, with decreased levels of SHBG and altered levels of the other sex hormones.

Homology between protein molecules can be detected by similarities in function, sequence, or structure (Schneider and Stephens, 1990; Murzin, 1998; Thornton et al., 1999). In the current study we started to develop our working hypothesis from genetic studies in mice (Lee et al., 2007; Oury et al., 2011). The supernatant of cultured wild-type osteoblasts was able to increase testosterone production by Leydig cells to far greater levels than those observed for other mesenchymal cells (Oury et al., 2011). Moreover, the supernatant of $Osteocalcin^{-/-}$ osteoblast cultures was ineffective in promoting testosterone production in Leydig cells (Oury et al., 2011). The higher osteocalcin expression was due to the stimulation of all genes necessary for testosterone biosynthesis in Leydig cells (Oury et al., 2011). Accordingly, circulating testosterone levels were low in $Osteocalcin^{-/-}$ mice and were high in $Esp^{-/-}$ mice, indirectly confirming the importance of the different γ–carboxylated forms of osteocalcin. Whereas an abundance of studies have tried to assess the possible relationship osteocalcin and energy metabolism in humans, data are lacking concerning osteocalcin and endogenous sex hormones. In our study we described for the first time a positive correlation between the ratio undercarboxylated osteocalcin/total osteocalcin and free testosterone, but we did not find a direct correlation between undercarboxylated osteocalcin and free testosterone. The latter could be due to changes that are related to metabolism or vitamin K intake, despite that our inclusion criteria excluded patients taking drugs

known to influence bone and calcium metabolism, or with hepatic failure and dietary derangements. The use of the ratio ucOC/OC could likely represent a more sensible parameter to describe the overall variation in osteocalcin pattern in pathophysiological condition with a multiple aetiology. The effects observed in mice with implanted osmotic minipumps containing undercarboxylated osteocalcin were seen, in fact, with an increase of undercarboxylated osteocalcin only to 14% (Ferron et al., 2010), which is within the intraindividual variation that is normal in humans consuming a varied diet. In our cohort there was a parallel decrement of free testosterone and SHBG, but we did not find a correlation between SHBG and undercarboxylated osteocalcin or ucOC/OC. The latter observation is not against our hypothesis. Free testosterone in our study is a direct expression of SHBG levels, because it was estimated by calculation from total testosterone and SHBG concentrations (Vermeulen et al, 1999). Moreover, the regulation of SHBG expression is still not clear and is multifactorial. In vitro studies have demonstrated, for example, that SHBG secretion is not only under the control of E and T stimulation (the previous exerting it in a dose-dependent manner whereas the second in a biphasic one) (Edmunds et al., 1990; Wallace et al. 2012), but is also under the control of, e.g., insulin and other hormone inhibition (Plymate et al. 1988; Wallace et al. 2012).

SHBG is specific for humans, whereas the plasma carrier protein for sex steroids in mice has not been characterized. Multiple evidence suggests that SHBG has functions in addition to that of regulating circulating concentrations of free sex steroids and their transport to target tissues. SHBG binds to plasma membranes, suggesting the presence of a specific plasma membrane receptor (Strel'chyonok et al. 1984). The binding of SHBG to plasma membranes has been demonstrated in a limited number of tissues, including prostate, proximal convoluted tubule cells of the kidney, liver and epididymis, largely correlating with tissues which are responsive to the sex steroids bound to SHBG (Fortunati et al., 1992). Unbound

SHBG binds to the SHBG receptor and it has been shown that the stronger the affinity of the sex steroid ligand for SHBG, the greater the inhibition of its interaction with the SHBG receptor (Rosner et al. 1988). The mechanism of action has not been elucidated yet, and it is possible that after SHBG binds to the SHBG receptor either a sex steroid then binds to SHBG and the complex is internalized, allowing delivery of the sex steroid to the nucleus, or SHBG directly exerts an effect on the cell, acting itself as a hormone (Rosner et al. 2010). The SHBG receptor is thought to be a G protein-coupled receptor, based on indirect evidence that shows that (i) when an appropriate steroid bound to the complex SHBG-SHBG receptor there was a rapid rise in cAMP (Nakhla et al. 1990; Nakhla et al., 1994; Nakhla et al. 1995); (ii) the exposure of cell membranes containing SHBG receptor to a non-hydrolysable analog of guanosine triphosphate (guanylyl-59-imidodiphosphate) caused a substantive decrease in the binding to the complex SHBG-SHBG receptor (Nakhla et al., 1999); and (iii) there was a reduction in cAMP concentration when the G_α subunit was replaced by a mutant form (i.e. as[Gly225Thr] and as[Gly226Ala]) which ineffectuated the signal transduction (Nakhla et al., 1999). In the current study we demonstrated that HEK-293T cells express GPRC6A receptor both at a genetic and protein level. Moreover, the pre-incubation of HEK-293T samples with an antibody anti-GPRC6A led to a meaningfully decrement of the fluorescence signal associated to the binding of SHBG. Despite that this is not conclusive, the current results tempt us to speculate that GPRC6A receptor could represent the putative SHBG receptor or, at least, SHBG can bind also to this protein. Conclusive results, however, will be obtained only by (i) demonstrating GPRC6A protein expression with western blot analysis; (ii) knocking down gene expression with, e.g., specific siRNA transfection, and the subsequent analysis of the fluorescence signal associated to the binding of SHBG to HEK-293T cells, or to another cell type expressing GPRC6A (e.g. LNCaP cells); and (iii) performing functional studies showing, e.g., a rapid rise in cAMP

when an appropriate steroid binds to the complex SHBG-SHBG receptor in an appropriate cell model (e.g. HEK-293T or LNCaP cells).

The demonstration that HEK-293T cells express GPRC6A is of particular importance, because HEK-293T cells represent an appropriate model to study the interaction between undercarboxylated osteocalcin and GPRC6A receptor, the former binding to their surface with the same pattern of expression as the latter (i.e. dotted signal at immunofluorescence assay). Interestingly, no other research group has ever reported a western blot analysis showing the protein expression of GPRC6A in the different cellular and ex vivo samples, e.g. mouse and human Leydig cells (Oury et al., 2011); RWPE-1 and LNCaP cells (Pi et Quarles, 2012[b]); transfected HEK-293 overexpressing *Gprc6A* (Pi et al., 2011); and mouse TC-6 pancreatic β-cells (Pi et al., 2011). Although Pi et al. state that HEK-293 do not express *Gprc6a* (Pi et al., 2010; Pi et al. 2011; Pi et Quarles, 2012[a]), our results do not show this. We obtained good expression using the same pair of primers and positive results using other two different primers at end-point PCR, as well as the primer *Gprc6a*_1 at quantitative RT-PCR analysis. Our immunofluorescence assays showed a pattern similar to those in testis coronal sections reported by Oury et al. (Oury et al., 2011), and the disappearance of the signal after pre-treatment with an antibody anti-GPRC6A support both the GPRC6A receptor expression and the undercarboxylated osteocalcin specificity binding. As previously explained, HEK-293T cells were generated by a human kidney cell line by transfection of adenovirus DNA; Wellendroph et al. reported that *Gprc6a* is expressed in mature cells of the kidney (Wellendorph et Bräuner-Osborne, 2004), and cytogenetic instability has been reported in the literature for some cell lines of HEK-293.

Structural motifs, including domain arrangements or small molecule binding pockets determine the biological function of protein families. The quality of a predicted structure partially depends on sequence similarity to the template structure and, despite the observed sequence identity above 20% between SHBG and osteocalcin,

a close to optimal sequence alignment can only be obtained for closely related protein sequences with identities over 40% (Sanchez et Šali, 1997), and a poor precision is seen for homologues with a sequence identity below 30%. As sequence similarity decreases, in fact, the alignment becomes more uncertain and is likely to contain an increasingly large number of gaps and alignment errors (Rost, 1999; Marti-Renom et al., 2000; Elofsson, 2002). In the current study we investigated possible protein-protein interaction predictors with a more appropriate and efficient 3-D protein structure alignment analysis between the crystal structure of SHBG and the osteocalcin model of the 3-D protein structure that was internally developed and validated. The two proteins, in fact, are largely different not only for the sequences with identities, but also from the dimension (40.5 KDa vs. around 5.8 kDa), and the secondary structure, which is constituted mainly of β motifs in SHBG vs. three α-helices in osteocalcin (Grishkovskaya et al. 2000; Hoang et al. 2003). Moreover, SHBG exerts its actions as a homodimer, whereas circulating osteocalcin seems to exist as a monomer in vivo (Strel'chyonok et Avvakumov, 1990; Hoang et al., 2003). Loops and side chains of SHBG have been hypothesized be necessary for the interaction with plasma membrane receptors in target tissues, despite that they are not essential for the steroid-binding activity of SHBG (Strel'chyonok et Avvakumov, 1990). Interestingly, inferring the results both from the cluster analysis of protein-protein alignments and those of the docking analysis, the predicted structure osteocalcin-like of SHBG is formed by a sequence of amino acids rich in proline residues forming a loop between the β-motifs, opposite to the steroid-binding site. Despite the small homology site and the lack of information about the site of interactions between osteocalcin and GPRC6A receptor, the osteocalcin displacement by excess SHBG in the experiments in vivo support our hypothesis. Moreover, in the preliminary experiment at the flow cytometry analysis, the relative displacement of osteocalcin by the excess of SHBG was higher for the uncarboxylated form than for the carboxylated one, which could resemble the

higher specificity for the binding, despite the minor structural difference in our molecular modeling studies developed using the amino acid residues from Pro13 to Val49.

Our experiments describe the structure of human osteocalcin, in its carboxylated and undercarboxylated forms for the first time. Recent studies on porcine osteocalcin revealed an excellent surface complementarity between the Ca^{2+} coordinating surface of osteocalcin and the prism face of hydroxyapatite, suggesting that Gla osteocalcin may also show selective binding characteristics to hydroxyapatite (Hoang et al. 2003). Our results extend this behaviour about Ca^{2+} affinity to human osteocalcin, and partially explain the lower affinity for hydroxyapatite exerted by undercarboxylated osteocalcin. The human Glu osteocalcin obtained through homology modelling based on 1Q8H porcine template (Hoang et al. 2003) has similar features previously described for the Gla osteocalcin model. Protein structures had high conformational changes in N-terminal and especially in the C-terminal, depending both on Gla residues and Ca^{2+} interactions. Ca^{2+} ions have a role in stabilizing the protein conformation of osteocalcin, which is supported by the experimental data of the current study describing the Ca^{2+}-dependent conformational changes in both human Gla osteocalcin, and mouse Glu osteocalcin. In particular, the spectroscopic measurements demonstrated that Ca^{2+} binding to osteocalcin results in a dramatic increase of α-helical secondary structure and that the N-terminal undergoes significant conformational changes with increasing concentration of Ca^{2+}. Interestingly, previous studies in fish osteocalcin similarly described that α-helical content of teleost osteocalcin increases and β-sheet structure decreases upon Ca^{2+} binding (Nishimoto et al. 2003). The experimental analyses have also shown that the presence of γ-carboxylated glutamic acid residues significantly modifies the Ca^{2+} binding capacity of human osteocalcin in agreement with the molecular dynamics data, as exemplified by, e.g., ClickMD RAINBOW RMSD analysis. Specifically, in the absence of Ca^{2+} Gla osteocalcin seem to

have a greater instability than Glu osteocalcin, probably attributable to the charge repulsion due to the presence of the carboxylation (i.e. COO^- groups). On the contrary, however, when the Ca^{2+} binds to the molecule, Gla osteocalcin acquire a higher rigidity compared to Glu osteocalcin. Overall, the influence of the binding of Ca^{2+} on the structure of the osteocalcin is stronger than the presence of γ-carboxylated glutamic acid residues, as exemplified by the heatmap analysis. One limitations of our and other studies (Hoang et al. 2003), however, is the lack of information about the N-terminal in the template structure. N-terminal, in fact, could not be modelled due to the high conformational flexibility. Moreover, due to the lack of commercially available human uncarboxylated osteocalcin, we were forced to perform wet chemistry analysis with mouse uncarboxylated osteocalcin. Despite the high homology (i.e. 88%) the lack, for example, of Trp-residue at position 5 prevented to resolve possible conformational changes due to Ca^{2+} binding at fluorescence spectroscopy in the far-UV region for osteocalcin, and a species-specificity should caution us in interpreting the results of the in vitro experiments. Conformational changes due the Ca^{2+} binding could have important effects at the level of the interactions between Glu osteocalcin and GPRC6A receptor. As previously explained, in fact, GPRC6A receptor senses Ca^{2+} via orthosteric binding sites in the VFTM. Moreover, Pi et al. showed how osteocalcin (up to 40 ng/ml) had no effect at sub-threshold extracellular Ca^{2+} (≤ 1.0 mM), and thereafter osteocalcin had a dose-dependent effect to stimulate GPRC6A-dependent increments in SRE-luciferase activity in experiments in vitro (Pi et al., 2005). Allosteric modulators, such as osteocalcin, may bind to distinct sites in the transmembrane domain, influencing or being influenced by Ca^{2+} and other extracellular positive cations. Interestingly, the serum concentration of human osteocalcin is approximately 60 mg/L, assuming the average serum concentration of free Ca^{2+} is about 1.2 mM, and the K_d estimated Gla osteocalcin is 90% Ca^{2+} saturated, and Glu osteocalcin is only 25% Ca^{2+} saturated. We could hypothesize that Glu osteocalcin could reach GPRC6A receptor largely

unbound to Ca^{2+} and then they could interact. Interestingly, also SHBG binds to its putative receptor unbound to SHBG, and it undergoes conformational changes after the steroid-binding, gaining its biological activity (Rosner et al. 2010). The completion of SHBG with osteocalcin could be implicated both in the regulation of testosterone synthesis (Oury et al., 2011), or in unravelled pathways. GPRC6A activity, in fact, may be modulated by multiple ligands or by mixtures of ligands working together, rather than the typical ligand-receptor interaction that characterizes most endocrine networks (Pi et Quarles., 2012[a]).

Our results did not investigate the functional consequences of the competition of SHBG and osteocalcin for the same binding site. Oury et al. hypothesized in a mouse model that the binding of osteocalcin to a GPRC6A receptor expressed in the Leydig cells of the testes regulates the expression of enzymes that are required for testosterone synthesis in a cAMP response element binding (CREB) protein-dependent manner (Oury et al. 2011). Pi et al. showed that the same receptor, GPRC6A, is also functionally important in regulating non-genomic effects of androgens in multiple tissues (Pi et al., 2010). Androgens, in fact, act both through classical binding to the nuclear receptor regulating steroid response elements in gene promoters (modulating gene expression over a period of hours) and by exerting illicit rapid (occurring in minutes) non-genomic effects that may also have important biological effects in many tissues. (Losel et al., 2003). The molecular mechanisms underlying these non-genomic actions are poorly understood, but *Gprc6a*^{-/-} mice exhibit significantly less ERK activation and *Egr-1* expression in response to pharmacological doses of testosterone in vivo in both bone marrow and testis, and different research teams have obtained opposite phenotypic pattern with *Gprc6a*^{-/-} mice (Pi et al., 2008; Wellendorph et al., 2009). However, the surface binding testosterone-BSA and GPRC6A receptor was validated both in in vitro experiments and at a structural level. GPRC6A receptor, in fact, has a unique pattern of hydrophobic residues in the second extracellular loop, which could play a role in

specific testosterone binding by the TM bundle of GPRC6A receptor (Pi M. et al. 2010). SHBG could exert its action by binding independently, as previously described, to its putative receptor, which our study has indicate to potentially be GPRC6A receptor, and/or by modulating the binding of free testosterone to the same receptor that has shown to mediate its non-genomic effects. There are many gaps in the knowledge not only of the possible ligand/modulator, but also in the downstream of the signaling pathways. GPRC6A receptor is purported to be coupled to $G_{\alpha q}$ and possibly $G_{\alpha i}$, and it was shown that testosterone binding resulted in an increased ERK activation and intracellular Ca^{2+} increase (Pi et al., 2010). However, GPRC6A receptor is atypical in that, although ERK activation is inhibited by a pertussis toxin, GPRC6A receptor fails to inhibit cAMP production in osteoblasts (Christiansen et al., 2007; Pi et al., 2005). Moreover, osteocalcin via GPRC6A receptor consistently induced cAMP production in Leydig cells to a level comparable to that induced by human chorionic gonadotropin, the positive control, but did not induce tyrosine phosphorylation, ERK activation, or intracellular calcium (Oury et al. 2011), suggesting the capacity to also couple to $G_{\alpha s}$. Interestingly, as previously explained, when an appropriate steroid binds to the complex SHBG-SHBG receptor, there is a rapid rise in intracellular cAMP (Nakhla et al. 1990; Nakhla et al., 1994; Nakhla et al. 1995).

Based on the current findings, we are currently knocking down *Gprc6a* gene with a pool target-specific siRNAs, in order to evaluate, after the confirmation throughout western blot analysis of the absence of the protein, the specificity of GPRC6A receptor binding both for SHBG and osteocalcin. Concurrently, from the structural side, we are synthesizing the target peptide that corresponds to the amino acid residues from Gly145 to Leu161 of SHBG in order to test its ability to compete with the binding of SHBG and osteocalcin in the same cellular model in experiments in vitro. The high content of proline residues could guarantee an own structure. The final step will be to study the functional consequences of binding of a combination

of (i) osteocalcin in different γ‑carboxylated forms and in the presence or absence of Ca^{2+}, (ii) SHBG in presence or not of dihydrotestosterone, and (iii) dihydrotestosterone alone. According to the literature, an increase in intracellular cAMP should be expected, but quantification of other transcriptional effectors should not be excluded.

CONCLUSIONS

The approach of whole-organism physiology, namely that all or most organs interact together, prompt us to explore new fields on the basis of a spectrum of clinical observations, and mouse genetics offer a unique key to open new research field. Molecular physiology represents the gold standard to investigate the function, in one particular cell type, of one protein or group of proteins, whether they are transcription factors, receptors, or hormones. Although to the best of our knowledge no molecule identified as a hormone in mice has lost its function in humans, gene, protein and enzymes can differ between species and genders as taught both by osteocalcin and SHBG.

The current two-step approach offers a target approach of investigation directly in humans, which has the potential to identify novel pathophysiological pathways as well as novel therapeutic possibilities, as exemplified by the current data. The computational basis of the possible binding of SHBG and osteocalcin has been experimentally validated and can directly lead to the synthesis of a peptide, whose physiological and therapeutic implications represent a feasible perspective for future research in an area of paramount importance, such as the cross-talk between bone, energy metabolism, and endogenous sex hormones.

REFERENCES

Anfinsen CB. Principles that govern the folding of protein chains. Science 1973;181:223-230.

Atkinson RA, Evans JS, Hauschka PV, Levine BA, Meats R, Triffitt JT, Virdi AS, Williams RJ. Conformational studies of osteocalcin in solution. Eur J Biochem 1995;232(2):515-21.

Avvakumov GV, Muller YA, Hammond GL. Steroid-binding specificity of human sex hormone-binding globulin is influenced by occupancy of a zinc-binding site. J Biol Chem 2000;275(34):25920-5.

Avvakumov GV, Grishkovskaya I, Muller YA, Hammond GL. Crystal structure of human sex hormone-binding globulin in complex with 2-methoxyestradiol reveals the molecular basis for high affinity interactions with C-2 derivatives of estradiol. J Biol Chem 2002;277(47):45219-25.

Aulestia FJ, Redondo PC, Rodríguez-García A, Rosado JA, Salido GM, Alonso MT, García-Sancho J. Two distinct calcium pools in the endoplasmic reticulum of HEK-293T cells. Biochem J 2011;435(1):227-35.

Bae SJ, Choe JW, Chung YE, Kim BJ, Lee SH, Kim HY, Koh JM, Kim HK, Kim GS. The association between serum osteocalcin levels and metabolic syndrome in Koreans. Osteoporos Int 2011;22(11):2837-46.

Bairoch A, Apweiler R, Wu CH, Barker WC, Boeckmann B, Ferro S, Gasteiger E, Huang H, Lopez R, Magrane M, Martin MJ, Natale DA, O'Donovan C, Redaschi N, Yeh LS. The Universal Protein Resource (UniProt). Nucleic Acids Res 2005;33(Database issue):D154-59.

Benton ME, Price PA, Suttie JW. Multi-site-specificity of the vitamin K-dependent carboxylase: in vitro carboxylation of des-gamma-carboxylated bone Gla protein and Des-gamma-carboxylated pro bone Gla protein. Biochemistry 1995;34(29):9541-51.

Berkner KL. The vitamin K-dependent carboxylase. Annu Rev Nutr 2005;25:127-49.

Bockaert J, Pin JP. Molecular tinkering of G protein-coupled receptors: an evolutionary success. EMBO J 1999;18(7):1723-29.

Booth SL, Centi A, Smith SR, Gundberg C. The role of osteocalcin in human glucose metabolism: marker or mediator? Nat Rev Endocrinol 2012;9(1):43-55.

Boskey AL, Gadaleta S, Gundberg C, Doty SB, Ducy P, Karsenty G. Fourier transform infrared microspectroscopic analysis of bones of osteocalcin-deficient mice provides insight into the function of osteocalcin. Bone 1998;23:187-196.

Boudreaux JM, Towler DA. Synergistic induction of osteocalcin gene expression: identification of a bipartite element conferring fibroblast growth factor 2 and cyclic AMP responsiveness in the rat osteocalcin promoter. J Biol Chem 1996;271:7508-15.

Boucher-Berry C, Speiser PW, Carey DE, Shelov SP, Accacha S, Fennoy I, Rapaport R, Espinal Y, Rosenbaum M. Vitamin D, osteocalcin, and risk for adiposity as comorbidities in middle school children. J Bone Miner Res 2012;27(2):283-93.

Bradbrook GM, Gleichmann T, Harrop SJ, Habash J, Raftery J, Kalb J, Yariv J, Hillier IH, Helliwell JR. X-ray and molecular dynamics studies of concanavalin-A glucoside and mannoside complexes - Relating structure to thermodynamics of binding. J Chem Soc 1998;94:1603.

Bräuner-Osborne H, Wellendorph P, Jensen AA. Structure, pharmacology and therapeutic prospects of family C G-protein coupled receptors. Curr Drug Targets 2007;8(1):169-84.

Carvallo L, Henríquez B, Paredes R, Olate J, Onate S, van Wijnen AJ, Lian JB, Stein GS, Stein JL, Montecino M. 1alpha,25-dihydroxy vitamin D3-enhanced expression of the osteocalcin gene involves increased promoter occupancy of basal transcription regulators and gradual recruitment of the 1alpha,25-dihydroxy vitamin D3 receptor-SRC-1 coactivator complex. J Cell Physiol 2008;214(3):740-49.

Case DA, Cheatham TE 3rd, Darden T, Gohlke H, Luo R, Merz KM Jr, Onufriev A, Simmerling C, Wang B, Woods RJ. The Amber biomolecular simulation programs. J Comput Chem 2005;26(16):1668-88.

Chenu C, Colucci S, Grano M, Zigrino P, Barattolo R, Zambonin G, Baldini N, Vergnaud P, Delmas PD, Zallone AZ. Osteocalcin induces chemotaxis, secretion of matrix proteins, and calcium-mediated intracellular signaling in human osteoclast-like cells. J Cell Biol 1994;127:1149-58.

Chothia C, Lesk AM. The relation between the divergence of sequence and structure in proteins. EMBO J 1986;5:823-826.

Christiansen B, Hansen KB, Wellendorph P, Bräuner-Osborne H. Pharmacological characterization of mouse GPRC6A, an L-alpha-amino-acid receptor modulated by divalent cations. Br J Pharmacol 2007;150(6):798-807.

Connolly ML. Solvent-accessible surfaces of proteins and nucleic acids. Science 1983;221(4612):709-13.

Cousin W, Courseaux A, Ladoux A, Dani C, Peraldi P. Cloning of hOST-PTP: the only example of a protein-tyrosine-phosphatase the function of which has been lost between rodent and human. Biochem Biophys Res Commun 2004;321(1):259-65.

Cristiani A, Brisotto N, Cedrati FC, Floris M, Scapozza L, Moro S. ClickMD: an intuitive web-oriented molecular dynamics platform. Future Med Chem 2011;3(8):923-31.

Desbois C, Hogue DA, Karsenty G. The mouse osteocalcin gene cluster contains three genes with two separate spatial and temporal patterns of expression. J Biol Chem 1994;269(2):1183-90.

Ding EL, Song Y, Malik VS, Liu S. Sex differences of endogenous sex hormones and risk of type 2 diabetes: a systematic review and meta-analysis. JAMA 2006;295(11):1288-99.

Ding EL, Song Y, Manson JE, Hunter DJ, Lee CC, Rifai N, Buring JE, Gaziano JM, Liu S. Sex hormone-binding globulin and risk of type 2 diabetes in women and men. N Engl J Med 2009;361(12):1152-63.

Dowd TL, Rosen JF, Mints L, Gundberg CM. The effect of Pb(2+) on the structure and hydroxyapatite binding properties of osteocalcin. Biochim Biophys Acta 2001;1535(2):153-63.

Dowd TL, Rosen JF, Li L, Gundberg CM. The three-dimensional structure of bovine calcium ion-bound osteocalcin using 1H NMR spectroscopy. Biochemistry 2003;42(25):7769-79.

Ducy P, Desbois C, Boyce B, Pinero G, Story B, Dunstan C, Smith E, Bonadio J, Goldstein S, Gundberg C, Bradley A, Karsenty G. Increased bone formation in osteocalcin-deficient mice. Nature 1996;382(6590):448-52.

Edmunds SE, Stubbs AP, Santos AA, Wilkinson ML. Estrogen and androgen regulation of sex hormone binding globulin secretion by a human liver cell line. J Steroid Biochem Mol Biol 1990;37(5):733-39.

Elofsson A. A study on protein sequence alignment quality. Proteins 2002;46:330-39.

Engelke JA, Hale JE, Suttie JW, Price PA. Vitamin K-dependent carboxylase: utilization of decarboxylated bone Gla protein and matrix Gla protein as substrates. Biochim Biophys Acta 1991;1078(1):31-34.

Fadini GP, Albiero M, Menegazzo L, Boscaro E, Vigili de Kreutzenberg S, Agostini C, Cabrelle A, Binotto G, Rattazzi M, Bertacco E, Bertorelle R, Biasini L, Mion M, Plebani M, Ceolotto G, Angelini A, Castellani C, Menegolo M, Grego F, Dimmeler S, Seeger F, Zeiher A, Tiengo A, Avogaro A. Widespread increase in myeloid calcifying cells contributes to ectopic vascular calcification in type 2 diabetes. Circ Res 2011;108(9):1112-21.

Fernández-Real JM, Izquierdo M, Ortega F, Gorostiaga E, Gómez-Ambrosi J, Moreno-Navarrete JM, Frühbeck G, Martínez C, Idoate F, Salvador J, Forga L, Ricart W, Ibañez J. The relationship of serum osteocalcin concentration to insulin secretion, sensitivity, and disposal with hypocaloric diet and resistance training. J Clin Endocrinol Metab 2009;94(1):237-45.

Fernández-Real JM, Ortega F, Gómez-Ambrosi J, Salvador J, Frühbeck G, Ricart W. Circulating osteocalcin concentrations are associated with parameters of liver fat infiltration and increase in parallel to decreased liver enzymes after weight loss. Osteoporos Int 2010;21(12):2101-07.

Ferron M, Hinoi E, Karsenty G, Ducy P. Osteocalcin differentially regulates beta cell and adipocyte gene expression and affects the development of metabolic diseases in wild-type mice. Proc Natl Acad Sci U S A 2008;105(13):5266-70.

Ferron M, Wei J, Yoshizawa T, Del Fattore A, DePinho RA, Teti A, Ducy P, Karsenty G. Insulin signaling in osteoblasts integrates bone remodeling and energy metabolism. Cell 2010;142(2):296-308.

Ferron M, McKee MD, Levine RL, Ducy P, Karsenty G. Intermittent injections of osteocalcin improve glucose metabolism and prevent type 2 diabetes in mice. Bone 2012;50(2):568-75.

Fleet JC, Hock JM. Identification of osteocalcin mRNA in nonosteoid tissue of rats and humans by reverse transcription-polymerase chain reaction. J Bone Miner Res 1994;9(10):1565-73.

Foresta C, Strapazzon G, De Toni L, Gianesello L, Calcagno A, Pilon C, Plebani M, Vettor R. Evidence for osteocalcin production by adipose tissue and its role in human metabolism. J Clin Endocrinol Metab. 2010 Jul;95(7):3502-06.

Foresta C, Strapazzon G, De Toni L, Fabris F, Grego F, Gerosa G, Vettore S, Garolla A. Platelets express and release osteocalcin and co-localize in human calcified atherosclerotic plaques. J Thromb Haemost 2012. doi:10.1111/jth.12088.

Fortunati N, Fissore F, Fazzari A, Berta L, Giudici M, Frairia R. The membrane receptor for sex steroid binding protein is not ubiquitous. J Endocrinol Invest 1992;15:617–20.

Frazão C, Simes DC, Coelho R, Alves D, Williamson MK, Price PA, Cancela ML, Carrondo MA. Structural evidence of a fourth Gla residue in fish osteocalcin: biological implications. Biochemistry 2005;44(4):1234-42.

Gallop PM, Lian JB, Hauschka PV. Carboxylated calcium-binding proteins and vitamin K. N Engl J Med 1980;302(26):1460-66.

Garnero P, Grimaux M, Seguin P, Delmas PD. Characterization of immunoreactive forms of human osteocalcin generated in vivo and in vitro. J Bone Miner Res 1994;9:255-64.

Gössl M, Mödder UI, Atkinson EJ, Lerman A, Khosla S. Osteocalcin expression by circulating endothelial progenitor cells in patients with coronary atherosclerosis. J Am Coll Cardiol 2008;52(16):1314-25.

Graham FL, Smiley J, Russell WC, Nairn R. Characteristics of a human cell line transformed by DNA from human adenovirus type 5. J Gen Virol 1977;36(1):59-74.

Gravenstein KS, Napora JK, Short RG, Ramachandran R, Carlson OD, Metter EJ, Ferrucci L, Egan JM, Chia CW. Cross-sectional evidence of a signaling pathway from bone homeostasis to glucose metabolism. J Clin Endocrinol Metab 2011;96(6):E884-90.

GrilloML,Jacobus AP, Scalco R, Amaral F, RodriguesDO,Loss ES, Wassermann GF. Testosterone rapidly stimulates insulin release from isolated pancreatic islets through a non-genomic dependent mechanism. Horm Metab Res 2005;37:662-665.

Grishkovskaya I, Avvakumov GV, Sklenar G, Dales D, Hammond GL, Muller YA. Crystal structure of human sex hormone-binding globulin: steroid transport by a laminin G-like domain. EMBO J 2000;19(4):504-12.

Grishkovskaya I, Avvakumov GV, Hammond GL, Catalano MG, Muller YA. Steroid ligands bind human sex hormone-binding globulin in specific orientations and produce distinct changes in protein conformation. J Biol Chem 2002; 277(35):32086-93. (a)

Grishkovskaya I, Avvakumov GV, Hammond GL, Muller YA. Resolution of a disordered region at the entrance of the human sex hormone-binding globulin steroid-binding site. J Mol Biol 2002;318(3):621-26. (b)

Hamann C, Goettsch C, Mettelsiefen J, Henkenjohann V, Rauner M, Hempel U, Bernhardt R, Fratzl-Zelman N, Roschger P, Rammelt S, Günther KP, Hofbauer LC.

Delayed bone regeneration and low bone mass in a rat model of insulin-resistant type 2 diabetes mellitus is due to impaired osteoblast function. Am J Physiol Endocrinol Metab 2011;301(6):E1220-28.

Hauschka PV, Lian JB, Gallop PM. Direct identification of the calcium-binding amino acid, gamma-carboxyglutamate, in mineralized tissue. Proc Natl Acad Sci U S A 1975;72(10):3925-29.

Hauschka PV. Specific tritium labeling of gamma-carboxyglutamic acid in proteins. Biochemistry 1979;18(22):4992-99.

Hauschka PV, Carr SA. Calcium-dependent alpha-helical structure in osteocalcin. Biochemistry 1982;21(10):2538-47.

Hauschka PV, Lian JB, Cole DE, Gundberg CM. Osteocalcin and matrix Gla protein: vitamin K-dependent proteins in bone. Physiol Rev 1989;69(3):990-1047.

Henneicke H HM, Street J, Modzelewski J, Buttgereit F, Zhou H, Seibel M. Glucocorticoid-induced fat accrual is mediated by the osteoblast. Arthritis Rheum 2009;60:609.

Hoang QQ, Sicheri F, Howard AJ, Yang DS. Bone recognition mechanism of porcine osteocalcin from crystal structure. Nature 2003;425(6961):977-80.

Hohm L, Sander C. Protein structure comparison by alignment of distance matrices. J Mol Biol 1993;233:123-38.

Holm L, Sander C. Mapping the protein universe. Science 1996;273:595-603.

Hornak V, Abel R, Okur A, Strockbine B, Roitberg A, Simmerling C. Comparison of multiple Amber force fields and development of improved protein backbone parameters. Proteins 2006;65(3):712-25.

Hryb DJ, Khan MS, Rosner W. Testosterone-estradiol-binding globulin binds to human prostatic cell membranes. Biochem Biophys Res Commun 1985;128(1):432-40.

Hubbard TJ, Murzin AG, Brenner SE, Chothia C. SCOP: a structural classification of proteins database. Nucleic Acids Res 1997;25:236-239.

Hughes-Fulford M, Li CF. The role of FGF-2 and BMP-2 in regulation of gene induction, cell proliferation and mineralization. J Orthop Surg Res 2011;6:8.

Humphrey W, Dalke A, Schulten K. VMD: visual molecular dynamics. J Mol Graph 1996;14(1):33-8, 27-28.

Iglesias P, Arrieta F, Piñera M, Botella-Carretero JI, Balsa JA, Zamarrón I, Menacho M, Díez JJ, Muñoz T, Vázquez C. Serum concentrations of osteocalcin, procollagen type 1 N-terminal propeptide and beta-CrossLaps in obese subjects with varying degrees of glucose tolerance. Clin Endocrinol (Oxf) 2011;75(2):184-88.

Iki M, Tamaki J, Fujita Y, Kouda K, Yura A, Kadowaki E, Sato Y, Moon JS, Tomioka K, Okamoto N, Kurumatani N. Serum undercarboxylated osteocalcin levels are inversely associated with glycemic status and insulin resistance in an elderly Japanese male population: Fujiwara-kyo Osteoporosis Risk in Men (FORMEN) Study. Osteoporos Int 2012;23(2):761-70.

Im JA, Yu BP, Jeon JY, Kim SH. Relationship between osteocalcin and glucose metabolism in postmenopausal women. Clin Chim Acta 2008;396:66–69.

Ingram RT, Park YK, Clarke BL, Fitzpatrick LA. Age- and gender-related changes in the distribution of osteocalcin in the extracellular matrix of normal male and female bone. Possible involvement of osteocalcin in bone remodeling. J Clin Invest 1994;93:989-97.

Ivaska KK, Hentunen TA, Vääräniemi J, Ylipahkala H, Pettersson K, Väänänen HK. Release of intact and fragmented osteocalcin molecules from bone matrix during bone resorption in vitro. J Biol Chem 2004;279:18361-69.

Jung C, Ou YC, Yeung F, Frierson HF Jr, Kao C. Osteocalcin is incompletely spliced in non-osseous tissues. Gene 2001;271(2):143-50.

Kanazawa I, Yamaguchi T, Yamauchi M, Yamamoto M, Kurioka S, Yano S, Sugimoto T. Adiponectin is associated with changes in bone markers during glycemic control in type 2 diabetes mellitus. J Clin Endocrinol Metab 2009;94(8):3031-37. (a)

Kanazawa I, Yamaguchi T, Yamamoto M, Yamauchi M, Kurioka S, Yano S, Sugimoto T. Serum osteocalcin level is associated with glucose metabolism and atherosclerosis parameters in type 2 diabetes mellitus. J Clin Endocrinol Metab 2009;94:45–49. (b)

Kanazawa I, Yamaguchi T, Yamauchi M, Yamamoto M, Kurioka S, Yano S, Sugimoto T. Serum undercarboxylated osteocalcin was inversely associated with plasma glucose level and fat mass in type 2 diabetes mellitus. Osteoporos Int 2011;22:187–94. (a)

Kanazawa I, Yamaguchi T, Tada Y, Yamauchi M, Yano S, Sugimoto T. Serum osteocalcin level is positively associated with insulin sensitivity and secretion in patients with type 2 diabetes. Bone 2011;48:270–75. (b)

Katchalski-Katzir E, Shariv I, Eisenstein M, Friesem AA, Aflalo C, Vakser IA. Molecular surface recognition: determination of geometric fit between proteins and their ligands by correlation techniques. Proc Natl Acad Sci U S A 1992;89(6):2195-99.

Keech A, Simes RJ, Barter P, et al. Effects of long-term fenofibrate therapy on cardiovascular events in 9795 people with type 2 diabetes mellitus (the FIELD study): Randomised controlled trial. Lancet 2005;366:1849–61.

Kerner SA, Scott RA, Pike JW. Sequence elements in the human osteocalcin gene confer basal activation and inducible response to hormonal vitamin D3. Proc Natl Acad Sci U S A 1989;86(12):4455-59.

Kim SH, Lee JW, Im JA, Hwang HJ. Serum osteocalcin is related to abdominal obesity in Korean obese and overweight men. Clin Chim Acta 2010;411(23-24):2054-57.

Knepper-Nicolai B, Reinstorf A, Hofinger I, Flade K, Wenz R, Pompe W. Influence of osteocalcin and collagen I on the mechanical and biological properties of Biocement D. Biomol Eng 2002;19:227-31.

Krieger E, Koraimann G, Vriend G. Increasing the precision of comparative models with YASARA NOVA--a self-parameterizing force field. Proteins 2002;47(3):393-402.

Kuang D, Yao Y, Lam J, Tsushima RG, Hampson DR. Cloning and characterization of a family C orphan G-protein coupled receptor. J Neurochem 2005;93(2):383-91.

Le TN, Nestler JE, Strauss JF 3rd, Wickham EP 3rd. Sex hormone-binding globulin and type 2 diabetes mellitus. Trends Endocrinol Metab 2012;23(1):32-40.

Lee NK, Sowa H, Hinoi E, Ferron M, Ahn JD, Confavreux C, Dacquin R, Mee PJ, McKee MD, Jung DY, Zhang Z, Kim JK, Mauvais-Jarvis F, Ducy P, Karsenty G. Endocrine regulation of energy metabolism by the skeleton. Cell 2007;130(3):456-69.

Levitt M, Gerstein M. A unified statistical framework for sequence comparison and structure comparison. Proc Natl Acad Sci USA 1998,95:5913-20.

Lian JB, Friedman PA. The vitamin K-dependent synthesis of gamma-carboxyglutamic acid by bone microsomes. J Biol Chem 1978;253(19):6623-26.

Lian JB, Tassinari M, Glowacki J. Resorption of implanted bone prepared from normal and warfarin-treated rats. J Clin Invest 1984;73:1223-26.

Lian J, Stewart C, Puchacz E, Mackowiak S, Shalhoub V, Collart D, Zambetti G, Stein G. Structure of the rat osteocalcin gene and regulation of vitamin D-dependent expression. Proc Natl Acad Sci U S A 1989;86(4):1143-47.

Liggett WH Jr, Lian JB, Greenberger JS, Glowacki J. Osteocalcin promotes differentiation of osteoclast progenitors from murine long-term bone marrow cultures. J Cell Biochem 1994;55:190-99.

Livak KJ, Schmittgen TD. Analysis of relative gene expression data using real-time quantitative PCR and the 2(-Delta Delta C(T)) Method. Methods 2001;25(4):402-08.

Losel RM, Falkenstein E, Feuring M, Schultz A, Tillmann HC, Rossol-Haseroth K, Wehling M. Nongenomic steroid action: controversies, questions, and answers. Physiol Rev 2003;83(3):965-1016.

Malone JD, Teitelbaum SL, Griffin GL, Senior RM, Kahn AJ. Recruitment of osteoclast precursors by purified bone matrix constituents. J Cell Biol 1992;92:227-30.

Martí-Renom MA, Stuart AC, Fiser A, Sánchez R, Melo F, Sali A. Comparative protein structure modeling of genes and genomes. Annu Rev Biophys Biomol Struct 2000;29:291-325.

Mauro LJ, Olmsted EA, Skrobacz BM, Mourey RJ, Davis AR, Dixon JE. Identification of a hormonally regulated protein tyrosine phosphatase associated with bone and testicular differentiation. J Biol Chem 1994;269(48):30659-67.

McDonnell DP, Scott RA, Kerner SA, O'Malley BW, Pike JW. Functional domains of the human vitamin D3 receptor regulate osteocalcin gene expression. Mol Endocrinol 1989;3:635-44.

Misra M, Miller KK, Cord J, Prabhakaran R, Herzog DB, Goldstein M, Katzman DK, Klibanski A. Relationships between serum adipokines, insulin levels, and bone density in girls with anorexia nervosa. J Clin Endocrinol Metab 2007;92(6):2046-52.

Mosavin R, Mellon WS. Posttranscriptional regulation of osteocalcin mRNA in clonal osteoblast cells by 1,25-dihydroxyvitamin D3. Arch Biochem Biophys 1996;332:142-52.

Mundy GR, Poser JW. Chemotactic activity of the gamma-carboxyglutamic acid containing protein in bone. Calcif Tissue Int 1983;35:164-68.

Murshed M, Schinke T, McKee MD, Karsenty G. Extracellular matrix mineralization is regulated locally; different roles of two gla-containing proteins. J Cell Biol 2004;165(5):625-30.

Murzin AG. How far divergent evolution goes in proteins. Curr Opin Struct Biol 1998; 8:380-87.

Muto T, Tsuchiya D, Morikawa K, Jingami H. Structures of the extracellular regions of the group II/III metabotropic glutamate receptors. Proc Natl Acad Sci U S A 2007;104(10):3759-64.

Nakhla AM, Khan MS, Rosner W. Biologically active steroids activate receptor-bound human sex hormone-binding globulin to cause LNCaP cells to accumulate adenosine 39,59-monophosphate. J Clin Endocrinol Metab 1990;71:398–404.

Nakhla AM, Khan MS, Romas NP, Rosner W. Estradiol causes the rapid accumulation of cAMP in human prostate. Proc Natl Acad Sci U S A 1994;91(12):5402-05.

Nakhla AM, Ding VDH, Khan MS, Romas NA, Rhodes L, Smith RG, Rosner W. 5a-Androstan-3a-17b-diol is a hormone: Stimulation of cAMP accumulation in human and dog prostate. J Clin Endocrinol Metab 1995;80:2259–62.

Nakhla AM, Leonard J, Hryb DJ, Rosner W. Sex hormone-binding globulin receptor signal transduction proceeds via a G protein. Steroids 1999;64(3):213-16.

Needleman SB, Wunsch CD. A general method applicable to the search for similarities in the amino acid sequence of two proteins. J Mol Biol 1970;48:443–53.

Nishimoto SK, Price PA. Secretion of the vitamin K-dependent protein of bone by rat osteosarcoma cells. Evidence for an intracellular precursor. J Biol Chem 1980;255(14):6579-83.

Nimptsch K, Hailer S, Rohrmann S, Gedrich K, Wolfram G, Linseisen J. Determinants and correlates of serum undercarboxylated osteocalcin. Ann Nutr Metab 2007;51(6):563-70.

Nussinov R, Wolfson HJ. Efficient detection of three-dimensional structural motifs in biological macromolecules by computer vision techniques. Proc Natl Acad Sci USA 1991;88:10495-99.

O'Donovan C, Martin MJ, Gattiker A, Gasteiger E, Bairoch A, Apweiler R. High-quality protein knowledge resource: SWISS-PROT and TrEMBL. Brief Bioinform 2002;3(3):275-84.

Okur A, Strockbine B, Hornak V, Simmerling C. Using PC clusters to evaluate the transferability of molecular mechanics force fields for proteins. J Comput Chem 2003;24(1):21-31.

Oury F, Sumara G, Sumara O, Ferron M, Chang H, Smith CE, Hermo L, Suarez S, Roth BL, Ducy P, Karsenty G. Endocrine regulation of male fertility by the skeleton. Cell 2011;144(5):796-809.

Overington JP, Al-Lazikani B, Hopkins AL. How many drug targets are there? Nat Rev Drug Discov 2006;5(12):993-96.

Ozono K, Liao J, Kerner SA, Scott RA, Pike JW. The vitamin D-responsive element in the human osteocalcin gene. Association with a nuclear proto-oncogene enhancer. J Biol Chem 1990;265:21881-88.

Pastoureau P, Vergnaud P, Meunier PJ, Delmas PD. Osteopenia and bone-remodeling abnormalities in warfarin-treated lambs. J Bone Miner Res 1993;8(12):1417-26.

Perry JR, Weedon MN, Langenberg C, Jackson AU, Lyssenko V, Sparsø T, Thorleifsson G, Grallert H, Ferrucci L, Maggio M, Paolisso G, Walker M, Palmer CN, Payne F, Young E, Herder C, Narisu N, Morken MA, Bonnycastle LL, Owen KR, Shields B, Knight B, Bennett A, Groves CJ, Ruokonen A, Jarvelin MR, Pearson E, Pascoe L, Ferrannini E, Bornstein SR, Stringham HM, Scott LJ, Kuusisto J, Nilsson P, Neptin M, Gjesing AP, Pisinger C, Lauritzen T, Sandbaek A, Sampson M; MAGIC, Zeggini E, Lindgren CM, Steinthorsdottir V, Thorsteinsdottir U, Hansen T, Schwarz P, Illig T, Laakso M, Stefansson K, Morris AD, Groop L, Pedersen O, Boehnke M, Barroso I, Wareham NJ, Hattersley AT, McCarthy MI, Frayling TM. Genetic evidence that raised sex hormone binding globulin (SHBG) levels reduce the risk of type 2 diabetes. Hum Mol Genet 2010;19(3):535-44.

Pi M, Garner SC, Flannery P, Spurney RF, Quarles LD. Sensing of extracellular cations in CasR-deficient osteoblasts. Evidence for a novel cation-sensing mechanism. J Biol Chem 2000;275(5):3256-63.

Pi M, Faber P, Ekema G, Jackson PD, Ting A, Wang N, Fontilla-Poole M, Mays RW, Brunden KR, Harrington JJ, Quarles LD. Identification of a novel extracellular cation-sensing G-protein-coupled receptor. J Biol Chem 2005;280(48):40201-29.

Pi M, Chen L, Huang MZ, Zhu W, Ringhofer B, Luo J, Christenson L, Li B, Zhang J, Jackson PD, Faber P, Brunden KR, Harrington JJ, Quarles LD. GPRC6A null mice

exhibit osteopenia, feminization and metabolic syndrome. PLoS One 2008;3(12):e3858.

Pi M, Parrill AL, Quarles LD. GPRC6A mediates the non-genomic effects of steroids. J Biol Chem 2010;285(51):39953-64.

Pi M, Wu Y, Quarles LD. GPRC6A mediates responses to osteocalcin in β-cells in vitro and pancreas in vivo. J Bone Miner Res 2011;26(7):1680-83.

Pi M, Quarles LD. Multiligand specificity and wide tissue expression of GPRC6A reveals new endocrine networks. Endocrinology 2012;153(5):2062-69. (a)

Pi M, Quarles LD. GPRC6A regulates prostate cancer progression. Prostate 2012;72(4):399-409. (b)

Pieper U, Eswar N, Braberg H, Madhusudhan MS, Davis FP, Stuart AC, Mirkovic N, Rossi A, Marti-Renom MA, Fiser A, Webb B, Greenblatt D, Huang CC, Ferrin TE, Sali A. MODBASE, a database of annotated comparative protein structure models, and associated resources. Nucleic Acids Res 2004;32(Database issue):D217-22.

Pierce BG, Hourai Y, Weng Z. Accelerating protein docking in ZDOCK using an advanced 3D convolution library. PLoS One 2011;6(9):e24657.

Pietschmann P, Schernthaner G, Woloszczuk W. Serum osteocalcin levels in diabetes mellitus: analysis of the type of diabetes and microvascular complications. Diabetologia 1988;31:892-95.

Pitroda AP, Harris SS, Dawson-Hughes B. The association of adiposity with parathyroid hormone in healthy older adults. Endocrine 2009;36(2):218-23.

Pittas AG, Harris SS, Eliades M, Stark P, Dawson-Hughes B. Association between serum osteocalcin and markers of metabolic phenotype. J Clin Endocrinol Metab 2009;94(3):827-32.

Pitteloud N, Hardin M, Dwyer AA, Valassi E, Yialamas M, Elahi D, Hayes FJ. Increasing insulin resistance is associated with a decrease in Leydig cell testosterone secretion in men. J Clin Endocrinol Metab 2005;90:2636-41.

Pollock NK, Bernard PJ, Gower BA, Gundberg CM, Wenger K, Misra S, Bassali RW, Davis CL. Lower uncarboxylated osteocalcin concentrations in children with prediabetes is associated with beta-cell function. J Clin Endocrinol Metab 2011;96(7):E1092-99.

Poser JW, Price PA. A method for decarboxylation of gamma-carboxyglutamic acid in proteins. Properties of the decarboxylated gamma-carboxyglutamic acid protein from calf bone. J Biol Chem 1979;254(2):431-36.

Poser JW, Esch FS, Ling NC, Price PA. Isolation and sequence of the vitamin K-dependent protein from human bone. Undercarboxylation of the first glutamic acid residue. J Biol Chem 1980;255(18):8685-91.

Poundarik A, Gundberg C, Vashishth D Non-collageneous proteins influence bone mineral size, shape and orientation: a SAXS study. J Bone Miner Res 2011;26:S36.

Price PA, Poser JW, Raman N. Primary structure of the gamma-carboxyglutamic acid-containing protein from bovine bone. Proc Natl Acad Sci U S A 1976;73(10):3374-75. (a)

Price PA, Otsuka AA, Poser JW, Kristaponis J, Raman N. Characterization of a gamma-carboxyglutamic acid-containing protein from bone. Proc Natl Acad Sci U S A 1976;73(5):1447-51. (b)

Price PA, Nishimoto SK. Radioimmunoassay for the vitamin K-dependent protein of bone and its discovery in plasma. Proc Natl Acad Sci U S A 1980;77(4):2234-38.

Price PA, Baukol SA. 1,25-dihydroxyvitamin D3 increases serum levels of the vitamin K-dependent bone protein. Biochem Biophys Res Commun 1981;99(3):928-35.

Price PA, Urist MR, Otawara Y. Matrix Gla protein, a new gamma-carboxyglutamic acid-containing protein which is associated with the organic matrix of bone. Biochem Biophys Res Commun. 1983;117(3):765-71.

Plymate SR, Matej LA, Jones RE, Friedl KE. Inhibition of sex hormone-binding globulin production in the human hepatoma (Hep G2) cell line by insulin and prolactin. J Clin Endocrinol Metab 1988;67(3):460-64.

Ponder JW, Case DA. Force fields for protein simulations. Adv Protein Chem 2003;66:27-85.

Prlić A, Domingues FS, Sippl MJ. Structure-derived substitution matrices for alignment of distantly related sequences. Protein Eng 2000;13(8):545-50.

Puchacz E, Lian JB, Stein GS, Wozney J, Huebner K, Croce C. Chromosomal localization of the human osteocalcin gene. Endocrinology 1989;124(5):2648-50.

Rosner W, Hryb DJ, Kahn SM, Nakhla AM, Romas NA. Interactions of sex hormone-binding globulin with target cells. Mol Cell Endocrinol 2010;316(1):79-85.

Qu Q, Perälä-Heape M, Kapanen A, Dahllund J, Salo J, Väänänen HK, Härkönen P. Estrogen enhances differentiation of osteoblasts in mouse bone marrow culture. Bone 1998;22:201-09.

Rammelt S, Neumann M, Hanisch U, Reinstorf A, Pompe W, Zwipp H, Biewener A Osteocalcin enhances bone remodeling around hydroxyapatite/collagen composites. J Biomed Mater Res A 2005; 73:284-94.

Raymond MH, Schutte BC, Torner JC, Burns TL, Willing MC. Osteocalcin: genetic and physical mapping of the human gene BGLAP and its potential role in postmenopausal osteoporosis. Genomics 1999;60(2):210-17.

Robinson PS, Goochee CF. Kidney-specific enzyme expression by human kidney cell lines generated through oncogene transfection. J Cell Physiol 1991;148(1):54-59.

Rosner W, Hryb DJ, Khan MS, Singer CJ, Nakhla AM. Are corticosteroid-binding globulin and sex hormone-binding globulin hormones? Ann N Y Acad Sci. 1988;538:137-45.

Rosner W, Hryb DJ, Khan MS, Nakhla AM, Romas NA. Androgens, estrogens, and second messengers. Steroids 1998;63(5-6):278-81.

Rosner W, Hryb DJ, Kahn SM, Nakhla AM, Romas NA. Interactions of sex hormone-binding globulin with target cells. Mol Cell Endocrinol 2010;316(1):79-85.

Rost B. Twilight zone of protein sequence alignments. Protein Eng 1999;12:85-94.

Saleem U, Mosley TH Jr, Kullo IJ. Serum osteocalcin is associated with measures of insulin resistance, adipokine levels, and the presence of metabolic syndrome. Arterioscler Thromb Vasc Biol 2010;30(7):1474-78.

Sanchez R., Sali A. Evaluation of comparative protein structure modeling by MODELLER-3. Proteins 1997;Suppl 1:50-58.

Schaller S, Henriksen K, Sørensen MG, Karsdal MA. The role of chloride channels in osteoclasts: ClC-7 as a target for osteoporosis treatment. Drug News Perspect 2005;18(8):489-95.

Schwede T, Kopp J, Guex N, Peitsch MC. SWISS-MODEL: An automated protein homology-modeling server. Nucleic Acids Res 2003;31(13):3381-85.

Shea MK, Gundberg CM, Meigs JB, Dallal GE, Saltzman E, Yoshida M, Jacques PF, Booth SL. Gamma-carboxylation of osteocalcin and insulin resistance in older men and women. Am J Clin Nutr 2009;90(5):1230-35.

Schneider TD, Stephens RM. Sequence logos: a new way to display consensus sequences. Nucleic Acids Res 1990;18:6097-6100.

Schneidman-Duhovny D, Inbar Y, Nussinov R, Wolfson HJ. PatchDock and SymmDock: servers for rigid and symmetric docking. Nucleic Acids Res 2005;33(WebServer issue):W363-67.

Shalhoub V, Aslam F, Breen E, van Wijnen A, Bortell R, Stein GS, Stein JL, Lian JB. Multiple levels of steroid hormone-dependent control of osteocalcin during osteoblast differentiation: glucocorticoid regulation of basal and vitamin D stimulated gene expression. J Cell Biochem 1998;69:154-68.

Shea MK, Booth SL, Gundberg CM, Peterson JW, Waddell C, Dawson-Hughes B, Saltzman E. Adulthood obesity is positively associated with adipose tissue concentrations of vitamin K and inversely associated with circulating indicators of vitamin K status in men and women. J Nutr 2010;140(5):1029-34.

Shen J, Hovhannisyan H, Lian JB, Montecino MA, Stein GS, Stein JL, Van Wijnen AJ. Transcriptional induction of the osteocalcin gene during osteoblast differentiation involves acetylation of histones h3 and h4. Mol Endocrinol 2003;17(4):743-56.

Silver IA, Murrills RJ, Etherington DJ. Microelectrode studies on the acid microenvironment beneath adherent macrophages and osteoclasts. Exp Cell Res 1988;175(2):266-76.

Sippl MJ, Wiederstein M. A note on difficult structure alignment problems. Bioinformatics 2008;24:426-27.

Spronk HM, Soute BA, Schurgers LJ, Cleutjens JP, Thijssen HH, De Mey JG, Vermeer C. Matrix Gla protein accumulates at the border of regions of calcification and normal tissue in the media of the arterial vessel wall. Biochem Biophys Res Commun 2001;289(2):485-90.

Stanley TB, Humphries J, High KA, Stafford DW. Amino acids responsible for reduced affinities of vitamin K-dependent propeptides for the carboxylase. Biochemistry 1999;38(47):15681-87.

Strel'chyonok OA, Avvakumov GV, Survilo LI. A recognition system for sex-hormone-binding protein-estradiol complex in human decidual endometrium plasma membranes. Biochim Biophys Acta 1984;802(3):459-66.

Strel'chyonok OA, Avvakumov GV. Specific steroid-binding glycoproteins of human blood plasma: novel data on their structure and function. J Steroid Biochem 1990;35(5):519-34.

Sullivan TR, Duque G, Keech AC, Herrmann M. An Old Friend in a New Light: The Role of Osteocalcin in Energy Metabolism. Cardiovasc Ther 2011. doi: 10.1111/j.1755-5922.2011.00300.x.

Thornton JM, Orengo CA, Todd AE, Pearl FM. Protein folds, functions and evolution. J Mol Biol 1999;293:333-42.

Tfelt-Hansen J, Brown EM. The calcium-sensing receptor in normal physiology and pathophysiology: a review. Crit Rev Clin Lab Sci 2005;42(1):35-70.

Thiede MA, Smock SL, Petersen DN, Grasser WA, Thompson DD, Nishimoto SK. Presence of messenger ribonucleic acid encoding osteocalcin, a marker of bone turnover, in bone marrow megakaryocytes and peripheral blood platelets. Endocrinology 1994;135(3):929-37.

Tovchigrechko A, Vakser IA. GRAMM-X public web server for protein-protein docking. Nucleic Acids Res 2006;34(Web Server issue):W310-14.

Ueland T, Fougner SL, Godang K, Lekva T, Schurgers LJ, Scholz H, Halvorsen B, Schreiner T, Aukrust P, Bollerslev J. Associations between body composition, circulating interleukin-1 receptor antagonist, osteocalcin, and insulin metabolism in active acromegaly. J Clin Endocrinol Metab 2010;95:361-68.

Urakawa I, Yamazaki Y, Shimada T, Iijima K, Hasegawa H, Okawa K, Fujita T, Fukumoto S, Yamashita T. Klotho converts canonical FGF receptor into a specific receptor for FGF23. Nature 2006;444(7120):770-74.

Vermeulen A. Testosterone in plasma. A physiopathological study. Verh K Acad Geneeskd Belg 1973;35(2):95-180.

Vermeulen A, Verdonck L, Kaufman JM. A critical evaluation of simple methods for the estimation of free testosterone in serum. J Clin Endocrinol Metab 1999;84:3666-3672.

Wallace I, McKinley M, Bell P, Hunter S. Sex Hormone Binding Globulin and Insulin Resistance. Clin Endocrinol (Oxf) 2012; doi: 10.1111/cen.12086.

Wang R, Lu Y, Wang S. Comparative evaluation of 11 scoring functions for molecular docking. J Med Chem 2003;46(12):2287-303.

Wass MN, Fuentes G, Pons C, Pazos F, Valencia A. Towards the prediction of protein interaction partners using physical docking. Mol Syst Biol 2011;7:469.

Wellendorph P, Bräuner-Osborne H. Molecular cloning, expression, and sequence analysis of GPRC6A, a novel family C G-protein-coupled receptor. Gene 2004;335:37-46.

Wellendorph P, Hansen KB, Balsgaard A, Greenwood JR, Egebjerg J, Bräuner-Osborne H. Deorphanization of GPRC6A: a promiscuous L-alpha-amino acid receptor with preference for basic amino acids. Mol Pharmacol 2005;67(3):589-97.

Wellendorph P, Burhenne N, Christiansen B, Walter B, Schmale H, Bräuner-Osborne H. The rat GPRC6A: cloning and characterization. Gene 2007;396(2):257-67.

Wellendorph P, Johansen LD, Jensen AA, Casanova E, Gassmann M, Deprez P, Clément-Lacroix P, Bettler B, Bräuner-Osborne H. No evidence for a bone phenotype in GPRC6A knockout mice under normal physiological conditions. J Mol Endocrinol 2009;42(3):215-23.

World Health Organization Obesity: Preventing and Managingthe Global Epidemic. Report of a WHO Convention, Geneva, 1999. Tech Rep Series 894. World Health Organization, Geneva 2000.

Ye Y, Godzik A. Flexible structure alignment by chaining aligned fragment pairs allowing twists Bioinformatics 2003;19:ii249-ii255.

Yu XP, Chandrasekhar S. Parathyroid hormone (PTH 1-34) regulation of rat osteocalcin gene transcription. Endocrinology 1997;138:3085-92.

Zee T, Settembre C, Levine RL, Karsenty G. T-cell protein tyrosine phosphatase regulates bone resorption and whole-body insulin sensitivity through its expression in osteoblasts. Mol Cell Biol 2012;32(6):1080-88.

Zhang C, Vasmatzis G, Cornette JL, DeLisi C. Determination of atomic desolvation energies from the structures of crystallized proteins. J Mol Biol 1997;267(3):707-26.

Zhang Y, Skolnick J. Scoring function for automated assessment of protein structure template quality. Proteins 2004;57:702-10.

Zhang Y, Skolnick J. TM-align: a protein structure alignment algorithm based on the TM-score. Nucleic Acids Res 2005;33:2302-09.

APPENDIX

Output of custer analysis of 3-D alignments Gla-OC and SHBG

	13	14	15	16	17	18	19	20	21	22	23	24	25	26	27	28	29	30	31	32	33	34	35	36	37	38	39	40
	P	P	A	V	H	L	S	N	G	P	G	Q	E	P	I	A	V	M	T	F	D	L	T	K	I	T	K	T
TopMatch	0	0	0	0	0	0	0	0	0	0	0	0	0	0	0	0	0	0	0	0	0	0	0	0	0	0	0	0
	0	0	0	0	0	0	0	0	0	0	0	0	0	0	0	0	0	0	0	0	1	1	1	1	1	1	0	0
	0	0	0	0	0	0	0	0	0	0	0	0	0	0	0	0	0	0	0	0	0	0	0	0	0	0	0	0
	0	0	0	0	0	0	0	0	0	0	0	0	0	0	0	0	0	0	0	0	0	0	0	0	0	0	0	0
	0	0	0	0	0	0	0	0	0	0	0	0	0	0	0	0	0	0	0	0	0	0	0	0	0	0	0	0
TriangleMatch	0	0	1	1	1	1	0	0	0	0	0	0	0	0	1	1	1	1	1	0	0	0	0	0	0	0	0	0
	0	0	0	0	0	0	0	0	0	0	0	0	0	0	0	0	0	0	0	0	0	0	0	0	0	0	0	0
	0	0	0	1	1	1	1	1	1	1	1	1	0	0	0	1	1	0	0	0	0	0	0	0	0	0	0	0
	0	0	0	0	0	0	1	1	1	0	1	0	0	0	0	0	0	0	0	0	0	0	0	0	0	0	0	0
	0	0	0	0	0	1	0	0	0	0	0	0	0	1	0	0	0	0	0	0	0	0	0	0	0	0	0	0
TWAlign	1	1	1	1	1	1	0	0	0	0	0	0	0	0	0	0	0	0	0	0	0	0	0	0	0	0	0	0
FatCat	0	0	0	0	0	0	0	0	0	0	0	0	0	0	0	0	0	0	0	0	0	0	0	0	0	0	0	0

41	42	43	44	45	46	47	48	49	50	51	52	53	54	55	56	57	58	59	60	61	62	63	64	65	66	67	68	69	70
S	S	S	F	E	V	R	T	W	D	P	E	G	V	I	F	Y	G	D	T	N	P	K	D	D	W	F	M	L	G
0	0	0	0	0	0	0	0	0	0	0	0	0	0	0	0	0	0	0	0	0	0	0	0	0	0	0	0	0	0
0	0	0	0	0	0	0	0	0	0	0	0	0	0	0	0	0	0	0	0	0	0	0	0	0	0	0	0	0	0
0	0	0	0	0	0	0	1	1	1	1	1	1	1	1	1	1	1	0	0	0	0	0	0	0	0	0	0	0	0
0	0	0	0	0	0	0	0	0	0	0	0	0	0	0	0	0	0	0	0	0	0	0	0	0	0	0	0	0	0
0	0	0	0	0	0	0	0	0	0	0	0	0	0	0	0	0	0	1	1	1	1	1	1	1	1	1	1	0	0
1	1	1	1	0	0	0	0	0	0	0	0	0	1	1	1	1	1	0	0	0	0	0	0	0	0	0	0	0	0
0	1	1	0	0	0	0	0	0	0	0	0	0	0	0	0	0	0	0	0	0	0	0	0	0	0	0	0	0	1
0	0	0	0	0	0	0	0	0	0	0	0	0	1	0	1	0	0	1	0	0	0	0	0	0	0	0	0	0	0
0	0	0	0	1	1	0	1	1	1	0	0	0	0	1	0	0	0	0	0	0	0	0	0	0	0	0	1	0	0
0	0	0	0	0	1	0	0	0	0	0	0	1	1	0	0	1	0	0	0	0	0	0	0	0	0	0	0	0	1
0	0	0	0	0	0	1	1	1	1	1	1	1	1	1	1	1	0	0	0	0	0	0	0	0	0	0	1	1	0
0	0	0	0	0	0	0	0	0	0	0	0	0	0	0	0	0	0	0	0	0	0	0	0	0	0	0	0	0	0

71	72	73	74	75	76	77	78	79	80	81	82	83	84	85	86	87	88	89	90	91	92	93	94	95	96	97	98	99	100
L	R	D	G	R	P	E	I	Q	L	H	N	H	W	A	Q	L	T	V	G	A	G	P	R	L	D	D	G	R	W
0	0	0	1	1	1	1	1	1	1	1	1	1	1	1	1	1	0	0	0	0	0	0	0	0	0	0	0	0	0
0	0	0	0	0	0	0	0	0	0	0	0	0	0	0	0	0	0	0	0	0	0	0	0	0	0	0	0	0	0
0	0	0	0	0	0	0	0	0	0	0	0	0	0	0	0	0	0	0	0	0	0	0	0	0	0	0	0	0	0
0	0	0	0	0	0	0	0	0	0	0	0	0	0	0	0	0	0	0	0	0	0	0	0	0	0	0	0	0	0
0	0	0	0	0	0	0	0	0	0	0	1	1	1	1	1	0	0	0	0	0	0	0	0	0	0	0	0	0	0
0	0	0	0	0	0	0	0	0	0	0	0	0	0	0	0	0	0	0	0	0	0	0	0	0	0	0	0	0	0
0	0	0	0	1	1	1	1	1	0	0	0	0	0	0	0	1	1	0	0	1	1	1	1	1	0	0	0	0	0
0	0	0	0	0	0	0	0	0	0	0	0	0	0	0	0	0	0	0	0	0	0	0	0	0	0	0	0	0	0
1	1	0	0	1	1	1	0	0	0	0	0	0	0	0	0	0	0	0	0	0	0	0	0	0	0	0	0	0	0
1	1	0	0	1	1	1	0	0	0	0	0	0	0	0	0	0	0	0	1	0	0	0	0	0	0	0	0	0	0
0	0	1	1	1	0	0	0	0	0	0	0	0	0	0	0	0	0	0	0	0	0	0	0	0	0	0	0	0	0
0	0	0	0	0	0	0	0	0	0	0	0	0	0	0	0	0	0	0	0	0	0	0	0	0	0	0	0	0	0

Positions 101–129

101	102	103	104	105	106	107	108	109	110	111	112	113	114	115	116	117	118	119	120	121	122	123	124	125	126	127	128	129
H	Q	V	E	V	K	M	E	G	D	S	V	L	L	E	V	D	G	E	E	V	L	R	L	R	Q	V	S	G
0	0	0	0	0	0	0	0	0	0	0	0	0	0	0	0	0	0	0	0	0	0	1	1	1	1	1	1	1
0	0	0	0	0	0	0	0	0	0	0	0	0	0	0	0	0	0	0	0	0	0	0	0	0	0	0	0	0
0	0	0	0	0	0	0	0	0	0	0	0	0	0	0	0	0	0	0	0	0	0	0	0	0	0	0	0	0
0	0	0	0	0	0	0	0	0	0	0	0	0	0	0	0	0	0	0	0	0	0	0	0	0	0	0	0	0
0	0	0	0	0	0	0	0	0	0	0	0	0	0	0	0	0	0	0	0	0	0	0	0	0	0	0	0	0
0	0	0	0	0	0	0	0	0	0	0	0	0	0	0	0	0	0	0	0	0	0	0	0	0	0	0	0	0
0	0	0	1	1	0	0	0	0	0	0	0	1	1	1	0	0	0	0	1	0	1	1	1	0	0	0	0	0
0	0	0	0	0	0	0	0	0	0	0	0	0	0	0	0	0	0	0	0	0	0	0	0	0	0	0	0	0
1	0	1	1	0	0	0	0	0	0	0	0	0	0	0	0	0	0	0	0	0	0	0	0	0	0	0	0	0
0	0	0	0	0	0	0	0	0	0	0	0	0	0	0	0	0	0	0	0	0	0	0	0	0	0	0	0	0
0	0	0	0	0	0	0	0	0	0	0	0	0	0	0	0	0	0	0	0	0	0	0	0	0	0	0	0	0
0	0	0	0	0	0	0	0	0	0	0	0	0	0	0	0	0	0	0	0	0	0	0	0	0	0	0	0	0

Positions 136–165

136	137	138	139	140	141	142	143	144	145	146	147	148	149	150	151	152	153	154	155	156	157	158	159	160	161	162	163	164	165
H	P	I	M	R	I	A	L	G	G	L	L	F	P	A	S	N	L	R	L	P	L	V	P	A	L	D	G	C	L
0	0	0	0	0	0	0	0	0	0	0	0	0	0	0	0	0	0	0	0	0	0	0	0	0	0	0	0	0	0
0	0	0	0	0	0	0	0	0	0	0	0	0	0	0	0	0	0	0	0	0	0	0	0	0	0	0	0	0	0
0	0	0	0	0	1	1	1	1	1	1	0	0	0	0	0	0	0	0	0	0	0	0	0	0	0	0	0	0	0
0	0	0	0	0	0	1	1	1	1	1	1	1	1	1	1	1	1	1	1	0	0	0	0	0	0	0	0	0	0
0	0	0	0	0	0	0	0	0	0	0	0	0	0	0	0	0	0	0	0	0	0	0	0	0	0	0	0	0	0
0	0	0	0	0	0	0	1	1	1	0	0	0	0	0	0	0	0	0	0	0	0	0	0	0	1	0	1	0	1
0	0	0	0	0	0	0	0	0	0	0	0	0	0	0	0	0	0	0	0	0	0	0	0	0	0	0	0	0	0
0	0	0	0	0	0	0	0	1	1	0	0	0	0	0	0	0	0	0	0	0	0	1	1	0	0	1	1	1	0
0	0	0	0	0	0	0	0	0	0	0	0	0	0	0	0	0	0	0	0	0	1	0	0	0	1	1	1	0	0
0	0	0	0	0	0	1	1	1	1	1	1	0	0	0	0	0	0	0	0	0	0	1	1	1	0	1	1	1	1
0	0	0	0	0	0	0	0	0	0	0	0	0	0	0	0	0	1	1	1	1	1	1	1	1	0	0	0	0	0
0	0	0	0	0	0	0	0	0	0	0	0	0	0	0	0	0	0	0	0	0	0	0	0	0	0	0	0	0	0

Positions 166–188

166	167	168	169	170	171	172	173	174	175	176	177	178	179	180	181	182	183	184	185	186	187	188
R	R	D	S	W	L	D	K	Q	A	E	I	S	A	S	A	P	T	S	L	R	S	C
0	0	0	0	0	0	0	0	0	0	0	0	0	0	0	0	0	0	0	0	0	0	0
0	0	0	0	0	1	1	1	1	1	1	1	1	1	0	0	0	0	0	0	0	0	0
0	0	0	0	0	0	0	0	0	0	0	0	0	0	0	0	0	0	0	0	0	0	0
0	0	0	0	0	0	0	0	0	0	0	0	0	0	0	0	0	0	0	0	0	0	0
0	0	0	0	0	0	0	0	0	0	0	0	0	0	0	0	0	0	0	0	0	0	0
0	1	0	1	0	0	0	0	0	0	0	0	0	0	0	0	0	0	0	0	0	0	1
0	0	1	1	1	0	0	0	0	0	0	0	0	0	0	0	0	0	0	0	0	0	0
0	0	0	0	0	0	0	0	0	0	0	0	0	1	1	1	0	0	0	0	0	0	1
0	0	0	0	0	0	0	0	0	0	0	0	0	0	0	0	0	0	0	0	0	0	0
0	0	0	0	0	0	0	0	0	0	0	0	0	0	0	0	0	0	0	0	0	0	0
0	0	0	0	0	0	0	0	0	0	0	0	0	0	0	0	0	0	0	0	0	0	0
0	0	0	0	1	1	1	1	1	1	1	1	0	0	0	0	0	0	0	0	0	0	0

Output of custer analysis of 3-D alignments Glu-OC and SHBG

	13	14	15	16	17	18	19	20	21	22	23	24	25	26	27	28	29	30	31	32	33	34	35	36	37	38	39	40
	P	P	A	V	H	L	S	N	G	P	G	Q	E	P	I	A	V	M	T	F	D	L	T	K	I	T	K	T
TopMatch	0	0	0	0	0	0	0	0	0	0	0	0	0	0	0	0	0	0	0	0	1	1	1	1	1	1	0	0
	0	0	0	0	0	0	0	0	0	0	0	0	0	0	0	0	0	0	0	0	1	1	1	1	1	1	1	0
	0	0	0	0	0	0	0	0	0	0	0	0	0	0	0	0	0	0	0	0	0	0	0	0	0	0	0	0
	0	0	0	0	0	0	0	0	0	0	0	0	0	0	0	0	0	0	0	0	0	0	0	0	0	0	0	0
	0	0	0	0	0	0	0	0	0	0	0	0	0	0	0	0	0	0	0	0	0	0	0	0	0	0	0	0
TriangleMatch	0	0	1	1	1	1	1	1	1	1	1	0	0	1	1	1	1	0	0	0	0	0	0	0	0	0	0	0
	0	0	0	0	0	1	1	0	0	0	0	0	0	0	0	0	0	0	0	0	0	0	0	0	0	0	0	0
	1	1	1	1	1	1	0	0	0	0	0	0	0	0	0	0	0	0	0	0	0	0	0	0	0	0	0	0
	0	0	0	0	1	1	1	1	0	0	0	0	0	0	1	1	1	1	1	0	0	0	0	0	0	0	0	0
	0	0	0	1	1	1	0	0	0	0	0	0	0	0	1	1	1	1	1	0	0	0	0	0	0	0	0	0
TWAlign	1	0	1	0	0	0	0	0	0	0	0	0	0	0	0	0	0	0	0	0	0	0	0	0	0	0	0	0
FatCat	0	0	0	0	0	0	0	0	0	0	0	0	0	0	0	0	0	0	0	0	0	0	0	0	0	0	0	0

41	42	43	44	45	46	47	48	49	50	51	52	53	54	55	56	57	58	59	60	61	62	63	64	65	66	67	68	69	70
S	S	S	F	E	V	R	T	W	D	P	E	G	V	I	F	Y	G	D	T	N	P	K	D	D	W	F	M	L	G
0	0	0	0	0	0	0	0	0	0	0	0	0	0	0	0	0	0	0	0	0	0	0	0	0	0	0	0	0	0
0	0	0	0	0	0	0	0	0	0	0	0	0	0	0	0	0	0	0	0	0	0	0	0	0	0	0	0	0	0
0	0	0	0	0	0	0	0	0	0	0	0	0	0	0	0	0	0	0	0	0	0	0	0	0	0	0	0	0	0
0	0	0	0	0	0	0	0	0	0	0	0	0	0	0	0	0	0	0	0	0	0	0	0	0	0	0	0	0	0
0	0	0	0	0	0	0	0	0	0	0	0	0	0	0	0	0	0	0	0	0	0	0	0	0	0	0	0	0	0
0	0	0	0	0	0	0	0	0	0	0	0	1	1	1	0	1	1	0	0	0	0	0	0	0	0	0	0	0	0
0	0	0	0	0	0	0	0	0	0	0	0	0	0	1	1	1	1	1	0	0	0	0	0	0	0	1	1	1	0
0	0	0	1	1	1	1	1	1	1	0	0	0	1	0	1	0	0	0	0	0	0	0	0	0	0	0	0	0	0
0	1	0	1	0	1	0	0	0	0	0	0	0	0	1	1	1	0	0	0	0	0	0	0	0	0	0	0	0	0
0	1	0	1	0	0	0	0	0	0	0	0	0	0	1	1	1	1	0	0	0	0	0	0	0	0	0	0	0	0
0	0	0	0	1	1	1	1	1	1	1	1	1	1	1	1	1	1	1	0	0	0	0	0	0	0	0	0	0	0
0	0	0	0	0	0	0	0	0	0	0	0	0	0	0	0	0	0	0	0	0	0	0	0	0	0	0	0	0	0

71	72	73	74	75	76	77	78	79	80	81	82	83	84	85	86	87	88	89	90	91	92	93	94	95	96	97	98	99	100
L	R	D	G	R	P	E	I	Q	L	H	N	H	W	A	Q	L	T	V	G	A	G	P	R	L	D	D	G	R	W
0	0	0	0	0	0	0	0	0	0	0	0	0	0	0	0	0	0	0	0	0	0	0	0	0	0	0	0	0	0
0	0	0	0	0	0	0	0	0	0	0	0	0	0	0	0	0	0	0	0	0	0	0	0	0	0	0	0	0	0
0	0	0	0	0	0	0	0	0	0	0	0	0	0	0	0	0	0	0	0	0	0	0	0	0	0	0	0	0	0
0	0	0	0	0	0	0	0	0	0	0	0	0	0	0	0	0	0	0	0	0	0	0	0	0	0	0	0	0	1
0	0	0	0	0	0	0	0	0	0	0	0	0	0	0	0	0	0	0	0	0	0	0	0	0	0	0	0	0	0
0	0	0	0	0	0	0	0	0	0	0	0	0	0	0	0	0	0	0	0	0	0	0	0	0	0	0	0	0	0
0	0	0	0	0	0	0	1	1	1	0	0	0	0	0	0	0	0	0	0	0	0	0	0	0	0	0	0	0	0
0	0	0	0	0	0	0	0	0	0	0	0	0	0	0	0	0	0	0	0	0	0	0	0	0	0	1	1	0	1
0	0	0	0	0	0	0	0	0	0	0	0	0	0	0	0	0	0	0	0	0	0	0	0	0	0	0	0	0	0
0	0	0	0	0	0	0	0	0	0	0	0	0	0	0	0	0	0	0	0	0	0	0	0	0	0	0	0	0	0
0	0	0	0	0	0	0	0	0	0	0	0	0	0	0	0	0	0	0	0	0	0	0	0	0	0	0	0	0	0
0	0	0	0	0	0	0	0	0	0	0	0	0	0	0	0	0	0	0	0	0	0	0	0	0	0	0	0	0	0

101	102	103	104	105	106	107	108	109	110	111	112	113	114	115	116	117	118	119	120	121	122	123	124	125	126	127	128	129
H	Q	V	E	V	K	M	E	G	D	S	V	L	L	E	V	D	G	E	E	V	L	R	L	R	Q	V	S	G
0	0	0	0	0	0	0	0	0	0	0	0	0	0	0	0	0	0	0	0	0	0	0	0	0	0	0	0	0
0	0	0	0	0	0	0	0	0	0	0	0	0	0	0	0	0	0	0	0	0	0	0	0	0	0	0	0	0
0	0	0	0	0	0	0	0	0	0	0	0	0	0	0	0	0	0	0	0	0	0	0	0	0	0	0	0	0
1	1	1	1	1	1	1	1	1	1	1	1	0	0	0	0	0	0	0	0	0	0	0	0	0	0	0	0	0
0	0	0	0	0	0	0	0	0	0	0	0	0	0	0	0	0	0	0	0	0	0	0	0	0	0	0	0	0
0	0	0	0	0	0	0	0	0	0	0	0	0	0	0	0	0	0	0	0	0	0	0	0	0	0	0	0	0
0	0	0	0	0	0	0	0	0	0	0	0	0	0	0	0	0	0	0	0	0	0	0	0	0	0	0	0	0
1	1	1	0	0	0	0	0	0	0	0	0	0	0	0	0	0	0	0	0	0	0	0	0	0	0	0	0	0
0	0	0	0	1	0	0	0	0	0	0	0	0	0	0	0	0	0	0	0	0	0	0	0	0	0	0	0	0
0	0	0	0	0	0	1	0	0	0	0	0	0	0	0	0	0	0	0	0	0	0	0	0	0	0	0	0	0
0	0	0	0	0	0	0	0	0	0	0	0	0	0	0	0	0	0	0	0	0	0	0	0	0	0	0	0	0
0	0	0	0	0	0	0	0	0	0	0	0	0	0	0	0	0	0	0	0	0	0	0	0	0	0	0	0	0

136	137	138	139	140	141	142	143	144	145	146	147	148	149	150	151	152	153	154	155	156	157	158	159	160	161	162	163	164	165
H	P	I	M	R	I	A	L	G	G	L	L	F	P	A	S	N	L	R	L	P	L	V	P	A	L	D	G	C	L
0	0	0	0	0	0	0	0	0	0	0	0	0	0	0	0	0	0	0	0	0	0	0	0	0	0	0	0	0	0
0	0	0	0	0	0	0	0	0	0	0	0	0	0	0	0	0	0	0	0	0	0	0	0	0	0	0	0	0	0
0	0	0	0	0	0	0	0	1	1	1	1	1	1	1	1	1	1	1	1	1	1	1	1	0	0	0	0	0	0
0	0	0	0	0	0	0	0	0	0	0	0	0	0	0	0	0	0	0	0	0	0	0	0	0	0	0	0	0	0
0	0	0	0	0	0	0	1	1	1	1	1	1	1	1	1	1	1	1	1	1	1	1	1	0	0	0	0	0	0
0	0	0	0	0	0	1	1	1	1	0	0	0	0	0	0	0	0	0	0	0	0	0	1	1	1	0	1	1	0
0	0	0	0	0	1	1	1	1	1	1	1	1	1	1	1	1	0	0	0	0	0	0	1	0	1	0	0	0	0
0	0	0	0	0	0	0	1	0	0	0	0	0	0	0	0	0	0	0	0	0	0	0	0	1	1	1	0	1	0
0	0	0	0	0	0	1	1	1	0	0	0	0	0	0	0	0	0	0	0	0	0	1	1	1	1	1	1	1	0
0	0	0	0	0	0	1	1	1	0	0	0	0	0	0	0	0	0	0	0	0	0	0	0	0	1	1	1	1	1
0	0	0	0	0	0	1	1	1	0	0	0	0	0	0	0	0	0	0	0	0	0	0	0	0	0	0	0	1	1
0	0	0	0	0	0	0	0	0	0	0	0	0	0	0	0	0	0	0	0	0	0	0	0	0	0	0	0	0	0

166	167	168	169	170	171	172	173	174	175	176	177	178	179	180	181	182	183	184	185	186	187	188
R	R	D	S	W	L	D	K	Q	A	E	I	S	A	S	A	P	T	S	L	R	S	C
0	0	1	1	1	1	1	1	1	1	1	1	0	0	0	0	0	0	0	0	0	0	0
0	0	0	0	1	1	1	1	1	1	1	1	0	0	0	0	0	0	0	0	0	0	0
0	0	0	0	0	0	0	0	0	0	0	0	0	0	0	0	0	0	0	0	0	0	0
0	0	0	0	0	0	0	0	0	0	0	0	0	0	0	0	0	0	0	0	0	0	0
0	0	0	0	0	0	0	0	0	0	0	0	0	0	0	0	0	0	0	0	0	0	0
1	0	0	0	0	0	0	0	0	0	0	0	0	1	1	0	0	0	0	0	0	0	0
0	0	0	0	0	0	0	0	0	0	0	0	0	0	0	0	0	0	0	0	0	0	0
0	0	0	0	0	0	0	0	0	0	0	0	0	0	0	0	0	0	0	0	0	0	1
0	0	0	0	0	0	0	0	0	0	0	0	0	0	0	0	0	0	0	0	0	0	0
1	0	1	0	0	0	0	0	0	0	0	0	0	0	0	0	0	0	0	0	0	0	1
0	0	0	0	0	0	0	0	0	0	0	0	0	0	0	0	0	0	0	0	1	1	1
0	0	0	0	1	1	1	1	1	1	1	1	0	0	0	0	0	0	0	0	0	0	0